Moloney murine leukemia virus RNA recruitment

by

Eric Luis Garcia

A dissertation submitted in partial fulfillment
of the requirements for the degree of
Doctor of Philosophy
(Cellular and Molecular Biology)
in the University of Michigan
2010

Doctoral Committee:

Associate Professor Alice Telesnitsky, Chair
Professor David R. Engelke
Professor Michael J. Imperiale
Associate Professor Mats E. D. Ljungman
Assistant Professor Akira Ono

To Erin.

ACKNOWLEDGEMENTS

I would first like to thank my mentor, Alice Telesnitsky. Alice is a tough boss and an excellent scientific mentor. She puts a lot of energy into the advancement and success of her students which is much appreciated. This dissertation would not have been possible without Alice, and it is the culmination of a lot of our hard work together.

I'd next like to acknowledge all of the help that I received from Steven R. King. Steve was very generous with his time, and he was an extremely valuable resource for day-to-day benchwork. Steve's kindness and calm temperament were also very much appreciated when I struggled with difficult concepts.

Next, I'd like to thank my student mentors, Jessica Flynn and Adewunmi Onafuwa-Nuga. Jessica was my rotation mentor, and she worked with me closely when I first joined the lab. I am very grateful for her patience and her insights at the beginning of my dissertation work. Adewunmi was an excellent scientific mentor and friend. She very directly helped me grow as an independent scientist and provided a great example for grace and charm under pressure.

I'm also very grateful to my other lab collegues over the years. Just to mention a few: Vicki Larson, Sarra Keene, Silas Johnson, Nisha Duggal, Leslie Goo, and Alyssa Borders. You somehow made work in the Telesnitsky lab fun.

Thank you to my thesis committee for helping shape this dissertation and for grappling with these difficult questions. I very much appreciated all of your advice and

encouragement. While not a member of the final group, I very much appreciated having Adam Hoppe on my committee for all of his direct and practical advice.

I'd like to specially thank my family, whose love and support have sustained me and without which this would not have been possible. I am very grateful for all of their sacrifices on my behalf. Perhaps most importantly, I'd like to thank my wife Erin. She is my best friend and an excellent partner in science as well as life.

Thank you!

Work in Chapter II was performed in collaboration with the Sandra Wolin lab at Yale University and previously published in:

Garcia, E. L., A. Onafuwa-Nuga, S. Sim, S. R. King, S. L. Wolin, and A. Telesnitsky. 2009. Packaging of host mY RNAs by murine leukemia virus may occur early in Y RNA biogenesis. J Virol 83:12526-34.

Soyeong Sim generated the Ro60 knockout MEFs used here. Adewunmi Onafuwa-Nuga performed the intial northern blots of Y RNAs packaged by MLV which are referred to here. Also, she worked in concert with Steve King to look at Ro60 and La protein incorporation into MLV particles in work which is referred to here. Vicki Larson cultured the cells, harvested the virus, and performed the RT assay which is presented as Figure 2-1. All authors were involved in useful discussions and textual edits that led to the final published manuscript.

Work in Chapter III was performed with assistance from Steve King and Vicki Larson. Steve King performed the intial transfections that were used for the two vector recombination assay. Vicki Larson helped culture and test the tetracycline-regulated MLV expressing cells.

Work in Chapter IV was performed in collaboration with the Michael Summers lab at the Howard Hughes Medical Institute and the University of Maryland Baltimore County. It was previously published in:

Miyazaki, Y., E. L. Garcia, S. R. King, K. Iyalla, K. Loeliger, P. Starck, S. Syed, A. Telesnitsky, and M. F. Summers. 2010. An RNA structural switch regulates diploid genome packaging by Moloney murine leukemia virus. J Mol Biol 396:141-52.

Yasu Miyazaki and collegues perfomed the *in vitro* experiments that are referred to here. Steve King generated the Ψ^{WT} and Ψ^{M} full length MLV vectors that were used in the experiments presented here. Steve performed the transfections, harvested the virus, and generated the single copy expressing cells for the experiments presented in Figure 4-2. Steve performed transfections and viral harvests for Figure 4-4. Steve also performed viral titers in experiments mentioned here.

TABLE OF CONTENTS

LIST OF FIGURES

ABSTRACT

Retroviruses recruit viral and cellular RNAs into assembling virions. This dissertation addresses where and how RNAs are first recruited in cells by the retrovirus Moloney murine leukemia virus (MLV). Although differences exist between retroviruses, findings in MLV may further our understanding of RNA recruitment by other retroviruses, such as human immunodeficiency virus type 1 (HIV-1).

MLV recruits high levels of cellular noncoding mouse Y RNAs (mY RNAs), the RNA component of Ro ribonucleoproteins (Ro RNPs). In cells, Ro RNPs likely function in noncoding RNA quality control. The Ro60 protein is the main protein component of Ro RNPs. Ro60 knockout mouse embryonic fibroblasts (MEFs) contain ~30-fold less mY RNAs than wild type MEFs. Residual mY1 RNAs in Ro60 knockout MEFs were redistributed between the nucleus and cytoplasm, in contrast to the mostly cytoplasmic localization of mY1 RNAs in wild type MEFs. Suprisingly, virions from Ro60 knockout MEFs continued to package high levels of mY RNAs. Together, these data suggest that MLV recruits mY RNAs early in their biogenesis.

Work performed here also addressed where MLV genomic RNAs (gRNAs) are first recruited. Here, specific tetracycline-regulated repression of MLV expression produced a more rapid decline in gRNA packaging than virion production. This is consistent with previous actinomycin D studies, and it suggests that MLV unspliced RNAs bisect into non-equilibrating pools of mRNAs and gRNAs. Additionally, transcription inhibition increased the randomness of gRNA dimer partner associations

and recombination rates, with residual biases consistent with ongoing partitioning between mRNAs and genomes. These observations support a model of nuclear MLV gRNA dimerization that functions as an initial step in recruitment.

Work reported here also addressed how MLV gRNAs are first recruited. Mutations to the gRNA packaging signal (Ψ), which stabilize Ψ stem loops and disrupt dimerization and nucleocapsid (NC) binding *in vitro*, led to ~100-fold decrease in gRNA packaging in a tissue culture system. This supports an RNA switch mechanism whereby dimerization exposes high affinity NC binding sites that recruit the gRNA into assembling virions.

Overall, findings in this dissertation suggest that MLV initially recruits cellular mY RNAs and viral gRNAs from cell nuclei.

CHAPTER I

INTRODUCTION

Retroviruses are large ribonucleoproteins (RNPs) composed of viral proteins and both viral and cellular RNAs. The viral RNA component of the retroviral RNP is a pair of unspliced sense-stranded RNAs, which function as the retroviral genomic RNA (gRNA). Unspliced viral RNA also functions as mRNA in the production of Gag and Gag/Pol polyproteins, which constitute the protein components of the retroviral RNP. The cellular RNAs that are recruited into retroviral RNPs at levels in excess of their abundance in host cells are predominantly noncoding RNA Polymerase III transcripts (149). Why retroviruses package these cellular RNAs and the function of these RNAs in retroviral replication is largely unknown. This dissertation works towards this knowledge by attempting to uncover where viral and cellular RNAs are first recruited. Assembly of retroviral RNPs culminates at host cell membranes (41), but the recruitment of RNAs into subassembly RNPs may occur earlier (160).

Work performed in this dissertation addresses the question of where viral and cellular RNAs are first recruited by Moloney murine leukemia virus (MLV), where viral and cellular RNAs first become part of an MLV RNP. This dissertation also explores the mechanisms of how viral and cellular RNAs are incorporated into the MLV RNP. Chapter I is an overview of the MLV RNP and the current knowledge in the field that provided the foundation for our study of how and where MLV gRNAs and noncoding host cell mY RNAs are first recruited into the MLV RNP.

The MLV RNP

As mentioned above, retroviruses may be viewed as large RNPs. While retroviral particles represent a cell-free form of the retroviral RNP, this dissertation details our work on earlier subassembly forms of the retroviral RNP. In this context, this dissertation takes the view that retroviral recruitment of RNA is defined as the initial routing of RNA into a subassembly retroviral RNP that precedes budding and maturation into cell-free retroviral RNPs. The point of initial routing of RNAs into retroviral RNPs likely differs among retroviruses. The overall goal of this dissertation was to better understand where and how RNAs first become recruited into subassembly retroviral RNPs by one retrovirus, MLV. This dissertation describes our work on the initial recruitment of cellular non-coding Y RNAs and the unspliced MLV gRNA into the MLV RNP.

Prior to a discussion of background relevant to retroviral RNA recruitment and subcellular RNA trafficking, the following beginning sections will provide a brief overview of the main RNA and protein components that make up the MLV RNP.

MLV RNAs

MLV unspliced RNA is an 8.3 kb transcript that is capped and polyadenylated (184) (Fig. 1-1A). Sense-stranded MLV unspliced RNAs function as retroviral genomes (gRNA) and as mRNAs in the translation of retroviral proteins. Full length transcripts contain a *cis*-acting packaging signal, called psi (Ψ), downstream of the 5' splice donor (SD). The Ψ sequences mediate specific recruitment and incorporation into assembling virions (36) (Fig. 1-1A). The role of Ψ in gRNA dimerization, gRNA packaging, and

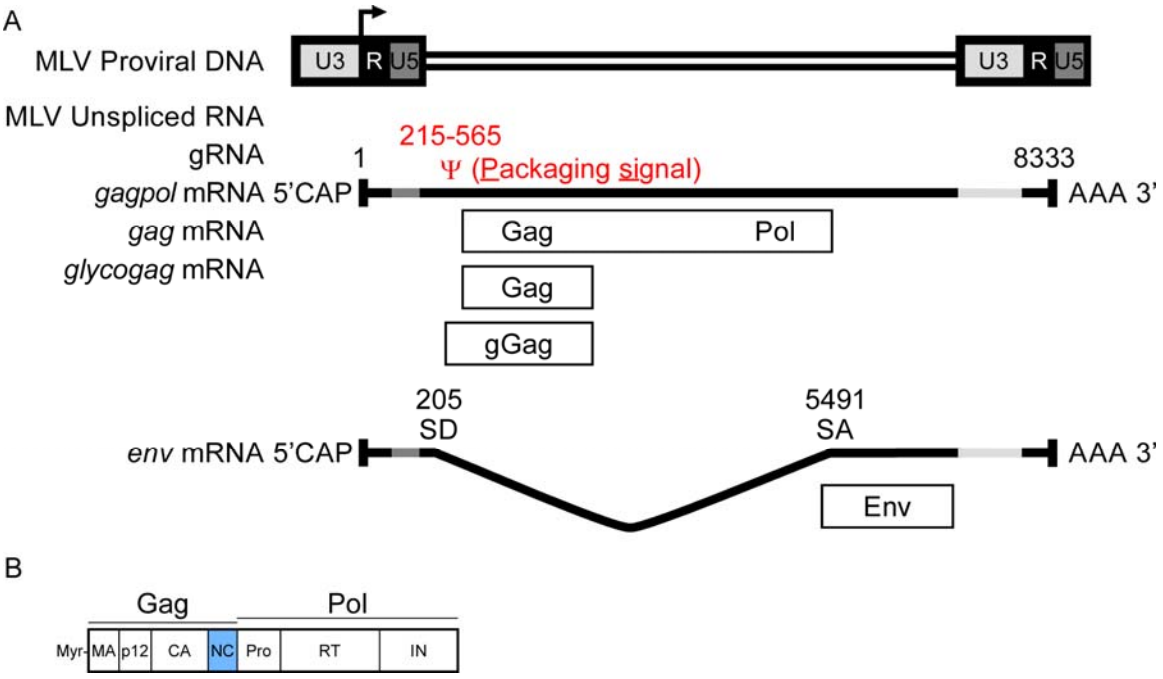

Figure 1-1. MLV RNAs and RNPs. (A) The main MLV RNAs are the unspliced RNA and spliced *env* mRNA. Locations are given for the "classic" Ψ (in red) and the splice donor (SD) and splice acceptor (SA). The arrow indicates the start of transcription of viral RNAs by RNA polymerase II at the 1st base of the 5' R (direct repeat). The provirus long terminal repeats at either end contain U3 (3' unique) and U5 (5' unique) sequences which are shaded in the lines that represent the RNA transcripts. The protein products of the MLV unspliced RNA are listed below the RNA: Gag/Pol, Gag, and glycosylated or glyco-Gag (gGag). Gag is an acronym for group-specific antigen and Pol refers to the polymerase proteins. The protein product of the spliced *env* transcript is also shown – Env (envelope). (B) The proteolytic products of Gag/Pol and the amino-terminal myristate (Myr). Listed domains are: matrix (MA), the p12 late domain, capsid (CA), nucleocapsid (NC) (shaded blue), protease (Pro), reverse transcriptase (RT), and integrase (IN). The drawing is not to scale.

unspliced RNA trafficking are discussed in greater detail in subsequent sections of this Chapter.

Subgenomic RNAs also function in MLV replication. Splicing and removal of the Ψ-containing sequences produces a subgenomic transcript for *env* which codes for the MLV ecotropic envelope glycoprotein (Fig. 1-1A). Alternative splicing also produces low levels of a 4.4 kb Ψ-containing subgenomic transcript (40). An alternative SD site, termed SD', in the capsid sequence of *gag* is spliced to the same splice acceptor SA that produces the *env* transcript (40). This alternative splice product is present at approximately 8% of full length unspliced transcript levels (83). Because it includes Ψ, this alternative splice product is packaged relatively efficiently at ~5% of the levels of full length transcript (83). The alternative splice product is capable of forming heterodimers with the full length MLV unspliced RNA, which may affect packaged gRNA dimer populations and recombination (120).

MLV ribonucleoproteins.

The full length MLV unspliced RNA is translated into Gag/Pol, Gag, and glyco-Gag (27) (Fig. 1-1A). Readthrough of an amber UAG stop codon, which occurs about 5% of the time, produces the Gag/Pol polyprotein (27). Rare use of a CUG codon upstream of the Gag AUG start codon produces a larger glycosylated form of Gag, called glyco-Gag, whose function in MLV replication is not fully understood (47), but recent observations suggest a function in viral release through lipid rafts in the plasma membrane (140). The p12 late domain of Gag functions in the release of budding virions from the host cells (41). After budding from host cells, proteolytic maturation of MLV Gag and Gag/Pol produces the MLV cleavage proteins. Cleavage of Gag yields matrix

(MA), the p12 late domain, capsid (CA), and the nucleocapsid (NC) protein (Fig. 1-1B and Fig. 1-2). MLV Pol is cleaved to the enzymatic proteins: protease (Pro), reverse transcriptase (RT), and integrase (IN) (Fig. 1-1B and Fig. 1-2). As mentioned above, spliced-*env* mRNA is translated into the MLV ecotropic envelope glycoprotein.

As part of the Gag polyprotein, the RT and NC domains function in the recruitment of RNAs into virions, and therefore, they likely nucleate formation of the retroviral RNP. RT functions in the incorporation of $tRNA^{Pro}$ (109, 110) which primes minus strand DNA synthesis during reverse transcription. NC has nucleic acid chaperone functions, and it likely participates in both specific and nonspecific RNA incorporation into virions (170). Human immunodeficiency virus type 1 (HIV-1) minimal virus-like particles (VLPs) (1), where NC is replaced with a leucine zipper, reportedly appear to be devoid of RNA (30); however, ongoing studies in our lab indicate that the host cell RNA 7SL is packaged but processed within the VLP (Keene and Telesnitsky, *in preparation*). These VLPs lack the NC domain but retain the carboxy terminal domain of CA-p2 and a P-P-P-P-Y late domain motif (P, proline and Y, tyrosine) (1). This suggests that, in addition to NC and RT, the CA domain of Gag may function in the incorporation of RNA into assembling virions. RNA, but not necessarily viral RNA, is necessary for retroviral assembly (132).

Co-packaged host cell RNAs

MLV selectively recruits a number of host cell noncoding RNAs (149). Among the cellular noncoding RNAs most highly packaged by MLV are $tRNA^{Pro}$, U6 snRNA, 7SL RNA, and the mY RNAs (149). The $tRNA^{Pro}$ serves to prime minus-strand DNA synthesis in MLV (113), and it is packaged in an RT-dependent manner (109). The

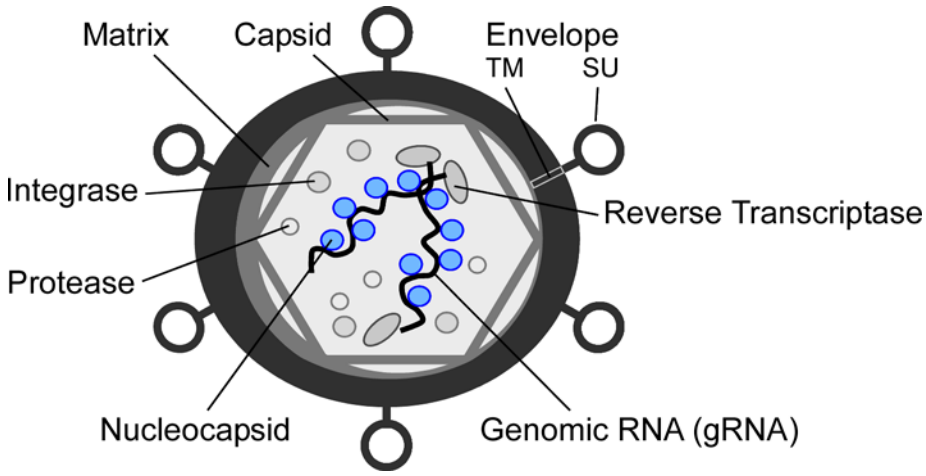

Figure 1-2. Diagram of mature MLV virion. MLV proteins are represented and labeled in the virion. The genomic RNA (gRNA) dimer is represented by the black squiggly lines in the center of the particle. Where the two gRNAs intersect is a representation of the dimer linkage site between the two sense stranded gRNAs. The dark gray outer circle depicts the lipid envelope that the virion acquires while budding from the cell's plasma membrane. The loops on the outside of the virus represent the MLV Env which is cleaved by the host protease, furan, into a surface unit (SU) and a transmembrane domain (TM), which is outlined in white. Co-packaged host cell RNAs are not represented in this figure, and the dimeric RNA genome is stylized to depict the dimer linkage near the 5' end. In the virion, the long gRNA is more likely wrapped like the "inside of a baseball" within capsids. The drawing is not to scale.

functions and manner of recruitment of other noncoding RNAs in MLV replication are relatively unknown.

MLV packages about one copy per virion of noncoding U6 snRNAs (149). Selective packaging of U6 snRNAs has also been reported in Rous sarcoma virus (RSV) (67) and HIV-1 (84). U6 snRNAs function in cells in the formation of the spliceosome and in the splicing of pre-mRNAs (208). U6 snRNAs form an initial snRNP with U4 RNAs in the host cell nucleus (4). Although U6 snRNAs are localized to and function in the host cell nucleus, they are recruited at high levels into MLV particles (149) which assemble and bud from the cell's plasma membrane (41, 179). This suggests that these RNAs are recruited into a subassembly viral RNP earlier in their biogenesis.

One of the most highly packaged noncoding RNAs by MLV is 7SL RNA (149). 7SL RNA is packaged into MLV particles in proportion to retroviral proteins (149, 174). As the RNA component of cellular signal recognition particles (SRP), 7SL RNA functions in the trafficking of nascent polypeptides to the endoplasmic reticulum (89). Packaging of 7SL has been observed in other retroviruses including RSV (16) and HIV-1 (150). In HIV-1, 7SL RNA is incorporated without the cellular 54 kd SRP protein (150). This suggests that 7SL may be recruited into retroviral particles from a pool of RNAs that are not associated with the 54 kd SRP protein and perhaps other SRP proteins.

High levels of the cellular mY1 and mY3 RNAs are recruited into MLV particles (149). In cells, mY RNAs are in RNPs with the Ro60 host cell protein, and they likely function together in the recognition and quality control of misfolded RNAs (24, 142, 171, 197). Y RNAs localize with the Ro60 protein to the host cell cytoplasm (141, 156). HIV-1 virions package lower levels of Y RNAs than MLV. However, one study used

RT-PCR analysis to demonstrate increased packaging of hY1, hY3, and hY4 in Ψ^- HIV-1 particles with decreased gRNA packaging, compared to Ψ^+ particles (91). This suggests that retroviral recruitment of Y RNAs may intersect with how retroviral genomic RNAs are recruited by the virus.

MLV replication cycle

MLV replicates its RNA genomes via proviral DNA intermediates (Fig. 1-3). The early steps of the viral replication cycle involve attachment of virions and entry of viral RNP components into host cells, immediately followed by reverse transcription to generate retroviral DNA from the RNA genome, translocation of the DNA to host cell nuclei, and integration into cellular chromosomes to form a provirus (Fig. 1-3). The late events of MLV replication begin with transcription of the unspliced MLV RNA (Fig. 1-3). MLV unspliced RNAs are exported out of the nucleus and function as mRNAs in the translation of retroviral proteins and as gRNAs that are recruited into assembling virions (Fig. 1-3). MLV assembly takes place at the host cell's plasma membrane. After budding from host cells, MLV virions undergo proteolytic maturation whereby the Gag and Gag/Pol polyproteins are cleaved by the viral protease into their constituent proteins (Fig. 1-3).

Mechanism of MLV gRNA recruitment

Retroviral RNAs are recruited in pairs, and this suggests that the mechanism for recruitment is coupled with RNA pair associations. All retroviruses except the spumaretroviruses package two gRNAs (36). Where retroviral gRNAs form dimer partner associations likely varies among retroviruses. However, the manipulation of *cis*-

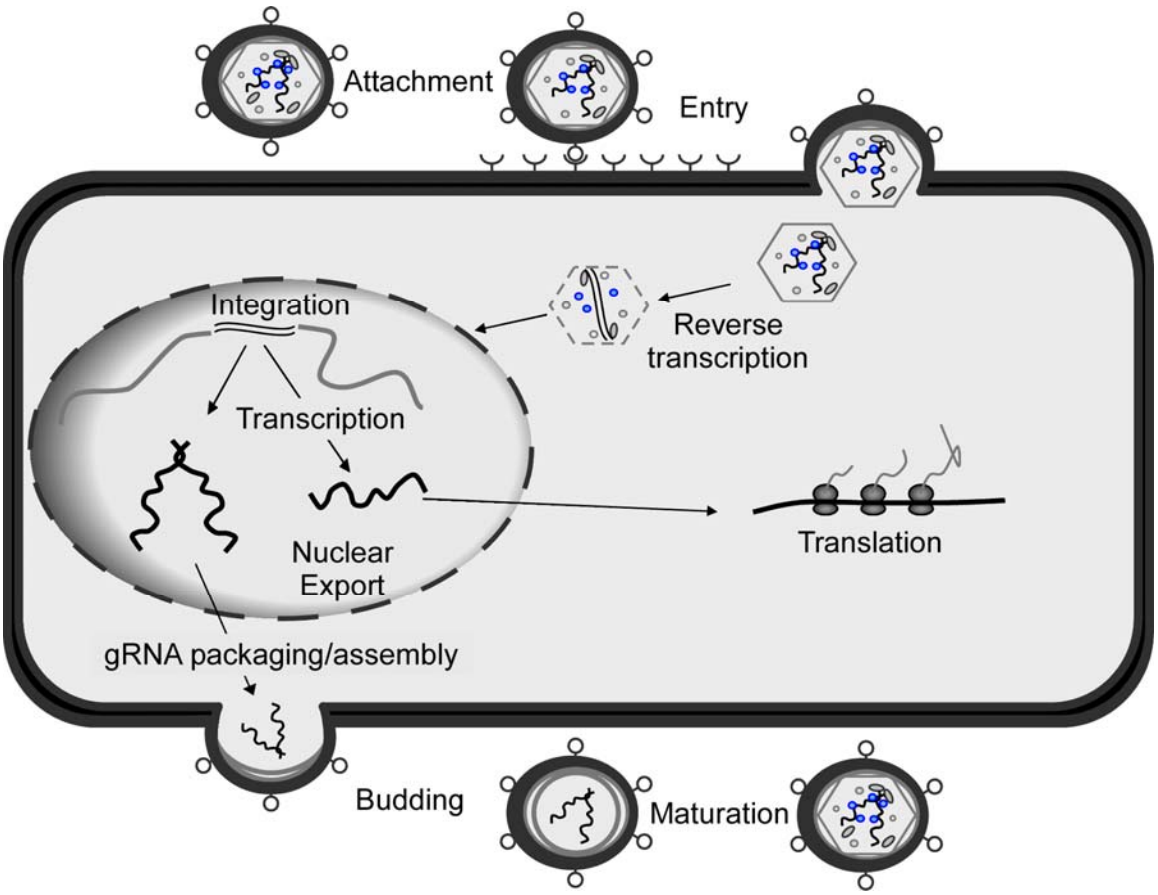

Figure 1-3. MLV replication cycle. The main steps of the MLV replication cycle are designated with particular focus on the unspliced viral RNA. Early events span attachment through integration. Late events, which are the focus of this dissertation, begin with transcription and culminate in a mature MLV particle. The diagram depicts the two main functions of MLV unspliced RNA, mRNA for translation and gRNA for packaging. The diagram of the replication cycle also depicts one of the main hypotheses tested in this dissertation, that MLV gRNAs form nuclear dimer partner associations. These nuclear gRNA dimer partner associations may function to partition MLV unspliced RNAs into separate pools of dimeric gRNAs and monomeric mRNAs. The focus of all of the work presented in this dissertation is on the events of viral RNP formation, from transcription through budding and maturation. In the context presented here of MLV as a retroviral RNP, the replication cycle depicts how MLV is a dynamic complex of nucleic acids and proteins. The mature virion is, therefore, only one form of the dynamic MLV RNP. Arrows within the cell indicate nucleic acid pathways required for MLV replication.

acting sequences involved in dimer initiation affects the frequency of heterodimer co-packaging and recombination, which suggests that gRNA dimerization likely precedes packaging (123, 127, 165). This, possibly weak (193), initial association becomes more stable after budding from the host cell and virion maturation (58, 81). Reflecting the link between gRNA dimerization and packaging, MLV gRNA sequences that are involved in dimer initiation and packaging are located in the 5' UTR within Ψ.

MLV cis-acting gRNA packaging elements

Cis-acting sequences that function in unspliced gRNA packaging are located within the 5' UTR of MLV unspliced RNA (168). A deletion of ~ 350 bases (b) in the 5' UTR abrogates MLV gRNA packaging (115), and relocation of these sequences to the 3' end of MLV RNAs or heterologous RNAs confers packaging into MLV particles (2, 114). This region is referred to here as the "classic" Ψ. A smaller segment of 64 b within the "classic" Ψ region has been demonstrated to be sufficient to confer packaging of heterologous RNA, and it has been termed the core encapsidation signal (CES) (bases 310 to 374, which includes SL-C and SL-D) (Fig. 1-4A) (129). While the CES is sufficient to achieve packaging of heterologous RNAs, the inclusion of downstream sequences that encompass the full "classic" Ψ and continue into sequences in the 5' portion of *gag* leads to increased titers of gene transfer vectors, which suggests that this region functions as an extended packaging signal (sometimes referred to as Ψ^+) (10, 153). The relatively efficient packaging of a MLV cryptic splice product that lacks the "classic" Ψ region has provided additional support for the function of sequences surrounding the "classic" Ψ in RNA packaging (153). Finally, a small stretch of 17 b downstream of the *env* stop codon also appears to function in RNA packaging, as a

deletion of these bases leads to a 10-fold decrease in titer and a 20- to 30-fold decrease in gRNA packaging (227).

MLV gRNA dimerization

The MLV dimer linkage site (DLS) is located near the 5' end of MLV gRNA dimers (74). Retroviral DLS linkages are visible in virion-extracted RNA dimers by electron microscopy (11, 100, 112, 134). The same *cis*-acting Ψ sequences above which have demonstrated functions in packaging also function in gRNA dimerization. *In vitro* transcribed Ψ sequences spontaneously form dimers at high concentrations in a NaCl-dependent manner, and purified NC can catalyze this RNA dimerization *in vitro* (154, 162). Computer predictions, phylogenetic analysis, chemical accessibility mapping, and mutagenesis have lead to a secondary structure model of stem loops that make up the MLV Ψ (Fig. 1-4A) (3, 97, 206). Nucleotides (nts) 204 to 228 and 283 to 298 function as a bipartite signal in MLV gRNA dimer initiation and are called DIS-1 and DIS-2, respectively (Fig. 1-4A) (111). MLV gRNA dimerization initiates through intermolecular base pair "kissing" interactions between DIS loops on separate gRNAs (Fig. 1-4B) which likely precede the formation of more stable intermolecular interactions in an extended dimer interface (Fig. 1-4C) (58, 111).

MLV NC function in gRNA recruitment

The MLV NC domain of Gag functions in the recruitment of MLV gRNAs (168). The importance of NC in MLV unspliced gRNA recruitment was first demonstrated by mutations in NC, and specifically the zinc finger domain of NC, that disrupt viral infectivity and gRNA packaging (72, 121). NC binds with high affinity to Py-Py-Py-G sequences (Py, pyrimidine and G, guanosine) within the MLV Ψ region (36, 42). In the

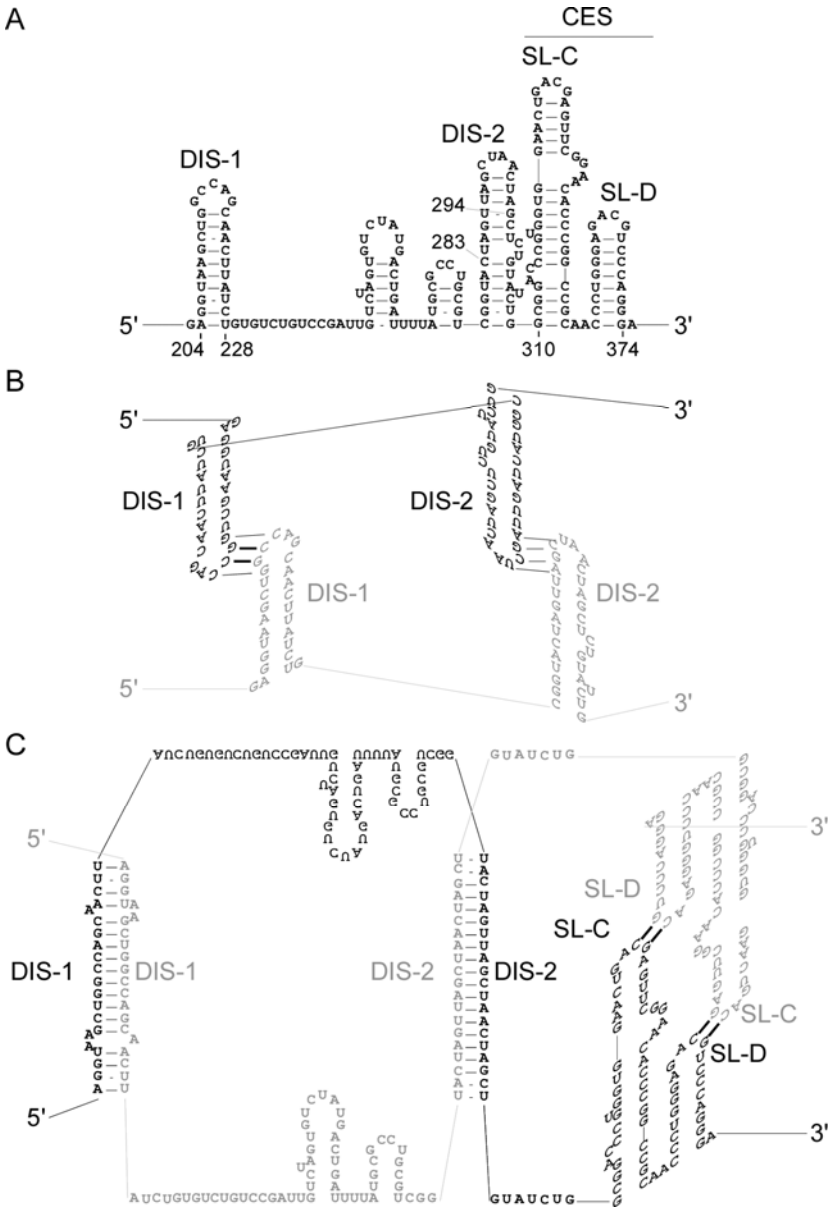

Figure 1-4. MLV Ψ – kissing complex and extended dimer. (A) The secondary structure of Ψ-associated stem loops with designations for the stem loops that have demonstrated functions as sites of dimer initiation (DIS-1 and DIS-2) and as a core encapsidation signal (CES)(SL-C and SL-D). (B) Horizontal lines in the center indicate intermolecular base pair "kissing" interactions that function in dimer initiation between separate gRNAs (black and gray) *Adapted from Ly and Parslow* (111). (C). Depiction of a more thermostable "extended" dimer structure. Lines indicate predicted structure stabilizing intermolecular "kissing" interactions between SL-C and SL-D stem loops on separate gRNAs that stabilize the "extended" dimer structure. *Adapted from Miyazaki et al.* (124).

context of full length Gag, a yeast three-hybrid study of MLV RNA-protein interactions suggests that the complete MLV RNA sequence from DIS-1 thru SL-D is important for strong Gag-RNA interactions (50). Further inferences from NMR structural observations of NC-RNA interactions suggest that MLV RNA dimerization may function to switch the RNA into a conformation that exposes high affinity NC binding sites on the dimeric RNA (34, 36, 37). In this manner, MLV gRNA dimerization functions as an RNA switch into a packaging-competent RNA fold (36).

Subcellular location of initial retroviral gRNA recruitment

Different retroviruses likely recruit gRNA from different subcellular locations. The *cis*-packaging of Line-1 retroelements (99, 214) and HIV-2 unspliced RNAs (76, 88) likely reflects a cytoplasmic point of initial recruitment from a microdomain near sites of translation. HIV-1 unspliced RNAs can be packaged in *trans* which suggests the potential for recruitment from a cellular site distinct from translation (88). A portion of RSV Gag molecules have been observed to traffic through the host cell nucleus and disrupting this trafficking impairs gRNA packaging (64), which suggests the potential for initial gRNA recruitment from the nucleus (176).

Retroviral unspliced RNA response to actinomycin D

Studies using actinomycin D (ActD) as a general transcription inhibitor have revealed differences in viral unspliced RNA sorting as mRNA or gRNA by different retroviruses. ActD treatment of MLV producing cells leads to a more rapid decline in packaged MLV gRNAs than virion-producing mRNAs, which suggests that MLV gRNAs and mRNAs exist in separate non-equilibrating pools (122). Hence, MLV gRNAs are likely recruited from sites distinct from sites of translation.

In contrast, HIV-1 and HIV-2 packaged gRNA levels decline at a similar rate as intracellular viral mRNA after ActD treatment, which suggests a single pool of viral unspliced RNAs (43). Similar to HIV-1 and HIV-2, ActD treatment of RSV producing cells leads to similar rates of decline in packaged gRNA and intracellular viral RNA (198); however, competition between Gag and ribosomes for an RNA structure upstream of RSV *gag* suggests that Gag autogenously regulates whether an RNA is encapsidated or translated (194). Thus, the location of RSV gRNA initial recruitment may vary as a function of intracellular Gag concentrations.

Cellular response to general transcription inhibition with ActD

General transcription inhibition with ActD has provided insights into retroviral RNA trafficking, but ActD can have indirect effects on cellular physiology and RNA trafficking. These indirect effects may lead to the observed differences in retroviral responses to general transcription inhibition with ActD. Used as a general transcription inhibitor, ActD can cause global changes in cellular physiology that lead to apoptosis (69, 95).

ActD can also have more specific off target effects on RNA trafficking which are well documented. General transcription inhibition with ActD disrupts the stability of cytoplasmic mRNA processing bodies (P bodies) (29), (212), reviewed in (49). P bodies are sites of mRNA decay and are therefore dependent on RNA availability (5, 29, 182, 202), reviewed in (49). Cougot et al. (29) used GFP fusion proteins to show that decapping-enzyme subunit hDcp1a-containing bodies disappear after treatment with ActD in HEK293 cells. The indirect disruption of P bodies by ActD transcription

inhibition was also observed by Wang et al. (212) in 293T cells by indirect immunofluroescense for the P body marker DDX6 (RCK/p54), a decapping co-activator.

ActD has also been shown to indirectly alter nuclear import of the influenza viral nucleoprotein and the nuclear-cytoplasmic shuttling of a number of cellular proteins. Transcription inhibition by ActD disrupts the nuclear translocation of incoming viral RNPs from influenza virus as measured by *in situ* hybridization for vRNA and indirect immunofluorescence for the virion nucleoprotein (209). In addition, GFP-protein fusions and indirect immunofluorescence have been used to show that ActD disrupts the normal nuclear-cytoplasmic trafficking of cellular proteins. Human-mouse heterokaryon experiments have shown that ActD treatment accelerates the nuclear-cytoplasmic shuttling of a heterogeneous nuclear ribonucleoprotein (hnRNP), the polypyrimidine tract binding protein (PTB/hnRNP I) (86). PTB reached equilibrium between mouse and human nuclei faster when Pol II and Pol III transcription were disrupted, which suggests that RNA binding is not necessary for PTB nuclear export and that RNA binding slows its nuclear export and subsequent import (86).

General transcription inhibition with ActD was used to classify whether the nuclear transport of other hnRNPs is dependent on or independent of transcription (159). The hnRNP proteins A1, A2, B1, B2, E, H, and L are abnormally retained in the cytoplasm after transcription inhibition (159). ActD also induces the cytoplasmic accumulation of JKTBP1 and JKTBP1Δ6 hnRNPs in HeLa cells (87). Therefore, their transport to the nucleus may be classified as transcription-dependent (159). In contrast, hnRNP C retains nuclear localization after transcription inhibition (159). Hence, its nuclear localization was classified as transcription independent (159).

Random and nonrandom retroviral gRNA dimer populations

The packaged gRNA dimer populations that result from co-expression studies also reveal differences among retroviruses, which also suggest different sites of initial gRNA recruitment. Our lab and others have demonstrated that co-expressed HIV-1 gRNAs randomly associate (53, 127). In combination with the observations of HIV-1 unpsliced RNAs post ActD treatment mentioned above, this suggests recruitment from a single pool of unspliced RNAs in the host cell cytoplasm. The random association of gRNAs expressed from separate nuclei in a cell fusion assay further supports this notion of cytoplasmic initial recruitment for HIV-1 gRNAs (126).

Co-expressed MLV gRNAs exhibit preferential self association, which supports an earlier point of initial gRNA recruitment for MLV than HIV-1 (53, 92, 166). Consistent with this hypothesis, MLV gRNAs that were expressed from a single nuclear locus formed dimer partner associations randomly (54). In combination with the observations of MLV unspliced RNAs post ActD treatment, these data suggest that MLV unspliced RNAs are subject to nuclear dimer partner associations that function in the bisection of MLV unspliced RNA to function as dimeric gRNAs or monomeric mRNAs.

Differences between HIV-1 and MLV in the randomness of gRNA dimerization are also reflected in differences between the two viruses in the levels of recombination in co-expression recombination assays (52, 151, 228). HIV-1 recombination is about ten-fold more frequent than MLV recombination (147). Onafuwa et al. (151) demonstrated that HIV-1 and MLV RT enzymes had similar rates of template switching, and thus could not account for differences in recombination. Rather, the differences in recombination could be fully accounted for in differences between HIV-1 and MLV in the levels of

heterozygous RNA co-packaging (52, 228). Therefore, levels of recombination also reflect the location of dimer pair formation and initial gRNA recruitment.

Intracellular RNA trafficking

How might MLV unspliced RNAs navigate out of the nucleus and through the cytoplasm to sites of assembly on the plasma membrane? Retroviruses use different cellular pathways to traffic gRNAs to sites of assembly and budding. The aforementioned studies of MLV, which support nuclear gRNA dimer partner associations, suggest that MLV gRNAs move rapidly and directly through the nucleus to sites of assembly on the plasma membrane. Much remains unknown about how MLV gRNAs translocate from the nucleus to the plasma membrane.

The remaining portion of Chapter I, before the dissertation overview, details how other retroviruses navigate viral unspliced RNA out of the nucleus and through the cytoplasm. The limited evidence for MLV unspliced RNA intracellular trafficking is also presented in this context. One of the first steps in the path of gRNA trafficking to sites of assembly is nuclear export. In order to navigate this trafficking step, retroviruses have evolved different mechanisms to hijack host cell machinery.

Cellular mRNA nuclear export

The nuclear export of most cellular mRNAs depends upon both 5'-cap addition and splicing (90). During transcription, nascent transcripts are bound by hnRNPs which function in various steps in the life of the mRNA, including nuclear export (18). Some hnRNPs, like the hnRNP A/B family, shuttle with the mRNA to the cytoplasm, and other hnRNPs, like the large hnRNP K, are retained in the nucleus (45). The first processing step in the life of a nascent pre-mRNA is the addition of a 7-methylguanosine cap to the

5’ end (181). This is followed by splicing which deposits a set of proteins on the mRNA termed the exon junction complex (EJC) (18). In higher eukaryotes, both the 5’-cap and the EJC function in the recruitment of the transcription and export (TREX) complex (18, 90). TREX is comprised of the THO complex (a transcription elongation complex) and other accessory molecules which include UAP56 and Ref/Aly (18). In spliced mRNAs, the THO complex interacts with hnRNPs and EJC components that recruit UAP56, which then recruits Ref/Aly (18). The non-karyopherin heterodimer Nxf1:Nxt1 displaces UAP56 and shuttles the mRNA out of the nucleus through the nuclear pore complex (NPC) (18).

In the nuclear export of some unspliced cellular mRNAs, THO complex proteins and other hnRNPs recruit UAP56 in the absence of EJC components (18). As with spliced mRNAs, UAP56 recruits Ref/Aly (18). The Nxf1:Nxt1 nuclear export factor then displaces UAP56 and traffics the RNA out of the nucleus (18). Ref/Aly function has been demonstrated in the export of unspliced histone H4 mRNAs (173). Like unspliced histone H4 mRNAs, unspliced retroviral RNAs that use this pathway must circumvent the requirement for EJC proteins which are deposited during splicing, as described below.

Subsets of cellular mRNAs use the karyopherin Crm1/Xpo1 to traffic out of the nucleus (18). This process requires the binding of adapter proteins to mRNAs because Crm1 lacks RNA binding activity (18). Potential adapter proteins have been discovered for a few cellular mRNAs that traffic via Crm1, including HuR for the nuclear export of spliced *Cd83* and unspliced c-*fos* mRNAs (18). HuR interacts with adenosine/uridine-rich elements (AREs) in these mRNAs. The coordination of specific adapters with different transcripts likely represents another level of nuclear export regulation. For the

unspliced retroviral RNAs that use this pathway, viral adapter molecules coordinate Crm1 binding and nuclear export.

Chapter II of this dissertation addresses an intersection in MLV replication with a host cell noncoding RNA quality control pathway and mY RNA biogenesis (Fig. 1-5). Prior to an introduction of retroviral mechanisms of nuclear export, the following section details the current knowledge in the field of cellular Y RNA biogenesis and nuclear egress.

Cellular Y RNA nuclear export.

Cellular Y RNAs are RNA polymerase III transcripts whose nuclear export likely differs from how cellular mRNAs are exported from the nucleus. Studies of human hY RNAs have identified sequences in the stems of the hY hairpins which function in the nuclear export of the RNAs (175, 188). After transcription, Y RNAs are bound by the cellular protein La which recognizes 3' terminal UUU-OH sequences (Fig. 1-5) (33, 156, 218). Subsequent to La binding, Y RNAs are bound by the Ro60 protein (Fig. 1-5B) (164). Ro60 binds to the stem of Y RNAs near the 3' and 5' ends (Fig. 1-5A) (220). Ro60 accelerates Y RNA nuclear export, but La has the opposite effect and slows export of Y RNAs (Fig. 1-5B) (188). Y RNA-La binding is thought to be more stable than other noncoding RNA-La interactions (164), and it is not fully known when 3' end maturation of Y RNAs takes place. Y RNAs mask a nuclear retention signal on Ro60, and Ro60 and Y RNAs translocate together as an RNP to the host cell cytoplasm (Fig. 1-5B) (188). Competition of adenoviral VA1 RNAs with hY RNAs for nuclear export has provided evidence that Y RNAs are exported from the nucleus by the RanGTP-dependent nuclear

export factor exportin-5 (79, 80). Thus, Y RNAs shuttle out of the nucleus using a separate pathway than the pathway used for bulk cellular mRNA nuclear export.

Retroviral unspliced RNA nuclear egress.

Different retroviruses use different cellular pathways to translocate their unspliced RNA out of the nucleus. Mason Pfizer monkey virus (M-PMV) uses an RNA sequence termed the constitutive transport element (CTE) to affect nuclear export (155). The CTE binds directly to the cellular nuclear export factor Nxf1 (32, 78). Together, the M-PMV unspliced RNA and Nxf1 are shuttled out of the nucleus (32). Simian retroviruses type 1 (SRV) also use a CTE to export unspliced RNA via Nxf1 (78, 201, 229). This mode of export entails direct binding of cellular export machinery to RNA elements in retroviral unspliced RNAs.

Other retroviruses use viral accessory proteins as adapters that join retroviral unspliced RNA and cellular RNA export proteins. Human immunodeficiency virus type 1 (HIV-1) uses the viral Rev protein to export its unspliced RNA from the host cell nucleus (31). Rev localizes to the nucleus after translation and binds to a Rev response element (RRE) on HIV-1 unspliced RNAs (31). Rev recruits Crm1 to transport the RNA out of the host cell nucleus (138). Binding of hnRNP A2 to A2-responsive elements also appears to function in Rev-dependent Crm1 nuclear export of HIV-1 unspliced RNA (131). Other viruses that use the Crm1 nuclear export pathway encode similar adapters. For example, human T-cell leukemia virus type 1 and type 2 (HTLV-1 and -2) encode the Rex adapter which mediates Crm1 export of RxRE-containing HTLV unspliced RNAs (66, 167, 196).

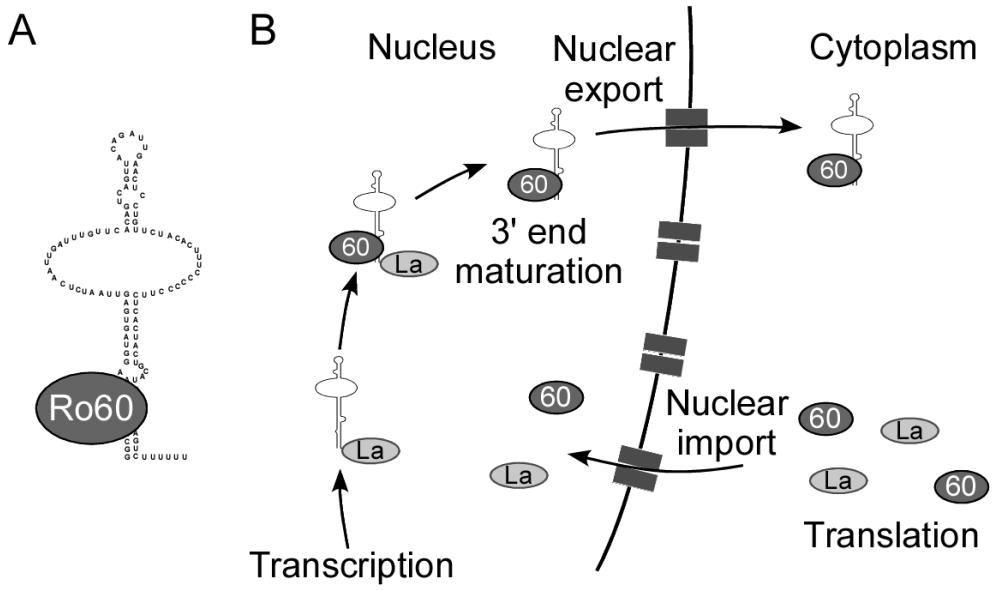

Figure 1-5. Model of Y RNA biogenesis. (A) A secondary structure model of mY1 RNA with the Ro60 protein bound to the stem of the mY1 RNA near the 5' end and the 3' uridylate tail. (B) Model for mY1 RNA biogenesis. Y RNAs are Pol III transcripts which are bound by La and subsequently by Ro60 in the nucleus. Y RNAs mask a nuclear retention signal on the Ro60 protein and translocate with the Ro60 out of the host cell nucleus. In cells, most Y RNAs reside in RNPs with the Ro60 protein in the cytoplasm. *(B) was adapted from the model of Pruijn et al.* (164).

A portion of Rous sarcoma virus (RSV) Gag molecules traffic through the nucleus en route to sites of assembly, and this may represent a retroviral example of nuclear Gag-gRNA recruitment (176). RSV Gag is transported out of the nucleus via the Crm1 pathway (176, 178). Disruptions to RSV Gag trafficking through the nucleus impair gRNA packaging, which suggests that gRNAs exit the nucleus with Gag via the Crm1 pathway (64). First, however, some RSV unspliced RNA must exit the nucleus to function as mRNA in the translation of Gag. Several studies suggest that two direct repeats (DRs) which flank the 3' *src* gene of RSV function in nuclear export of RSV unspliced RNA (145, 146, 189, 224). Using a RSV DR reporter construct, Leblanc et al. (103) demonstrated that this mode of RNA export likely occurs via Nxf1 and the DEAD box RNA helicase Dbp5. This mode of nuclear export was independent of Gag (103). Speculatively, this suggests that RSV unspliced RNAs which function as mRNAs and gRNAs may traffic out of the nucleus via separate cellular pathways. However, the low level packaging of RSV unspliced RNAs with premature termination codons (PTCs) suggests that at least some RSV RNAs may first be translated (102).

The pathway MLV uses to traffic its unspliced RNA out of the nucleus is unknown, but sequences in the 5' UTR, including portions of Ψ, may function in this process. In the SL3 strain of MLV, mutations to a stem loop in the 5' R region impaired the cytoplasmic accumulation of full length transcripts, but not the accumulation of spliced *env* transcripts (207). Fusing the 5' UTR to a reporter, Trubetskoy et al. (207) showed that mutation of this R region stem loop (RSL) led to a two-fold decline in intron-containing reporter expression but a greater than ten-fold decline in intronless reporter expression. This suggests that the RSL may function in nuclear export of MLV

SL3 unspliced RNAs which function as mRNAs. However, gRNA packaging was not addressed in these experiments.

In addition to the RSL, the RNA stem loops associated with MLV Ψ may contribute to MLV unspliced RNA nuclear export. Placing the MLV Ψ signal within an HTLV-1 expression cassette led to Rex independent reporter expression, which suggests that sequences in Ψ provided a nuclear RNA export function (94). With minimal MLV Ψ constructs that contain flanking SD and SA sites, Ψ stem loops associated with dimerization and packaging increase cytoplasmic levels of unspliced RNAs relative to spliced RNAs in comparison to an RNA lacking these stem loops (192). Also, minimal Ψ-containing RNAs appear to compete with full length MLV unspliced RNAs for nuclear export as reported in a co-expression study (192). With fluorescent in situ hybridization (FISH) of tagged MLV unspliced RNAs, Basyuk et al. (7) showed that deletions of individual Ψ stem loops disrupted nuclear export of the tagged MLV unspliced RNAs. Together these data suggest that MLV Ψ may function in nuclear egress of MLV unspliced RNAs.

The mode of nuclear export used by retroviral unspliced RNAs can affect viral assembly and gRNA sorting. Changing the mode of HIV-1 nuclear export from the Crm1 pathway to the Nxf1 pathway relieves the restriction of HIV-1 assembly in murine cells (200). Also, co-expressing HIV-1 gRNAs that either use Crm1 or Nxf1 for nuclear export decreases levels of recombination between the two co-expressed gRNAs (128). These observations suggest that the mode of nuclear export affects downstream functions of retroviral unspliced RNAs and partitioning within the cytoplasm.

Retroviral cytoplasmic unspliced RNA trafficking

Different retroviruses use different mechanisms to sort and regulate the trafficking of their unspliced RNA within the host cell cytoplasm. Trafficking of retroviral unspliced RNAs to microdomains within the cytoplasm can regulate whether the RNA functions as gRNA or mRNA. Retroviruses can co-opt cellular cytoplasmic trafficking machinery to move viral unspliced RNA to different microdomains within the cytoplasm (199).

A perinuclear/pericentriolar area termed the microtubule-organizing center (MTOC) may represent a cytoplasmic microdomain where M-PMV and HIV-1 gRNAs are routed while trafficking to sites of assembly (135, 199). A cytoplasmic targeting-retention signal (CTRS) in M-PMV MA traffics nascent Gag molecules to the MTOC (180). Sfakianos et al. (180) observed ribosomes and polyribosomes in the vicinity of assembling immature capsids at the MTOC. Also, cycloheximide treatment depleted Gag localization at the MTOC more rapidly than nocodazole treatment, which suggests that Gag translation is ongoing at the MTOC (180). Together, these data may suggest that M-PMV has a *cis*-packaging preference for gRNAs at the MTOC.

HIV-1 RNAs do not exhibit a *cis*-packaging preference, but confocal microscopy observations of fluorescence energy transfer (FRET) between HIV-1 Gag molecules and HIV-1 unspliced RNAs at the MTOC suggest that this may represent the site of initial recruitment of HIV-1 gRNAs during assembly (160). HIV-1 unspliced RNA trafficking to and from the MTOC appears to be partially regulated by hnRNP A2, as knockdown of this cellular hnRNP results in the rapid nuclear export and accumulation of HIV-1 unspliced RNAs at the MTOC (106).

Cytoplasmic mRNA processing bodies (P bodies) may function as another microdomain in retrovirus unspliced RNA cytoplasmic trafficking. P bodies are sites of RNA storage and 5' to 3' RNA degradation (49, 118). Yeast Ty3 RNAs, proteins, and VLPs co-localize with P body proteins, and knockout of P body proteins decreases Ty3 retrotransposition (9). This suggests that Ty3 uses this cytoplasmic RNA quality control pathway as a microdomain for assembly and RNP formation. Retroviruses might use P bodies or P body proteins to stall translation and re-route unspliced RNAs towards sites of assembly and packaging.

How MLV gRNA navigates through the cytoplasm is relatively unknown, but one study has reported MLV gRNA trafficking on endosomal vesicles (8). Basyuk et al. (8) used live cell imaging of MS2-GFP bound to MS2-binding site-containing MLV RNAs to show colocalization of these RNAs with transferrin-positive endosomes. This localization required both Gag and Env proteins (8). This suggests that vesicular trafficking may function in the movement of MLV RNPs to sites of assembly at the plasma membrane, and may therefore represent a subassembly microdomain in MLV replication.

The localization of retroviral proteins and RNAs to and from cytoplasmic microdomains suggests retroviruses co-opt microtubule motor proteins to move viral RNP cargos throughout the cell. Knockdown of the microtubule plus-end-directed kinesin motor protein KIF4 disrupts HIV-1 particle production, slows cytoplasmic trafficking of Gag, and leads to increased Gag degradation (117). Upon Kif4 knockdown, Gag colocalized with a perinuclear marker which has also been shown to colocalize with M-PMV Gag (117, 215). This suggests that the KIF4 microtubule motor protein may

function in cytoplasmic HIV-1 Gag trafficking. A yeast two-hybrid screen revealed a carboxy-terminal KIF4-MLV Gag interaction that was also demonstrated by *in vivo* pull down assays (93). Therefore, KIF4 may also function in MLV Gag cytoplasmic trafficking towards the plasma membrane in a microtubule plus-end directed fashion.

An interaction of MLV MA with IQGAP may also function in Gag-cytoskeleton interactions in MLV RNP trafficking. The cellular proteins IQGAP1 and IQGAP2 bind directly to actin (60), and they modulate cytoskeletal rearrangements (61, 213). Yeast two-hybrid analysis revealed an MLV MA-IQGAP interaction (105). Overexpression of a C-terminal fragment of IQGAP1 inhibited MLV release, and shRNA knockdown of IQGAP1 and/or IQGAP2 decreased viral spread (105). This suggests that Gag MA interactions with IQGAP1 are also important for late Gag trafficking steps.

The double-stranded RNA-binding protein Staufen may function in the cytoplasmic trafficking of retroviral unspliced RNAs. Staufen is a dsRNA-binding protein that functions in RNA localization in *Drosophila* (195). The human and mouse orthologs bind dsRNA and tubulin in vitro, and they localize to the endoplasmic reticulum (216). Human Staufen I (hStau) copelleted with HIV-1, HIV-2, and MLV virions, and it co-sedimented with HIV-1 viral proteins and RNA on sucrose density gradients (130). Incorporation of hStau into HIV-1 particles also correlated with levels of HIV-1 gRNA incorporation (130). Subsequent studies in HIV-1 demonstrated an interaction between the HIV-1 NC zinc fingers and the double-stranded RNA binding domain of hStau (20, 21). Thus, mounting evidence suggests a function for Staufen in HIV-1 gRNA recruitment, and its incorporation into MLV particles may suggest a similar function in MLV.

The preliminary observations mentioned above suggest that cellular proteins like KIF4, IQGAP, and Staufen may function in MLV unspliced RNA cytoplasmic trafficking through interactions with the host cell cytoskeleton. However, the differences in unspliced RNA sorting and trafficking between MLV and other retroviruses like HIV-1 described in previous sections suggest that where and when the MLV RNP first encounters these cellular proteins may differ from other retroviral RNPs. Prior studies and observations reported in this dissertation suggest that cellular mY RNAs and MLV gRNAs are routed towards sites of assembly prior to nuclear egress. Thus, early recruitment of these proteins to the MLV RNP as it exits the nucleus could provide a means of directly navigating from the nucleus to sites of assembly.

Dissertation overview

This dissertation addresses the question of where RNAs are first recruited for assembly by MLV. To address this question and test the hypothesis that cellular Y RNAs are recruited from the host cell nucleus, Chapter II details our observations of cellular mY RNA packaging in MLV virions produced from Ro60 knockout cells, which have ~30-fold less cellular mY RNAs than wild type cells. Our observations of high level packaging of mY1 and mY3 RNAs in virions from Ro60 knockout cells is consistent with our hypothesis that these RNAs form a subassembly retroviral RNP in the host cell nucleus.

Next, Chapter III relates our observations of MLV gRNA packaging to virion production after specific tetracycline-repression of MLV transcription. The results, which indicate viral mRNAs have longer half-lives than gRNAs, are consistent with prior observations obtained with general transcription inhibition with ActD, and they are consistent with our hypothesis that MLV unspliced RNAs are bisected into separate pools of gRNA and viral mRNA. Chapter III also tests the hypothesis that this bisection occurs at or near sites of transcription by testing outcomes of inhibiting transcription on the randomness of gRNA dimer co-packaging and on recombination in co-expression studies. Results again are consistent with our hypothesis of a nuclear bisection, but the moderate increases in the randomness of gRNA dimerization and recombination are consistent with an ongoing bisection of MLV unspliced RNA.

In Chapter IV, we address the hypothesis that MLV gRNA dimerization functions as a molecular switch to package MLV gRNA. Our results are consistent with this hypothesis, and they provide *in vivo* support for *in vitro* observations of high affinity NC-

RNA interactions that were performed in collaboration with the work discussed here. In Chapter IV, we test the hypothesis that gRNA dimerization represents an initial point of recruitment into a MLV RNP subassembly complex. Our preliminary results are consistent with this hypothesis.

Finally, in Chapter V, our observations of a potential intersection in MLV mY RNA and gRNA recruitment are discussed in the context of an additional preliminary finding of an inverse relationship between packaged gRNA levels and packaged mY RNA levels. This finding supports the notion of an intersection in MLV gRNA recruitment with a host cell RNA quality control pathway.

CHAPTER II

Packaging of host mY RNAs by murine leukemia virus may occur early in Y RNA biogenesis.

Abstract

Moloney murine leukemia virus (MLV) selectively encapsidates host mY1 and mY3 RNAs. These noncoding RNA polymerase III transcripts are normally complexed with the Ro60 and La proteins, which are autoantigens associated with rheumatic disease that function in RNA biogenesis and quality control. Here, MLV replication and mY RNA packaging were analyzed using Ro60 knockout embryonic fibroblasts, which contain only ~3% as much mY RNA as wild type cells. Virus spread occurred at the same rate in wild type and Ro knockout cells. Surprisingly, MLV virions shed by Ro60 knockout cells continued to package high levels of mY1 and mY3 (about 2 copies of each) like those from wild type cells, even though mY RNAs were barely detectable within producer cells. As a result, for MLV produced in Ro60 knockout cells, encapsidation selectivity from among all cell RNAs was even higher for mY RNAs than for the viral genome. Whereas mY RNAs are largely cytoplasmic in wild type cells, fractionation of knockout cells revealed that the residual mY RNAs were relatively abundant in nuclei, likely reflecting the fact that most mY RNAs were degraded shortly after transcription in the absence of Ro60. Together these data suggest that these small, labile host RNAs may

be recruited at a very early stage of their biogenesis and may indicate an intersection of retroviral assembly and RNA quality control pathways.

Introduction

Retroviruses are ribonucleoprotein (RNP) complexes that assemble at host cells' plasma membranes. Their predominant RNA component is the unspliced retroviral genome, but virions also contain a number of host cell noncoding RNAs (13, 149, 174). Subsets of these RNAs are over-represented in virions relative to their abundance in host cells (149). Other than the primer tRNA, which anneals to the primer binding site on viral genomic RNA (gRNA) and initiates minus-strand DNA synthesis, the manner of recruitment of these RNAs and whether or not they function in retrovirus biology is unknown (19, 109, 110). Virion assembly does not require viral gRNA, but RNA of some sort is required for assembly, thus suggesting host RNA can serve this role (96, 132). Although prevailing notions suggest nonspecific RNA interactions drive retrovirus assembly (63), the concentration within virions of particular subsets of host cell noncoding RNAs suggests that their recruitment may have functional significance for viral assembly or other replication processes.

Among the most highly recruited noncoding cellular RNAs in MLV are mY1 and mY3 (149). These RNAs are enriched in MLV particles to a similar degree as the highly packaged 7SL RNA (7S or SRP RNA) (149). Packaging of 7SL RNA, the scaffolding RNA of host cell signal recognition particles, is observed for a number of retroviruses including Rous sarcoma virus (RSV) (15), MLV (46, 149, 157) and HIV-1 (150). In MLV, 7SL is present at three- to four-fold molar excess to gRNA, and therefore packaged at approximately six to eight copies per virion (149). HIV-1 particles contain roughly 10 to 14 molecules of 7SL per gRNA dimer (150). Like MLV, HIV-1 also

packages at least some Y RNAs, albeit at a lower level of enrichment than 7SL (6, 91, 204).

mY1 and mY3 are host RNA polymerase III transcripts of ~100 nucleotides. Both these mouse RNAs fold into similar structures consisting of 5' and 3' ends joined in a base-paired stem surrounding an internal, largely single-stranded, loop (25). Within cells, most mY RNAs are complexed with the host cell protein Ro60, which appears to function in quality control of misfolded noncoding RNAs (24, 142, 171). Structural analysis suggests Y RNA binding may inhibit Ro60 access to misfolded RNAs, as Ro60 binding sites for Y RNAs partially overlap those for misfolded RNAs (59, 197, 220). In agreement with this hypothesis, a bacterial Y RNA inhibits the function of its Ro orthologue in 23S rRNA maturation (26). It has been suggested that Y RNA binding might sequester Ro60 in the cytoplasm, thereby preventing Ro60's interaction with nascent nuclear transcripts (142, 164). Consistent with this view, the mouse Ro protein was recently shown to contain a signal for nuclear accumulation that is masked by Y RNA binding (186).

Chapter II includes work published in Garcia et al. (65) that addressed a potential intersection in mY RNA biogenesis and MLV virion assembly. This work builds on the initial findings of Onafuwa-Nuga (148) that demonstrated a surprisingly high level of mY1 and mY3 RNA packaging in MLV virions from Ro60 knockout cells which lack Ro60 and contain ~30 fold less mY RNAs. Here, the levels of mY1 RNA packaging were quantified by RNase protection assays, and results demonstrated that MLV virions from Ro60 knockout cells package ~2 copies of mY1 RNA per virion. Also, measurements of mY1 RNA levels in nuclear and cytoplasmic fractions revealed a

subcellular redistribution of mY1 RNAs in Ro60 knockout cells. Finally, analysis of mY RNA processing intermediates revealed a lack of bias in the length of mY1 RNAs that were packaged by MLV. Together, these findings support the initial work of Onafuwa-Nuga (148), and they demonstrate a remarkable degree of selectivity in mY RNA encapsidation into MLV particles. These results also suggest mY RNAs are recruited for MLV packaging from a very early stage in their biogenesis.

Materials and Methods

Cells and virus. NIH 3T3 and derivative cell lines were maintained in Dulbecco's modified Eagle medium (DMEM; Invitrogen) supplemented with 10% bovine serum (Invitrogen). Wild type mouse embryonic fibroblasts (MEFs) and Ro60 -/- MEFs were maintained in Dulbecco's modified Eagle medium (DMEM; Invitrogen) supplemented with 10% fetal bovine serum (Gemini). Wild-type and Ro60 -/- MEFs were prepared by backcrossing 129/Sv x C57BL/6 $Ro^{-/-}$ mice (221) with C57BL/6 mice for six successive generations (186). Embryonic fibroblasts were prepared and immortalized by repeated passage (205). Wild-type MLV particles were obtained by collecting supernatants from 70% to 100% confluent NIH/3T3 cells, wild type MEFs, and Ro60 -/- MEFs chronically infected with wild type MLV at 8- to 16-h intervals.

Plasmids. All riboprobe templates were derivatives of pBSII SK(+) (Stratagene). pEG604-1 was constructed with synthetic oligos for 95 nt of mY1 (nt 1 to 95) with SalI and EcoRI sticky ends and 65 nt of mouse 7SL RNA (nt 125 to 189) with PstI and NotI sticky ends. The insert in pEG467-10, which was generated by PCR and subcloned into the EcoRV site, included complementary portions to both the MLV 5' untranslated region (nt 55 to 214) and 100nt of 7SL RNA (149).

Viral and cellular RNA extraction. All supernatants were filtered using 0.2µm MCE syringe filters (Fisher Scientific), and stored at -70 °C prior to use. Virus was concentrated at 4 °C by centrifugation at 25,000 rpm for 90 min using the AH629 rotor in a Sorvall discovery ultracentrifuge. Viral pellets were resuspended in TRIzol (Invitrogen), and RNA extracted following the manufacturer's instructions. RNA from chronically

infected cells was also extracted with TRIzol. Samples were resuspended in either DEPC-treated ddH_2O or TENS (10 mM Tris [pH 8.0], 1 mM EDTA, 1% SDS, 100 mM NaCl).

Northern blots. Northern blots were used to visualize RNAs. Hybridization probes were oligonucleotides complementary to the RNAs of interest, 5' end labeled using γ-^{32}P ATP (Perkin-Elmer) and T4 polynucleotide kinase (NEB). Labeled oligonucleotides were separated from unincorporated nucleotides on G-25 sephadex columns (Roche). Oligonucleotides included:
5'-CTGACTGTGAACAATCAATTGAGATAACTCACTAC-3' for mY1;
5'-CGTGTCATCCTTGCGCAGGGGCCATGCTAATCTTCTCTGT-3' for U6;
and 5'-GAGTCCCACGCTCTACCAACTGAGCTAGCTG-3' for $tRNA^{Lys1}$.
Fractionated cellular RNAs were separated by 8% polyacrylamide-8M urea gel electrophoresis in 1X TBE. For high resolution denaturing northerns, viral and cellular RNAs were separated on 8% polyacrylamide-8M urea gels (0.4 mm thickness) in 1X TBE using glass plates pre-treated with Sigmacote® (Sigma) to facilitate separation from the glass plates prior to transfer. RNAs were subsequently transferred by electroblotting to Zeta-probe GT Nylon membranes (Bio-Rad) in 0.5X TBE. Membranes were air dried, UV crosslinked (Stratalinker; Stratagene), and prehybridized at 45 $^{\circ}$C in 6X SSC-5X Denhardt's solution-0.5% SDS-0.025M sodium phosphate-625μg/ml denatured salmon sperm DNA. Oligonucleotide probes were denatured at 85 $^{\circ}$C for 5 minutes before adding to the membranes, and hybridization was at 45 $^{\circ}$C. Blots were washed first in 2X SSC-0.1% SDS at 52 $^{\circ}$C, and then in 0.33X SSC-0.1% SDS at 52 $^{\circ}$C. Damp blots were wrapped in plastic wrap and exposed to phosphorimager screens and/or film. For re-

probing, blots were stripped by at least 2 washes in 0.1% SDS at 80°C, then prehybridized and probed as above.

Ribonuclease protection assays. To detect mY1 and 7SL, pEG604-1 was linearized with XhoI and transcribed with T3 RNA polymerase (Promega) and [α-^{32}P] rCTP to create a 217 nt transcript which protected 95 nt of mY1 and 65 nt of 7SL RNA. To detect 7SL and MLV genomic RNA, pEG467-10 was linearized with HindIII and transcribed with T3 RNA polymerase to create a 364 nt transcript which protected 160 nt of MLV genomic RNA and 100 nt of 7SL RNA. Previously described RPA approaches [Onafuwa-Nuga, 2005 #8] were modified by extending hybridization times to 16h and by digesting with a 5-fold excess of RNase T1 (Applied Biosystems). Bands were quantified by PhosphorImager analysis using a Typhoon for detection and ImageQuant TL for analysis. Bands were adjusted for the number of radiolabelled Cs incorporated.

Exogenous RT assay. Quantification of RT activity of cell-free media supernatants was used to measure levels of virus per volume of media. Media supernatants were harvested, filtered through 0.2 μM MCE syringe filters (Fisher Scientific) and stored at -70 ºC. RT assays were based on (70) as described previously (203). Briefly, 3 μl of viral supernatant was incubated with 12 μl of a 1.2x solution (60 mM Tris [pH 8.3], 24 mM dithiothreitol, 0.7 mM $MnCl_2$, 75 mM NaCl, 0.06% NP-40, 6 μg/ml oligo(dT), 12 μg/ml poly(rA), 10 μCi/ml [α-^{32}P]TTP at 3 Ci/mmol) at 37ºC for 2 h. Following incubation, 3 μl of reaction mix was spotted onto DEAE paper, dried, washed with 2xSSC followed by 95% ethanol, and once again dried. Spots were quantified by PhosphorImager analysis.

Cellular fractionation. Wild type and Ro60 -/- MEFs were fractionated using a modification of the procedure of Siomi et al. (191). Briefly, nuclear and cytoplasmic fractions were obtained by washing adherent cells twice with ice cold 1x phosphate buffered saline (PBS) followed by one wash with buffer RSB100 (10 mM Tris-HCl pH 7.4, 2.5 mM $MgCl_2$, and 100 mM NaCl). Adherent cells were permeabilized by incubation with 4 mls RSB100 supplemented with .01% (w/v) digitonin (Sigma) on ice for 5 min. The RSB100 buffer-digitonin mix was removed from the adherent cells and spun at 200 x g for 5 min to pellet residual cell debris. The RSB100 buffer supernatant served as the cytoplasmic fraction, and RNA was extracted from this aqueous mix with TRIzol LS (Invitrogen) according to the manufacturer's recommended protocol. The remaining nuclei were washed once with ice cold PBS before the addition of 1 ml of TRIzol (Invitrogen) and RNA extraction according to the manufacturer's protocol.

Results

MLV replication is unaltered in Ro60 -/- cells.

Ro RNP RNAs mY1 and mY3 are among the most highly enriched host RNAs in MLV particles (149). Within cells, most Y RNAs exist in RNPs containing the Ro60 cellular protein, and most Ro60 protein is associated with Y RNAs (156, 219). When Y1 RNA levels were used to normalize parallel viral and cellular protein extracts, the Ro60 protein in virus was below the limit of detection by western blot (148). To test the inference that Y RNAs were not recruited as parts of Ro RNPs, the kinetics of viral spread and Y RNA recruitment were analyzed in Ro60 knockout cells.

Ro60 binding is necessary for the stable accumulation of Y RNAs (23, 101, 221). Accordingly, embryonic fibroblasts prepared from Ro knockout mice contain only very low levels of mY1 and mY3 (186). Thus, studying MLV infectivity in Ro60 knockout cells allowed an examination of the effects of limiting mY RNA availability on viral replication, as well as possible roles of Ro60 itself. Ro60 -/- mouse embryonic fibroblasts (MEFs) and isogenic wild type cells were infected with MLV, and infected and control uninfected cells were serially passaged. Culture media were collected and assayed for reverse transcriptase (RT) activity at various time points post-infection to monitor virus spread (Fig. 2-1). Control uninfected cells retained only background levels of RT activity throughout the time course. For media samples from wild type and Ro60 -/- infected MEFs, the levels of RT activity rose above background on the same day (day 7) (Fig. 2-1). Thereafter, the kinetics of virus spread in infected wild type and Ro60 -/- cells remained approximately equal, with infected Ro60 -/- supernatants containing levels of RT activity that differed by less than 2 fold from those of infected wild type MEFs (not

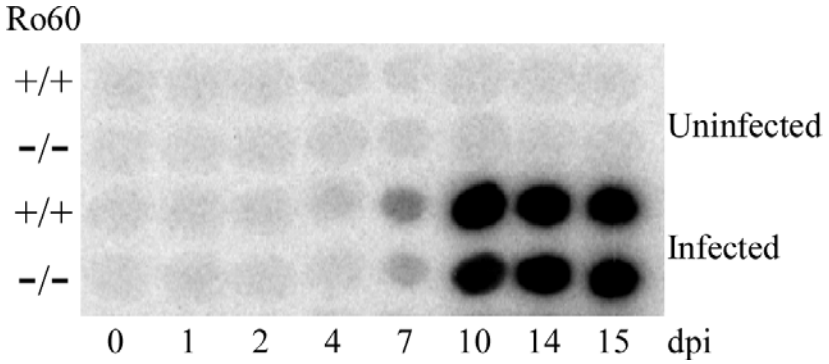

Figure 2-1. Time course of MLV spread in Ro60 -/- cells and wild type MEFs. Wild type and Ro knockout cells were infected with identical amounts of MLV, and virus spread was monitored by assaying for RT activity at the indicated time points. (dpi designates days post infection)

shown). Thus, Ro60 was dispensable for infectious MLV particle assembly and infectivity.

MLV virions from wild type and Ro60 -/- MEFs package high levels of mY1 and mY3.

Because MLV replicated normally in cells containing very low levels of mY RNAs, it initially seemed likely that virions shed from Ro knockout cells would contain correspondingly low levels of mY RNAs. Surprisingly, despite the very low levels of mY RNAs in R060 -/- cells, MLV virions produced from these cells continued to package high levels of mY RNAs (65, 148). When normalized to the co-packaged 7SL RNA, which is undiminished in Ro60 -/- cells, virus produced from the Ro60 -/- cells contained nearly the same amount of mY RNA per virion as virus from wild type cells (65, 148).

Because the Y/7SL RNA ratios in virus vs. those in cells were the same for both mY1 and mY3 RNAs, this suggests that each MLV virion encapsidates the same number of mY1 molecules as mY3 molecules. However, because the previous observations of mY RNA per 7SL packaging were obtained by northern blots which involved co-probing with two separate oligonucleotide probes--one for mY RNA and the other for 7SL--the absolute number of Y RNAs per virion could not be addressed by the radioactive signals (65, 148). Thus, to ensure uniformity in probe specific activities and estimate the number of mY1 RNAs packaged per virion, virus and cell RNA samples were subsequently probed with a single radiolabeled oligonucleotide complementary to both 7SL and mY1. The results indicate that approximately two-fold less mY1 than 7SL RNA was encapsidated into MLV produced by wild type cells, and slightly less mY1 was packaged into MLV produced from Ro60 knockouts (65, 148).

Here, ribonuclease protection assays (RPA) for mY1 and 7SL RNA confirmed the previous quantification and revealed a near 2:1 ratio of 7SL:mY1 in virus from wild type cells (Fig. 2-2A, lane 7). When normalized to 7SL, a detectable but less than two-fold decrease in mY1 packaging was observed in virus from Ro60 knockouts (Fig. 2-2A, lane 8). The gRNA to 7SL ratios in virus from both cell types (Fig. 2-2B, lanes 3 and 4) were consistent with previously established levels of 7SL packaging (three- to four-fold molar excess to gRNA (149)). Taken together these results indicated that each MLV virion from wild type MEFs contained four to five copies of both mY1 and mY3, and virions from Ro60 knockouts contained approximately 2 copies of mY1 and mY3.

The subcellular distribution of mY1 RNA is altered in Ro60 -/- cells.

Ordinarily, most Y RNA localizes to the cytoplasm, where it is bound to Ro60 in RoRNPs (141, 156). The reduced levels of mY RNAs in Ro60 -/- cells are believed to reflect their decreased intracellular stability when their cognate RNP protein is not present (23, 101, 221). Thus, a reduction in mY RNA stability in Ro60 -/- cells would likely be accompanied by a more severe deficit of mY RNA in the cytoplasm than in the nucleus.

To determine the subcellular distribution of the residual mY1 RNA in Ro60 -/- cells, RNA was extracted from total, nuclear and cytoplasmic fractions of knockout and isogenic wild type MEFs (Fig. 2-3). Northern blots were probed for mY1 or co-probed for nuclear U6 snRNA and cytoplasmic $tRNA^{Lys1}$ to control for fractionation efficiency. The results indicated that the cytoplasm of wild type cells contained at least four-fold more mY1 RNA than their nuclei (Fig. 2-3A, lanes 3 and 5). In contrast, nuclear and cytoplasmic fractions of Ro -/- MEFs contained similar amounts of mY RNA (nuclear

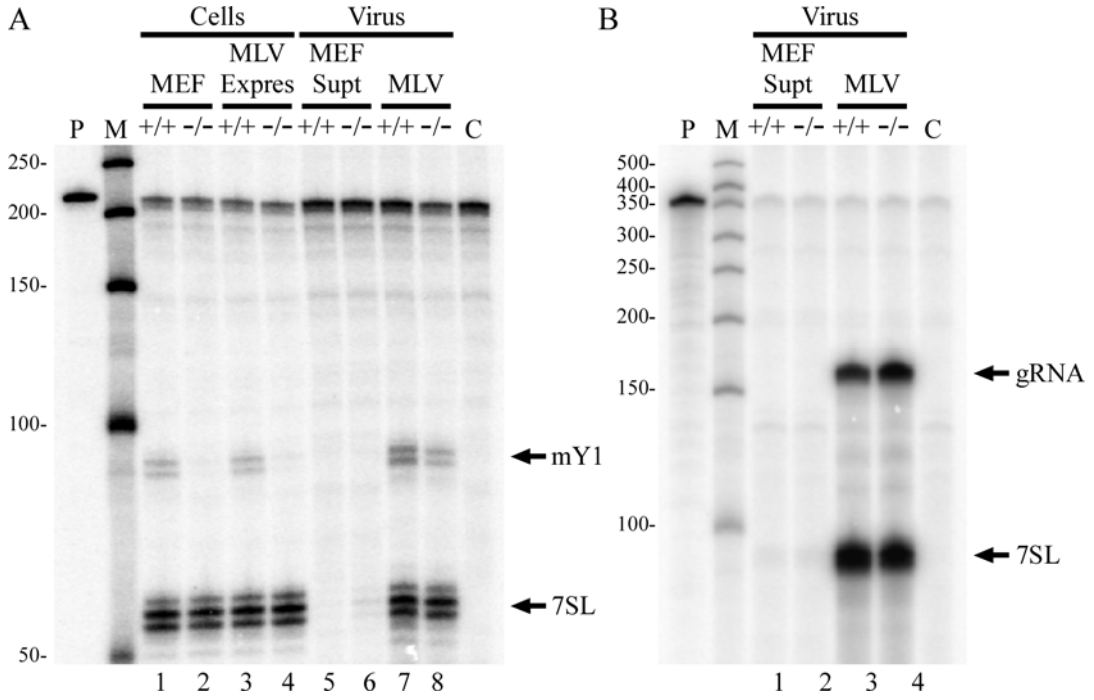

Figure 2-2. Stoichiometric analysis of mY1 RNA packaging. (A) RPA of cellular and supernatant/viral RNA for mY1 and 7SL RNA. Lanes show: undigested probe (P); RNA size markers (M); experimental samples indicated at top either Ro60 wt (+/+) or Ro60 knockout (-/-); and digested probe alone control (C). (B) RPA of supernatant/viral RNA for gRNA and 7SL RNA (C). Quantification of 4 to 5 mY1 RNAs per virion (gRNA dimer) was performed by quantifying the bands in two separate RPAs represented in (B), correcting for 18 [α-^{32}P] rCTPs for mY1 and 25 [α-^{32}P] rCTPs for 7SL, and multiplying by 7.75 7SL RNAs per virion as determined by two separate RPAs represented in (C). The bands in (C) were corrected for 53 [α-^{32}P] rCTPs in the MLV gRNA and 35 [α-^{32}P] rCTPs in the 7SL RNA. These data were consistent with quantification by direct MLV gRNA per mY1 RPAs performed in triplicate (data not shown).

fraction lane contains 10% more Y1 than cytoplasmic fraction; Fig. 2-3A, lanes 4 and 6). Compared to wild type cells, knockout cell cytoplasmic amounts of mY1 were reduced about 20-fold, and nuclear amounts were reduced about four-fold. Because the nuclear levels of the control RNA U6 are not reduced in knockout cells, the fourfold decrease of nuclear Y1 in the knockouts suggest at least some of the RNA degradation associated with the absence of Ro60 may initiate in the nucleus. These findings confirm a marked alteration in the subcellular location of mY RNAs, from their cytoplasmic prominence in wild type cells to a far greater depletion from cytoplasm than from nucleus for the residual mY RNAs in Ro60 knockout cells.

The results here showed mY RNAs were recruited at wild type levels from Ro60 knockout cells, despite 20 to 30-fold reductions in mY RNA intracellular levels. When mY to gRNA ratios in wild type cells and virus are compared, mY RNAs are selected for packaging 3 to 4 fold less well than MLV gRNAs (149). Thus, whereas virions produced by wild type cells package mY RNAs slightly less effectively than viral gRNAs, when MLV replicated in Ro knockout cells, mY1 and mY3 displayed a roughly 5- to 10-fold higher packaging selectivity than gRNAs.

mY RNA packaging is independent of Y RNA processing step.

The biosynthesis of host ribonucleoprotein complexes involves a series of RNA processing steps and alternate protein associations. Significant uncertainty remains about both temporal and spatial aspects of these steps in Ro RNP assembly (156, 164, 187, 188, 218). Nonetheless, it is clear that transcription of Y RNAs, as is the case for all RNA polymerase III transcripts, terminates in a run of uridines, and that the resulting 3’ ends

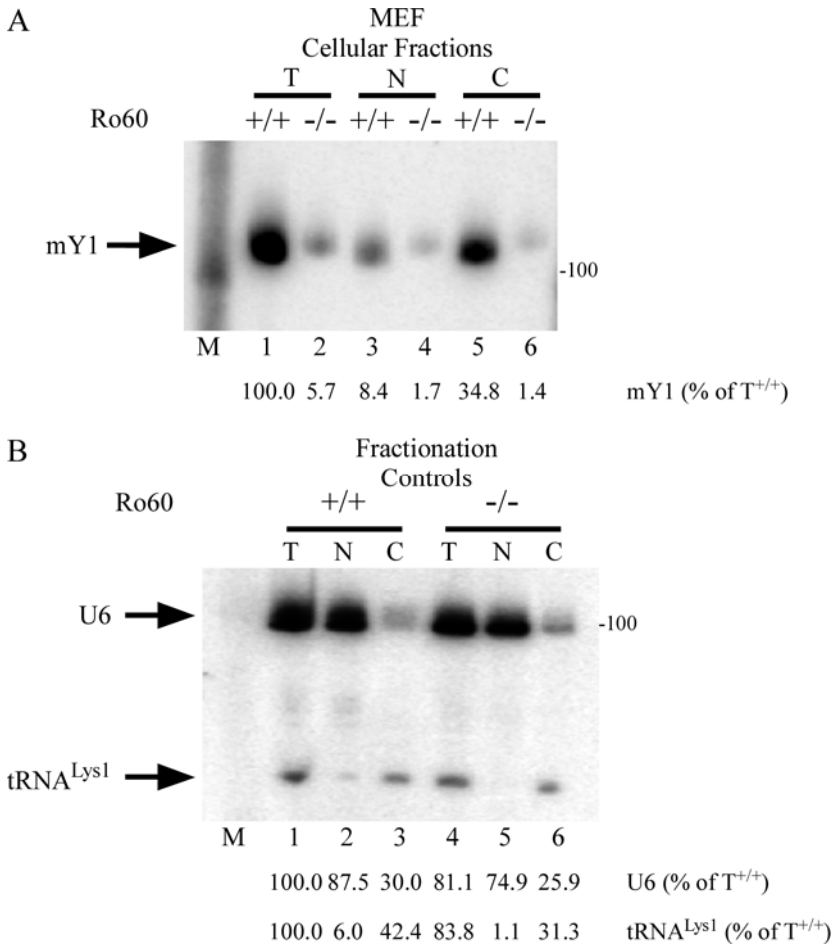

Figure 2-3. mY1 RNA redistribution in Ro60 -/- cells. (A) Northern blot of RNA from total (T), nuclear (N), and cytoplasmic (C) fractions of both wild type Ro60 +/+ MEFs and knockout Ro60 -/- MEFs, probed for mY1. (B) Northern blot of RNA from total (T), nuclear (N), and cytoplasmic (C) fractions of both wild type Ro60 +/+ MEFs co-probed for U6 snRNA, a nuclear RNA control, and $tRNA^{Lys1}$, a cytoplasmic RNA control. Quantification of the levels of mY1, U6, and $tRNA^{Lys1}$ are given below each blot as a % of total cellular RNA from wild type MEFs ($T^{+/+}$).

are bound by the La protein, which recognizes RNAs ending in three or more uridines (33, 116, 218). Subsequent end-trimming by exonucleases removes some of the terminal uridines, resulting in a population of RNAs slightly shorter than the initial transcription products; some of these no longer possess La binding sites (218). Neither the identity of the exonuclease nor its subcellular location is known. Ro travels to the nucleus prior to Ro RNP assembly, and binds the bulged Y RNA stem region (75, 187). Ro and La can bind a single Y RNA simultaneously (164). Although La has been observed to shuttle between the nucleus and cytoplasm (55), La binding retards nuclear export of Y RNAs (77, 188). Thus, Y RNA 3' end shortening and elimination of the La binding site may occur prior to nuclear export (80, 175). In unstressed wild type cells, most Y RNAs exist in the cytoplasm in a shorter, matured form, in an RNP complex containing Ro but not La (shorter mY1 RNAs lack the 3' La binding site (Fig. 2-3A) and (116, 218)).

To address whether or not mY RNA encapsidation into MLV represented diversion of the RNAs from a specific stage in their maturation pathway, RNAs from wild type and Ro60-/- cells were first analzyed for signatures of Y RNA processing intermediates. Consistent with the Y RNAs in the knockout MEFs representing newly synthesized RNAs, the residual Y RNAs in Ro60-/- cells migrated slightly slower than the majority of the Y RNAs in wild-type cells, and thus exhibited the pattern observed for nascent La-bound Y RNAs (Fig. 2-3A and (24)).

Next, the lengths of Y RNA processing intermediates in cells and virions were examined by high resolution denaturing acrylamide gels (Fig. 2-4A). These results confirmed that the spectrum of mY RNAs in knockout cells was longer than that in wild type cells. The short length of mY RNAs in virions from wild type cells suggested that

La binding was not necessary for mY RNA packaging. However, the encapsidated RNAs from knockout cells were longer than those from wild type cells. In both cell types, the RNA length distribution in virus was found to resemble that in the producer cells (Fig. 2-4A), suggesting that packaging did not require mature 3' end formation.

To further address possible packaging of specific Y RNA subsets, high resolution gels were used to examine mY1 processing species distribution in cytoplasmic and nuclear fractions (Fig. 2-4B). Under the fractionation conditions used, the spectra of RNAs in knock-out cells' cytoplasmic and nuclear fractions were indistinguishable (Fig. 2-4B lanes 5 and 6). A subtle but reproducible slight bias toward more completely processed products was observed both in wild type cells' cytoplasmic fractions (Fig. 2-4B lane 3) and in virions (Fig. 2-4A lane 6), compared to these cells' nuclear RNA spectrum (Fig. 2-4B lane 2).

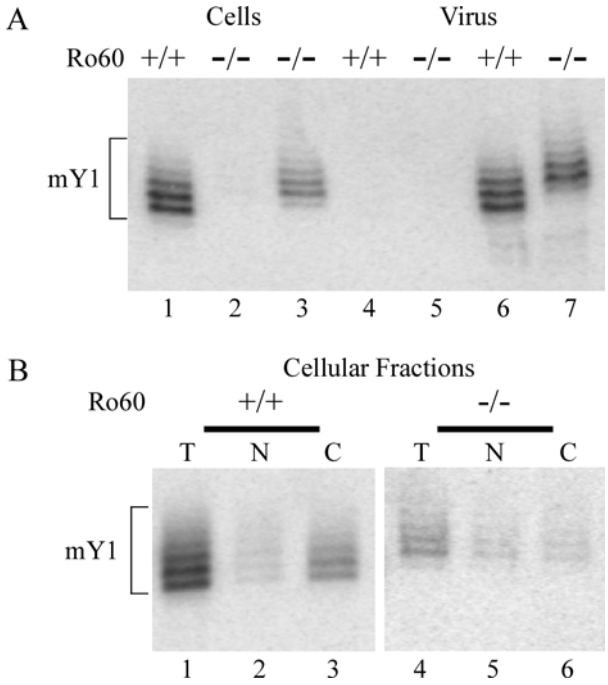

Figure 2-4. mY1 RNA processing intermediates in cell and virus samples. (A) Northern blot of RNA from total cell and viral samples from wild type Ro60 +/+ MEFs and knockout Ro60 -/- MEFs, separated on 8% acrylamide, 8M urea sequencing gel and probed for mY1. Note that whereas lanes 1 and 2 contain equivalent samples, 20 times as much -/- cell sample was loaded in lane 3 as +/+ cell sample in lane 1 to facilitate qualitative comparison; lane 4 and lane 5 are RNA samples from supernatants of uninfected cells – the same volume of cell-free media as was used in lane 6; and virus samples (lane 6 and lane 7) were normalized to 7SL. (B) Northern blot of RNA from total, nuclear, and cytoplasmic fractions from wild type Ro60 +/+ MEFs and knockout Ro60 -/- MEFs, separated on 8% acrylamide, 8M urea sequencing gel and probed for mY1.

Discussion

Retroviruses like MLV encapsidate distinct subsets of cellular non-coding RNAs (13, 149). Data here demonstrated that mY1 and mY3 RNA were recruited into budding MLV at four to five copies apiece from wild type MEFs and about 2 copies apiece from Ro60 knockout cells. Although most mY RNA in cells resides in Ro RNPs, these RNAs were recruited into MLV without their cognate RNP protein, Ro60.

Similar observations of host protein-independent packaging of RNP RNA have been made for the SRP RNA, 7SL, which is packaged without the 54-kd SRP protein in both MLV and HIV-1 ((91, 150) and unpublished). Because of its essential role in signal recognition particles, direct knock-down of 7SL RNA is not readily achievable ((6) and unpublished). Facilitating our analysis of MLV mY RNA packaging, viable Ro60 knockout mice have been generated. Their cells lack Ro RNPs and display vastly reduced levels of mY RNAs (221).

We therefore used Ro60 -/- cells to examine the intersection of mY RNA biogenesis with MLV replication. The normal spread of MLV in Ro60 -/- embryonic fibroblasts demonstrated that the Ro60 protein is not necessary for virus replication. Because mY1 and mY3 are highly labile in the absence of Ro60, knockout of Ro60 leads to a 30-fold reduction in these RNAs (221). Strikingly, this intracellular reduction was not accompanied by a proportional reduction in mY RNA packaging. Instead, mY1 and mY3 were so highly enriched that MLV's selectivity for mY RNAs, from among all RNAs in Ro60 knockout cells, was 5- to 10-fold higher than selectivity for its own genome.

MLV's high level of selectivity for mY RNAs led to our model in which Ro RNP and MLV assembly pathways intersect at an early step in Ro RNP biogenesis (Fig. 2-5). In this model for the encapsidation of mY RNAs without Ro60, the pathways of mY RNA biogenesis and MLV assembly intersect, and a virion-specifying factor diverts Ro60-free mY RNAs away from host cell RNA degradation machinery toward assembly sites on the plasma membrane (Fig. 2-5).

The similar Y RNA packaging observed in virions produced by cells with either high or very low intracellular Y RNA levels suggests that these RNAs are not recruited from RoRNPs, but from a separate intracellular pool of Ro60-free RNAs. Towards localizing this intracellular pool, cell fractionation suggested MLV recruitment from an early pool of nascent mY RNAs. Consistent with the role of Ro60 in stabilizing mY RNAs (23, 101, 221), as well as the likely importance of Ro60 binding to Y RNA nuclear export (188), cytoplasmic pools of mY RNAs decreased more than the residual pool of nuclear mY RNAs in Ro60 knockout cells. Because this redistribution did not result in a corresponding decrease in Y RNA recruitment by MLV, it suggests that recruitment occurs at an unaffected, and possibly earlier, step in Y RNA biogenesis.

Precisely where this occurs was not resolved by monitoring 3' end modifications that accompany Y RNA maturation. In virus from wild type cells, encapsidated RNAs resembled the biased pattern of Y RNAs in the cytoplasm. However, encapsidated RNAs from Ro60 knockouts resembled more nascent RNAs. The Y RNAs in knockout cells resembled longer nascent transcripts which have not undergone 3' end maturation. Thus, rather than indicating a cytoplasmic point of recruitment, these data suggest that recruitment into particles is independent of 3' end maturation.

Assuming that mY RNAs are recruited at the same step of their biosynthesis in both cell types, these results suggest that recruitment for packaging occurs before 3' end maturation is completed but does not preclude subsequent 3' end maturation. Because both La and Ro recognize and act on RNA motifs in the Y RNA stem and 3' tail region, while other factors such as nucleolin and hnRNP I are known to interact with some Y RNAs via the internal loop (51, 56, 75), these findings may indicate that recruitment of Y RNAs occurs via interactions with the loop region that prevent degradation of Ro-deficient RNAs but do not preclude 3' end maturation (Fig. 2-5). Speculatively, the slower migration of residual Y RNAs in knockout cells may be suggestive of a role for Ro60 in exposing Y RNA 3' ends for completing their exonucleolytic processing by an as yet unknown mechanism.

Because they are recruited early, one possibility is that mY RNAs may be selected for encapsidation into MLV from near their site of transcription in the nucleus (Fig. 2-5). The possibility of nuclear recruitment is plausible, considering that known pools of protein-free Y RNAs localize to perinucleolar sites of early RNP assembly (119). Although assembly of MLV, as for all retroviruses classically described as type C, is first visualized at the plasma membrane (57), the notion that retroviral late replication phases may include a nuclear step is not unprecedented. A portion of avian sarcoma virus Gag molecules transit through the nucleus prior to assembly (176-178). Although one study reported that 18% of MLV infected cell-associated Gag immunoprecipitated from nuclear fractions, it remains controversial whether or not retroviruses other than ASV share this step (137).

The recruitment of mY RNAs at a nuclear subassembly step may involve MLV gRNA. The notion that MLV gRNAs transit directly from the nucleus to sites of assembly is supported by the propensity of sibling MLV gRNAs, but not those of HIV-1, to self-associate for packaging (53). When sibling gRNAs are expressed from a single nuclear locus or proximal integration sites, they associate randomly (54, 92, 166). The impact of nuclear distance on gRNA dimer partner selection argues for an early association of gRNA siblings and an early formation of a subviral RNP destined for encapsidation at the plasma membrane. If mY RNAs are recruited in the nucleus, they may join this hypothetical subviral RNP and accompany it to the plasma membrane, with the possibility that mY RNA binding may modulate the RNP's intracellular trafficking, as it does for Ro RNPs (Fig. 2-5) (186).

These findings of highly specific recruitment and enrichment of host RNP RNAs into MLV particles, even when the particles are produced by cells in which the RNAs are barely detectable, adds to growing evidence that the pathway of retroviral assembly—from nuclear provirus to plasma membrane released virion—may be less linear than previously believed (199). Whether the apparent intersection of host and viral RNP biogenesis pathways is a fortuitous convergence, represents a viral evolved reliance on host RNP biosynthetic machinery, or is indicative of an abortive attempt of the host RNA quality control circuitry to thwart viral attack is not clear. The comparable packaging of similar subsets of noncoding RNAs in several different retroviral species does not immediately differentiate between these possibilities (6, 91, 149, 204), although the argument for chance interactions may be weakened if some retroviruses include a nuclear preassembly step while others do not (43, 53). Accumulating evidence suggests that some

viruses co-opt protein quality control machinery to aid their replication (217): the work here adds to evidence for a similar intersection between retrovirus assembly and cellular machinery associated with RNA quality control (9, 62).

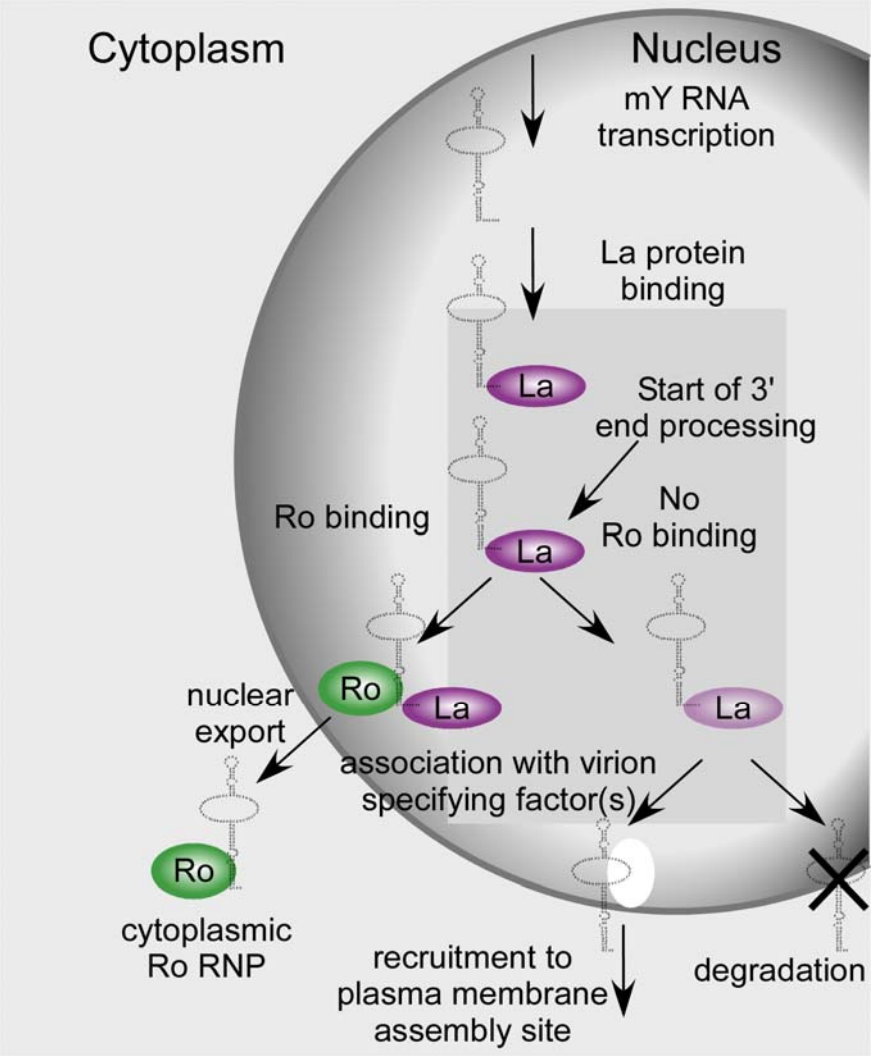

Figure 2-5. Ro RNP biogenesis and late stages of MLV replication. A speculative model for their intersection based on observations reported here and Ro RNP assembly properties, as described in the text. The oval represents the nucleus; the light gray box within the nucleus indicates the most parsimonious locations of mY RNA recruitment for packaging.

CHAPTER III

Specific repression of Moloney murine leukemia virus transcription supports the early bisection in viral unspliced RNA into mRNA and genome fates.

Abstract

Unspliced retroviral RNAs function as genomes (gRNA) for packaging and mRNAs for translation. Where and when gRNAs initially form dimer partner associations or are recruited for packaging likely differs among retroviruses. For Moloney murine leukemia virus (MLV), previous findings with actinomycin D treated cells suggest that MLV unspliced RNAs sort into non-equilibrating pools of gRNAs and mRNAs. Prior work from our lab and others on the randomness of gRNA dimer populations suggests that unlike HIV-1, MLV gRNA dimer partner selection may occur before RNAs exit the nucleus, suggesting that the bisection in gRNA and mRNA fates occurs before nuclear egress. Here, tetracycline-regulated MLV transcription was used to repress MLV transcription in a more targeted fashion in order to re-address the two pool phenotype of MLV unspliced RNA. Specific repression of MLV transcription led to a more rapid decline in gRNA packaging than virion production, which is consistent with earlier findings where transcription was inhibited globally with actinomycin D. Additionally, packaged gRNA dimer populations were analyzed at various time points after both specific and general transcription inhibition. The results indicated that

transcription inhibition led to increased randomness in gRNA dimer partner associations and a parallel increase in recombination under both conditions, albeit with residual biases consistent with an ongoing partitioning between mRNAs and genomes. These data suggest that the small population of heterodimers in MLV co-expression studies arise from a subset of gRNAs that escape early dimer partner associations and form dimer associations more randomly later. Together, our observations suggest that MLV unspliced RNA fates are determined early in the host cell nucleus and support the early separation of MLV unspliced RNAs into two largely non-equilibrating pools.

Introduction

Retroviruses use unspliced RNA as either genome (gRNA) or mRNA. In order to package gRNA into viral particles, retroviruses must sort gRNA away from viral mRNA. All retroviral gRNAs are packaged in pairs, and this shared property may provide a mechanism for the separation and recruitment of paired gRNAs from the pool of unpaired viral mRNAs. Where gRNAs form pairs and diverge from viral mRNAs likely varies among retroviruses.

Where are retroviral unspliced RNAs initially recruited into assembling virions? Different packaging mechanisms contribute to diversity in the potential subcellular locations where RNAs might first encounter packaging machinery. The *cis*-preference for Line-1 genomic RNA incorporation into ribonucleoprotein (RNP) retrotransposition intermediates supports a cytoplasmic site of initial recruitment (99, 214). Similarly, the recruitment of human immunodeficiency virus type 2 (HIV-2) RNAs from the pool of translating viral mRNAs indicates a cytoplasmic point of initial recruitment (76, 88). Studies using actinomycin D (ActD) as a general transcription inhibitor suggest that HIV-1 and HIV-2 gRNAs are recruited from the same pool of RNAs that function as mRNA (43). This suggests that, like HIV-2, the initial point of recruitment for HIV-1 gRNAs is in the host cell cytoplasm. Unlike HIV-2 gRNAs, HIV-1 gRNAs can be packaged in *trans*, which suggests a potential cytoplasmic recruitment from a location separate from translating viral mRNA (17, 88, 139).

For murine leukemia virus (MLV), studies using ActD have suggested that the MLV unspliced RNA that functions as mRNA is unavailable for packaging (107, 108). This implies packaging occurs in *trans* and suggests that MLV unspliced RNA segregates

into separate nonequilibrating pools of mRNA and gRNA (108). By quantifying packaged MLV gRNA and intracellular viral RNA after ActD treatment, Messer et al. (122) showed that intracellular viral RNA had a half-life three to four times greater than packaged gRNA. This suggests that MLV gRNAs move rapidly from the initial point of recruitment to sites of assembly.

Prior studies of gRNA dimer partner selection between two distinct co-expressed gRNAs have provided evidence that MLV gRNAs form pairs at or near sites of transcription and further suggest an early separation of gRNAs from unpaired viral mRNAs (53, 54). It was observed that MLV gRNAs expressed from separate nuclear loci preferentially self associate and therefore exhibit nonrandom dimerization (53). In contrast, when distinct MLV gRNAs were expressed from a single locus or proximal nuclear loci, they dimerized randomly (54, 92, 166).

Flynn et al. (53) showed that, unlike MLV, co-expressed HIV-1 gRNAs dimerize randomly, which is consistent with more recent observations of the random association of fluorophore-tagged HIV-1 gRNAs tagged in a single virion visualization assay (22). Through manipulation of palindromic sequences within the dimer initiating signal (DIS) of HIV-1 gRNAs, Moore et al. (127) provided evidence that gRNA dimerization precedes packaging in HIV-1. Recently, a cell fusion assay was used to compare the recombination of HIV-1 gRNAs produced from separate nuclei to the rate of recombination of HIV-1 gRNAs produced from the same nucleus (128). The observations that recombination rates were similar between the two conditions and that nuclei remained separate and intact further suggest that HIV-1 gRNAs form dimers randomly in the host cell cytoplasm (128).

This difference in RNA trafficking between MLV and HIV-1 also accounts for observed differences in recombination rates between the two in single cycle recombination assays (52, 151, 228). The more random dimerization of HIV-1 leads to greater genetic marker cosegregation and recombination than MLV, which displays relatively low rates of recombination due to preferential packaging of homodimers. The nonrandom dimerization of MLV gRNAs and its comparatively low level of recombination are consistent with the ActD inhibitor studies. Together, these observations suggest that MLV gRNAs form pairs and separate from viral mRNA early in their biogenesis.

Although general transcription inhibition with ActD has suggested a bifurcation in MLV unspliced RNA fates, it remains a strong possibility that the two nonequilibrating pools of MLV RNA may arise from indirect consequences of this mode of general transcription inhibition. Some indirect or off target effects of ActD treatment include disruptions to translation initiation (190), disruptions to cytoplasmic mRNA processing body (P body) stability (29, 212) (reviewed in (49)), and disruptions to nuclear-to-cytoplasmic shuttling of host cell proteins (86, 87, 104, 143). These disruptions could lead to changes in MLV unspliced RNA trafficking patterns, or to disruptions of cellular physiology that might sequester viral or cellular factors required for gRNA packaging.

Here, we sought to address whether or not the two-pool hypothesis could withstand more stringent testing by using targeted repression of MLV transcription to eliminate indirect/off target effects of general transcription inhibition. Notably, we observed a bifurcation in the fates of MLV unspliced RNA that was similar to the bifurcation which results from ActD treatment when we inhibited MLV transcription

specifically. Testing the prediction that this separation in gRNA from viral mRNA is linked to early dimer partner selection, we also demonstrate here that both the randomness of gRNA dimerization and the levels of recombination increased when early events were disrupted by transcription inhibition. Lastly, we show a long half-life for MLV unspliced RNA in nuclear fractions which paralleled MLV unspliced RNA decreases in the host cell cytoplasm. Together, these data support an early separation of MLV gRNA from viral mRNA from within a long-lived pool of unspliced RNA in the host cell nucleus.

Materials and Methods

Cells. 293T cells (human embryonic kidney cells expressing SV40 T antigen) were grown in Dulbecco's modified Eagle's medium (DMEM) (Invitrogen) supplemented with 10% fetal calf serum (Gemini). NIH 3T3 cells, 3T3 cells chronically infected with MLV, and D17/pJET cells (144) (canine osteosarcoma cells expressing murine ecotropic receptor) were maintained in DMEM (Invitrogen) supplemented with 10% bovine serum (Invitrogen).

A tetracycline (Tet) (Sigma)-inducible MLV cell line was constructed by site-specific recombination of MLV under control of $TetO_2$ operator sequences into Flp-In™ T-REx™ -293 cells (derived from human embryonic kidney cells (73)) (Invitrogen). This was done by co-transfection of pEG483-4 (described below) with pOG44 (which expresses the Flp recombinase under the control of the human CMV promoter) into Flp-In™ T-REx™ -293 cells. Flp-In™ T-REx™ -293 cells contain two stable, independently integrated plasmids pFRT/*lacZeo* and pcDNA6/TR. pFRT/*lacZeo* introduced a single Flp Recombination Target site (FRT) site into the 293 cell genome, and it stably expresses the lacZ-Zeocin™ fusion gene by the SV40 early promoter. pcDNA6/TR constitutively expresses the TetR repressor from the cytomegalovirus (CMV) immediate-early enhancer/promoter. Flp-In™ T-REx™ -293 cells and Tet-inducible MLV cells were grown in DMEM supplemented with 10% fetal calf serum (Gemini).

Virus – tetracycline-regulated repression of MLV transcription. For our study of the selective repression of MLV transcription, virus was harvested from cells maintained under induction with 1 μg/ml tetracycline (Tet) (Sigma) and from cells where MLV transcription was shut off by removal of Tet. After ~96 hours of induction and 72

hours of serum deprivation, virus was harvested at 2 hour time intervals from media supernatants of cells either maintained under induction in the presence of Tet or from media of cells where MLV transcription was repressed by removal of Tet.

Virus – general transcription inhibition with ActD or DRB. To recapitulate previously reported observations of the MLV unspliced RNA response to actinomycin D, virus was harvested from chronically infected 3T3 cells at two hour time intervals before and after treatment with 1 ug/ml actinomycin D (Sigma).

For two vector dimerization and recombination experiments, virus was produced by transient transfection of plasmids into 293T cells by calcium phosphate precipitation (225), and virus-containing media was harvested at indicated time points pre or post treatment of transfected 293T cells with 1 μg/mL actinomycin D (Sigma) or 100 μM 5,6-dichlorobenzimidazole riboside (DRB) (Sigma). All virus was filtered through a 0.2-μM MCE syringe filter (Fisher Scientific), and stored at -70ºC prior to use.

Plasmids. pMLV is an infectious MLV proviral clone also known as pNCA (28). pMΨPuro is an MLV-based vector containing cis-acting sequences for RNA dimerization and packaging as well as a puromycin resistance gene driven by a simian virus 40 (SV40) early promoter (pAM86-5) (98). The helper plasmid pNGVL-3'-gagpol, which expresses MoMuLV Gag and Gag-Pol from a 5' leader-deleted transcript driven by the CMV promoter, has been described previously (225). The MLV recombination vectors MLV Lac (also called pNR1755-1) and MLV L^cPuro (also called pNR1727-1) have been described previously (151). Briefly, MLV Lac contains *lacZ* driven by the MLV long terminal repeat (LTR). MLV L^cPuro was derived from the same plasmid as MLV Lac,

but it contains a 117-bp deletion between the EcoRV and SspI sites of *lacZ* and a SV40 early promoter followed by a puromycin resistance gene.

Riboprobes were templated by pBluescript II SK or KS (+/-) (Stratagene)-derived plasmids. pAO993-11 is an MLV 5' UTR-7SL chimeric riboprobe template that has been described previously and was used here to quantify gRNA/RT activity and gRNA/7SL (149). pD1040-2 is a *gag* riboprobe template that has been described previously and was used here to detect MLV RNA in Tet-inducible cells and MLV/MΨPuro RNAs in RNA captures (53, 183). pSRK38-7 is an HIV-1 *pol*-7SL chimeric riboprobe template that has been described previously and used here as a probe for 7SL RNA in Tet-inducible cells (150). pEG623-1 is a β-actin mRNA riboprobe template generated by PCR of mouse cDNA with oligos EG96 5'-CGCCGACTAGTAGCCATGTACGTAGCCATCC-3' and EG97 5'-CGAGTGCGGCCGCCTCTCAGCTGTGGTGGTGAA-3' that was blunt end cloned into the EcoRV site of pBluescript II SK (+/-).

For generation of a MLV inducible cell line, MLV from pNCA was sub-cloned into pcDNA5/FRT/TO© (Invitrogen). For Tet-regulated expression of MLV, overlap extension PCR was used to fuse the MLV transcription start site in R with the hybrid hCMV/$TetO_2$ promoter from pcDNA5/FRT/TO©. The internal oligos for this were: EG82 5'-GCTCGTTTAGTGAACCGCGCCAGTCCTCCGATTG-3' and EG83 5'-CAATCGGAGGACTGGCGCGGTTCACTAAACGAGC-3'. The resulting plasmid was pEG483-4.

Exogenous RT assay. Media supernatants were harvested, filtered through 0.2-μM MCE syringe filters (Fisher Scientific) and stored at -70 ºC. RT assays were based

on a protocol by (70) as described previously (203) to measure the amount of RT activity in media supernatants with an exogenous template.

Dimeric viral RNA extraction. Previously reported dimeric viral RNA extraction methods, which isolate MLV gRNAs without disrupting their non-covalent dimer associations (53), were modified by using 30 ml of virus-containing medium over 2 ml of 20% sucrose in phosphate-buffered saline and centrifuging at 113,000 × *g* for 2 h at 4ºC.

RPAs. To quantify gRNA packaging in virus from ActD treated cells and gRNA/7SL in virus from Tet-inducible cells, pAO993-11 was linearized with Hind III and transcribed using T3 RNA polymerase (Promega) and [α-^{32}]CTP to create a 436-nt transcript which protected 201 nt of MLV RNA and 99 nt of 7SL RNA. To quantify 7SL in Tet-inducible MLV cells, pSRK38-7 was linearized with SalI and transcribed with T7 RNA polymerase (Promega) to generate a 344-nt transcript that protects 101 nt of 7SL RNA. To quantify MLV unspliced RNA in Tet-inducible MLV cells and to detect MLV/MΨPuro in RNA captures, pD1040-2 was linearized with EcoRI and transcribed using T3 RNA polymerase (Promega) to create a 400-nt transcript which protected 330 nt of MLV RNA and 289 nt of MΨPuro RNA. To quantify β-actin mRNA in nuclear and cytoplasmic fractions, pEG623-1 was linearized with EcoRI and transcribed using T7 RNA polymerase (Promega) to create a 311-nt transcript which protects 228 nt of exon 4 of mouse β-actin mRNA.

Previously described RNase protection assay (RPA) approaches using RNase T1 (Ambion) and RNase A (Roche) (53) were modified by extending hybridization times to 16 h (Applied Biosystems). Bands were quantified by PhosphorImager for detection and

ImageQuant TL for analysis. Bands were adjusted for the number of radiolabeled Cs incorporated.

Cell fractionation. NIH 3T3 cells and chronically infected 3T3 cells were fractionated using a modification of the digitonin (Sigma) procedure of Siomi et al. (191) as previously described (65) which selectively permeabilizes the plasma membrane.

Northern blots. Northern blots were used to visualize RNAs for fractionation controls. Hybridization probes were oligonucleotides complementary to the RNAs of interest, 5' end labeled using γ-^{32}P ATP (Perkin-Elmer) and T4 polynucleotide kinase (NEB). Labeled oligonucleotides were separated from unincorporated nucleotides on G-25 sephadex columns (Roche). Oligonucleotides included 5'-GGATAAACCTCGCCCTGGGAAAACCACCTTCGTGATCATG-3' for U1 and 5'-GAGTCCCACGCTCTACCAACTGAGCTAGCTG-3' for $tRNA^{Lys1}$. Viral and cellular RNAs were separated by 8% polyacrylamide-8M urea gel electrophoresis in 1X TBE. RNAs were subsequently transferred by electroblotting to Zeta-probe GT Nylon membranes (Bio-Rad) in 0.5X TBE. Membranes were air dried, UV crosslinked (Stratalinker; Stratagene), and prehybridized at 52 °C in 6X SSC-5X Denhardt's solution-0.5% SDS-0.025M sodium phosphate-625µg/ml denatured salmon sperm DNA. Oligonucleotide probes were denatured at 85 °C for 5 minutes before adding to the membranes, and hybridization was at 52 °C. Blots were washed first in 2X SSC-0.1% SDS at 50 °C, and then in 0.33X SSC-0.1% SDS at 50 °C. Damp blots were wrapped in plastic wrap and exposed to phosphorimager screens and/or film. For re-probing, blots were stripped by at least 2 washes in 0.1% SDS at 80 °C, then prehybridized and probed as above.

Infection and functional assay for LacZ activity. D17/pJET cells in 6-cm-diameter dishes were infected for 1 h in the presence of 5 μg of hexadimethrine bromide (Polybrene; Sigma) per ml at low multiplicities of infection (<0.01). After 24 h, cells were transferred to 10-cm-diameter dishes using 0.5 ml of 0.05% trypsin (Invitrogen). 48 h after infection, cells were placed in selection media containing 1 μg/ml puromycin (Sigma). Selection, cell fixation, and 5-bromo-4-chloro-β-D-galactopyranoside (X-Gal) (Sigma) staining were performed as previously reported (158).

RNA capture assay. The RNA capture assay protocol, a biotinylated-oligo mediated method for the capture/pull down of dimeric RNA, was adapted from that previously described (53). The modifications included increasing the number of washes to 7 and increasing the stringency of the washes by lowering the salt concentration of the wash buffer to 0.33× SSC (50 mM NaCl) and heating to 50ºC.

Tet induction and shut-off. Sub-confluent 10-cm diameter dishes of Tet-inducible MLV cells (~2×10^6 cells/10-cm diameter dish) were split 1:8 (~2.5×10^5 cells/10-cm diameter dish) onto new 10-cm diameter dishes with 0.05% Trypsin-EDTA (Invitrogen). The cells were placed in fresh DMEM supplemented with 10% fetal calf serum (Gemini) either with or without 1 μg/ml Tet (Sigma). After 24 hours, the serum-containing media was replaced with serum-free media to obtain a more synchronous cell population and lessen the experimental variation in our study, and cells were maintained with or without Tet. Serum-free media with and without Tet was replaced every 24 hours for the next 48 hours. After 48 hours, the serum-free media with and without Tet was replaced every six hours until approximately 72 hours. At 72 hours, cells were placed back in DMEM supplemented with 10% fetal calf serum (Gemini). At this same time

point, Tet was removed from a subset of cells to shut off MLV transcription. MLV expression was monitored by media RT activity of cells that were under continual induction, cells that were never induced, and cells that were shut off following induction. RT levels and virion RNA levels were monitored every 2 hours from the time of shut off until 10 hours later.

Results

Consistent with previous studies, general transcription inhibition results in a more rapid decline in MLV gRNA packaging than virion production.

Previous studies of MLV unspliced RNA sorting used general transcription inhibition to reveal a separation of MLV gRNA from viral mRNA (107). For comparison with specific inhibition of MLV transcription, this earlier experiment was reproduced here by actinomycin D (ActD) treatment of chronically infected mouse fibroblasts, measuring RT activities and packaged gRNA levels after ActD treatment (Fig. 3-1A and 1B). RT activities, which provided an indication of virion production and an indirect measure of intracellular viral mRNA levels, declined gradually over time to around 40% by 10 hours post ActD treatment (Fig. 3-1A). When viral supernatants were normalized to RT activity, packaged gRNA levels declined rapidly to less than 20% of initial levels by 4 hours post ActD treatment, and gRNA levels were barely detectable by 10 hours post ActD treatment (Fig. 3-1B). These data recapitulate the earlier data, which suggests a two-pool phenotype of MLV unspliced RNA and significant difference in the half lives of packageable gRNA versus virion-producing intracellular viral mRNA.

Specific repression of MLV transcription results in a more rapid decline in gRNA packaging than virion production.

In order to determine if the functional separation of MLV unspliced RNA fates was a direct or indirect result of treatment with ActD, a more targeted inhibition of MLV transcription was used to minimize global disruptions to cell physiology and RNA trafficking. In order to specifically shut off MLV transcription, a full length MLV provirus was placed under control of tetracycline (Tet) by replacing the 5' U3 region with

a CMV promoter regulated by Tet operator sequences. This construct was site-specifically recombined into 293 cells that constitutively express the TetR repressor. In this system, transcription of MLV unspliced RNA is turned on in the presence of Tet and turned off in the absence of Tet, or upon Tet removal.

The rate of MLV shut off in this system was first tested by repressing MLV transcription after a period of induction and monitoring virion production by RT activity in media supernatants(Fig. 3-1C). The rate of decline in virion production was determined for cells deprived of Tet (after a period of induction) and compared to levels for cells under constant induction (Fig. 3-1C). The rate of decline in RT activity upon MLV transcription shut was comparable to the rate of decline in RT activity post ActD treatment. Both methods of MLV transcriptional shut off reduced RT to ~40% of uninhibited levels by 10 hours (Fig. 3-1A and 1C). Therefore, specific shut off of MLV transcription produces a rate of decline in virion production which is consistent with the rate observed with ActD-mediated transcription inhibition.

Upon specific shut off of MLV transcription, changes in packaged gRNA levels were determined through direct comparison with copackaged 7SL RNA, a host RNA packaged by MLV at levels proportionate to virion proteins (149) (Fig. 3-1D). An RNase protection assay (RPA) was used to determine the ratio of gRNA to 7SL in virion RNA from cells under constant induction to that from cells where MLV transcription was repressed (Fig. 3-1D). Quantification of gRNA to 7SL ratios over time revealed a two-fold decline in gRNA/7SL in virus from cells in which MLV transcription had been switched off (Fig. 3-1D). The gRNA to 7SL ratios appeared to level off between 6 to 10 hours, with a final ratio of 43(± 8) % of levels observed under continuous induction. By

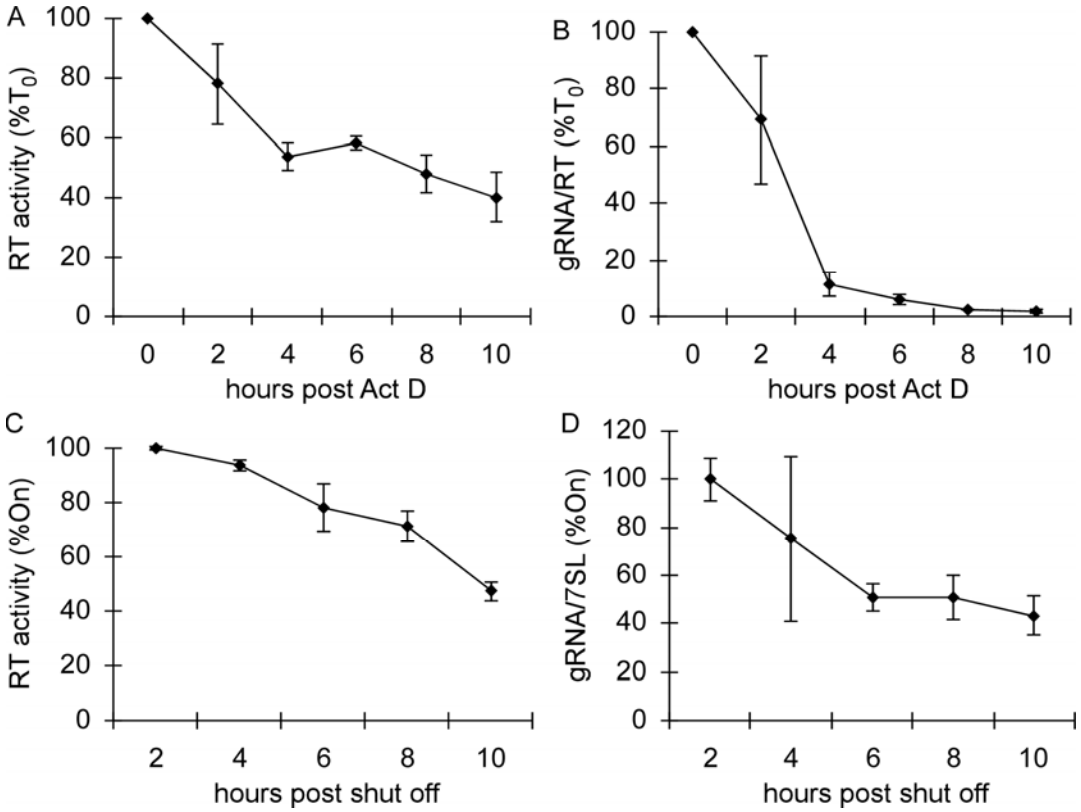

Figure 3-1. RT activities and packaged gRNA levels post transcription inhibition. (A) RT activities of media samples were quantified before and after the addition of 1 μg/ml ActD to chronically-infected NIH-3T3 fibroblasts. For all 2 hour time points, data are represented as values relative to RT activities of media before ActD, which was set at 100%. (B) gRNA packaging from virus harvested before and after ActD treatment was measured by RPA and normalized to RT activity. The gRNA packaging levels per RT before ActD were set to 100% and subsequent time points are plotted as a percentage of this value, T_0. (C) RT activities of media supernatants were quantified for 2 hour time points post specific repression of MLV by Tet removal from cells previously under induction. Data are expressed as values relative to media supernatants harvested at corresponding time points from cells kept under induction. Maximum RT activities were achieved 2 hours after Tet shut off and serum replacement, and this average value was set to 100%. (D) gRNA packaging was quantified by RPA of gRNA per 7SL from virus harvested from 2 hour time points after specific repression of MLV transcription. Large error bar at 4 hours post shut off may indicate no change at this time point, but the subsequent time points reveal a ~2-fold drop in gRNA/7SL. Levels are presented as a percentage of the values obtained for virus harvested from cells kept under induction. Maximum levels again achieved 2 hours after specific repression, and this average value was set to 100%. Data from all the experiments presented here represent the average of two independent experiments.

demonstrating an apparent shorter half-life of gRNA than viral mRNA, these data are consistent with the separation in MLV unspliced RNA fates revealed by ActD treatment. However, the observed decline in gRNA packaging was more modest than seen after ActD treatment.

Transcription inhibition leads to an increase in the randomness of gRNA dimer partner selection.

Previous studies suggest that the majority of MLV gRNAs likely form dimer partner associations at or near sites of transcription (53, 54). This suggests that the bisection in MLV unspliced RNA fate occurs early in the biogenesis of the RNA. Because previous evidence suggests that gRNA packaging persists 8-10 hours post transcription inhibition with ActD (43, 122), albeit at low levels, it was possible to disrupt early events with transcription inhibition and test outcomes on the randomness of dimer partner associations over time after transcription ceased. Therefore, the randomness of dimer partner selection was measured by an RNA capture assay before and after 10-12 hours of ActD treatment (Fig 3-2A and 2B). Untreated samples displayed nonrandom elution ratios that were consistent with previous findings of MLV gRNA preferential self-associations (Fig. 3B) and (53). In contrast, an approximately a two-fold increase in the level of randomness was observed at 10-12 hours after ActD treatment (Fig. 3-2A and 2B). When the elution ratio expected from randomness is set to one, a change in elution ratio from 4.9 pre-ActD treatment to 2.5 at 10-12 h post-ActD treatment was observed. This suggests that a small portion of coexpressed MLV gRNAs are capable of escaping early self-associations and forming dimer partners more

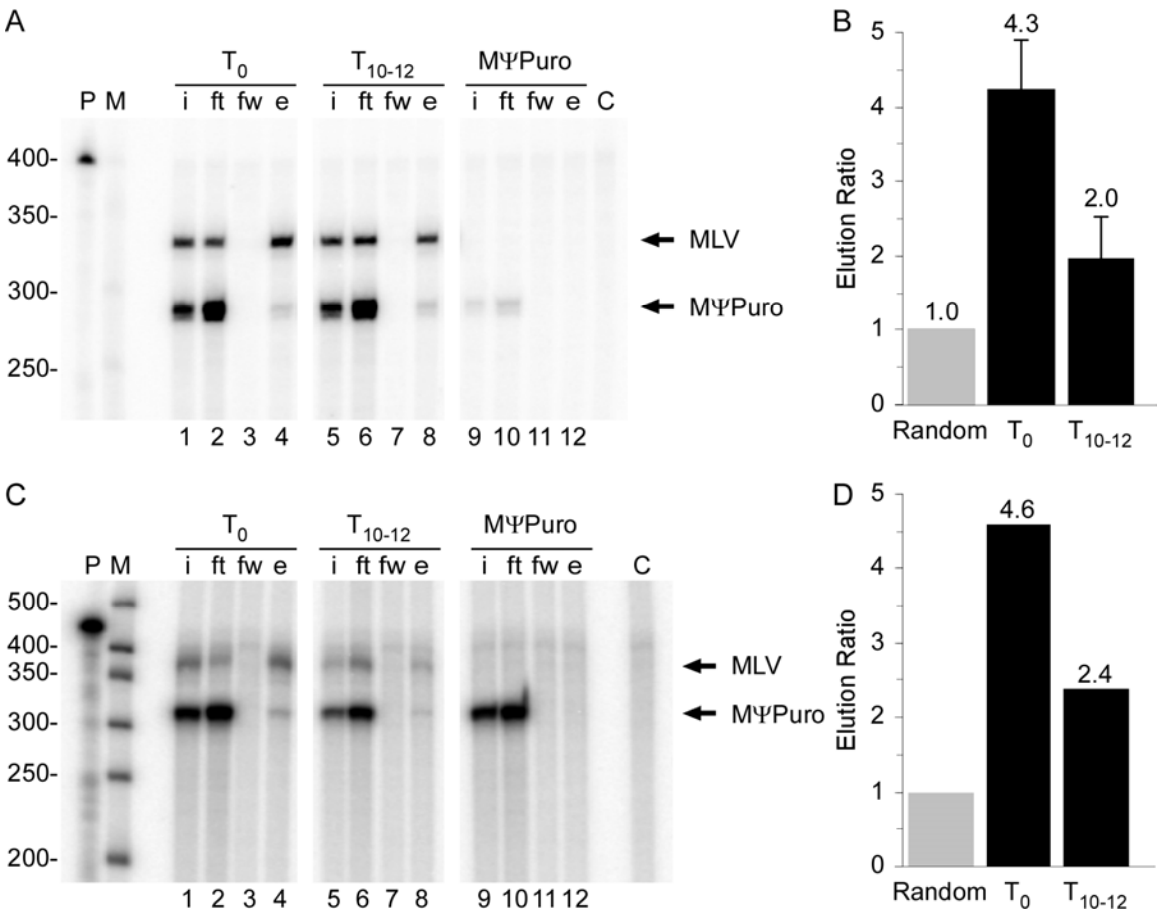

Figure 3-2. Randomness of MLV gRNA dimer partner associations before and after transcription inhibition. (A) RPA of viral RNA from an RNA capture assay of untreated samples, T_0, and samples from 10 to 12 hours after the addition of 1 μg/ml ActD, $T_{10\text{-}12}$. Lane designations indicate the following: i, input; ft, flow through; fw, final wash; e, elution; P, undigested probe; M, RNA marker; and C, no RNA digested probe control. Using the Hardy-Weinberg equation (53), the ratio of MLV and MΨPuro gRNAs in input (i) lanes was used to calculate the ratio of the two gRNAs in the elution lanes expected from randomness. The expected ratio was then compared to empirical elution (e) ratios. (B) comparison of the elution ratios before and 10-12 hours after ActD treatment. The expected elution ratio was set to 1. Data represent the average of two independent RNA capture experiments. (C) RPA of an RNA capture assay of RNA extracted from virions before and 10 to 12 hours after the addition of 100 μm DRB. (D) comparison of the elution ratios before and 10-12 hours after DRB treatment. The elution ratio expected from randomness was set to one. Data represent the quantification of the RPA shown in (C).

randomly later. When the nascent gRNA population is disrupted by transcription inhibition, the remaining gRNAs formed dimer partner associations more randomly.

Increases in randomness of gRNA dimer partner selection are independent of the mode of transcription inhibition.

As another way to address if the randomness of gRNA dimerization seen at late time points post ActD was a direct or indirect effect of ActD treatment, the randomness of dimerization was measured before and after the use of an alternate transcription inhibitor, DRB. DRB specifically disrupts RNA polymerase II (Pol II) elongation by inhibiting phosphorylation of the carboxy terminal domain of the largest Pol II subunit by positive transcription elongation factor b (p-TEFb), a cyclin dependent kinase (211, 223). DRB also activates the DRB-sensitivity inducing factor (DSIF) (210, 223), which causes Pol II pausing in conjunction with negative elongation factor (NELF) (136, 222).

After 10 -12 hours of treatment with 100 μM DRB, a two-fold increase in the level of encapsidated gRNA randomness was observed (Fig. 3-2C and 2D). When the elution ratio expected from random dimer partner associations is set to one, a change from measured elution ratios of 4.6 prior to DRB treatment to 2.4 at 10-12 h post DRB treatment was observed. This result reconfirmed that the increase in the randomness of dimerization that is seen at late time points post transcription inhibition is independent of the mode of transcription inhibition.

A post transcription inhibition increase in recombination parallels the increase in randomness of dimer partner selection.

The tendency of MLV gRNAs to preferentially self associate can fully account for the low rate of MLV recombination relative to that of HIV-1, as measured in two vector

recombination assays (52, 228). Recombination, therefore, provides a sensitive, albeit indirect, measure of the randomness of gRNA dimer associations. To test if disruptions to early events which lead to increased randomness in dimer partner associations also lead to increases in recombination, MLV gRNA recombination was measured from virus harvested at various time points post transcription inhibition (Fig. 3-3A). In the two vector recombination assay used here, recombination between co-packaged gRNAs is monitored using markers for puromycin resistance and β-galactosidase activity (Fig. 3-3A). Only when gRNA heterodimers are packaged is there a potential for the generation of a provirus that will contain both genetic markers (Fig. 3-3A).

Coupling this recombination assay with transcription inhibition provided a means of testing outcomes of disrupting nascent transcript associations on the frequency of gRNA heterodimer packaging. Post transcription inhibition with ActD, a two log drop in titer was observed (Fig. 3-3B). This two log drop was accompanied by a 3-fold increase in recombination at 10 hours after ActD treatment (Fig. 3-3C). Thus, an increase in recombination paralleled the increase in the randomness of dimer partner associations seen above by RNA capture.

The general inhibition of transcription with ActD can alter RNA trafficking pathways, possibly contributing to the observed changes in the randomness of dimer partner associations and recombination. Thus, to further test the notion that a portion of MLV gRNAs can escape early partner associations and form dimers after the completion of transcription, MLV transcription was specifically ablated by taking advantage of the transient nature of gene expression after plasmid DNA transfections. Using the two vector recombination assay, recombination levels were monitored for two time windows

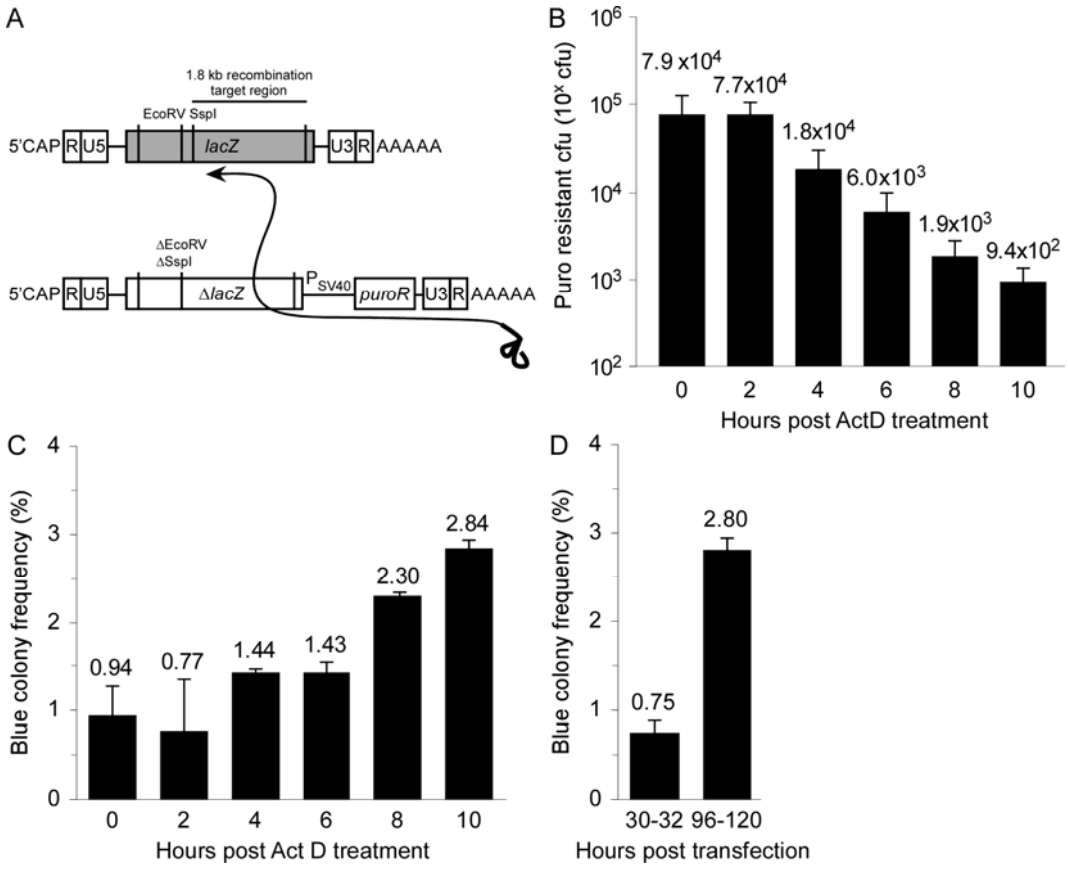

Figure 3-3. Recombination frequency between co-expressed MLV gRNAs post transcription inhibition. (A) heterodimeric recombination in a two-vector single cycle assay. The diagram illustrates recombinogenic template switching between co-packaged gRNAs in the reverse transcription of proviral DNA with a functional β-galactosidase gene and a puromycin resistance cassette. (B) titer after ActD treatment. Titer is displayed as puromycin resistant colony forming units (cfu) from pre-ActD treatment, hour 0, to 10 hours after ActD treatment. (C) levels of recombination reported as the percent of blue colony frequency before and after ActD treatment. Data represent the average of two independent experiments with at least 500 colonies counted per time point per experiment. (D) levels of recombination four to five days after transfection compared to a 30-32 hour time window. The 30-32 hour represents a time window where virion production was at or near peak levels, and the 96-120 hour time point corresponds to more than a two fold drop in virion production as measured by RT activity. Data represent the average of two independent infections, with a minimum of 300 colonies counted per time point per infection.

after transfection: one window for active MLV gene expression and the other when MLV gene expression was likely shutting down. To determine the appropriate time point post transfection, RT assays of media were first used to determine when virion production declined to a similar extent as was observed at 10 hours after ActD treatment. Taking RT assays of media supernatant every 24 hours, a drop of RT activity to at or below 45% of maximum levels was observed 96 to 120 hours after transfection. Therefore, the recombination rate observed with virus harvested at this time point was compared to an earlier time point, 30-32 hours post transfection, that represented a time of active transcription and high virion production. The results indicated a four fold increase in the rate of recombination to a 2.8% blue colony frequency at the late time point post transfection (Fig. 3-3D). This increase was equivalent to the increase observed at 10 hours post ActD treatment (Fig. 3-3C) which suggests that the rise in recombination was a direct consequence of inhibiting MLV gene expression and not an indirect consequence of general transcription inhibition with ActD.

Abundant nuclear MLV unspliced RNA exhibits a low rate of decay that is paralleled by MLV unspliced RNA in the cytoplasm.

The results above point to an early gRNA sorting event, and suggest that MLV gRNA is likely recruited to sites of assembly prior to nuclear export. Dorman and Lever (43) showed that the cytoplasmic MLV unspliced RNA population has a very slow decline compared to encapsidated viral gRNA levels after transcription inhibition. This suggests that gRNA takes a rapid and direct route from its site of synthesis to encapsidation.

To measure the decline in the nuclear MLV unspliced RNA relative to cytoplasmic MLV unspliced RNA, chronically-infected cells were fractionated with digitonin over a 10 hour time window after ActD treatment. Nuclear and cytoplasmic MLV unspliced RNA levels (Fig. 3-4A and 4B) were quantified by RPA and compared to total mouse β-actin mRNA levels (Fig. 3-4C and 4D). A northern blot separately probed for nuclear U1 snRNA and cytoplasmic $tRNA^{Lys1}$ served as a control for the fractionation (Fig. 3-4E and 4F). At all time points, more than 90% of MLV gRNA co-purified with the nuclear fraction (Fig. 3-4A and 4B). In contrast, nuclear and cytoplasmic fractions contained near equal levels of mouse β-actin mRNA prior to ActD treatment (Fig. 3-4C and 4D); however, the levels of β-actin mRNA shifted away from the cytoplasm and became elevated, near 80% of total, in the nucleus after ActD treatment (Fig. 3-4C and 4D), possibly indicating that β-actin mRNA localization is disrupted by ActD. Nuclear U1 levels, which varied by less than 24% throughout the time points tested, were used to normalize relative cell amounts and to determine an approximate rate of decay of nuclear MLV unspliced RNA. Normalizing to U1, nuclear MLV unspliced RNA exhibited a half-life of approximately 11 hours. Over the tested time course, the $tRNA^{Lys1}$ control for the cytoplasmic fraction declined by more than 50%. However, the ratio of cytoplasmic to total MLV unspliced RNA varied by less than 2% over the same time course. Thus, the decline in the levels of cytoplasmic viral RNA per volume paralleled the declines in the nucleus per volume which suggests that the half-life of MLV cytoplasmic unspliced RNA is similar, ~11 hours, to that of the nuclear pool.

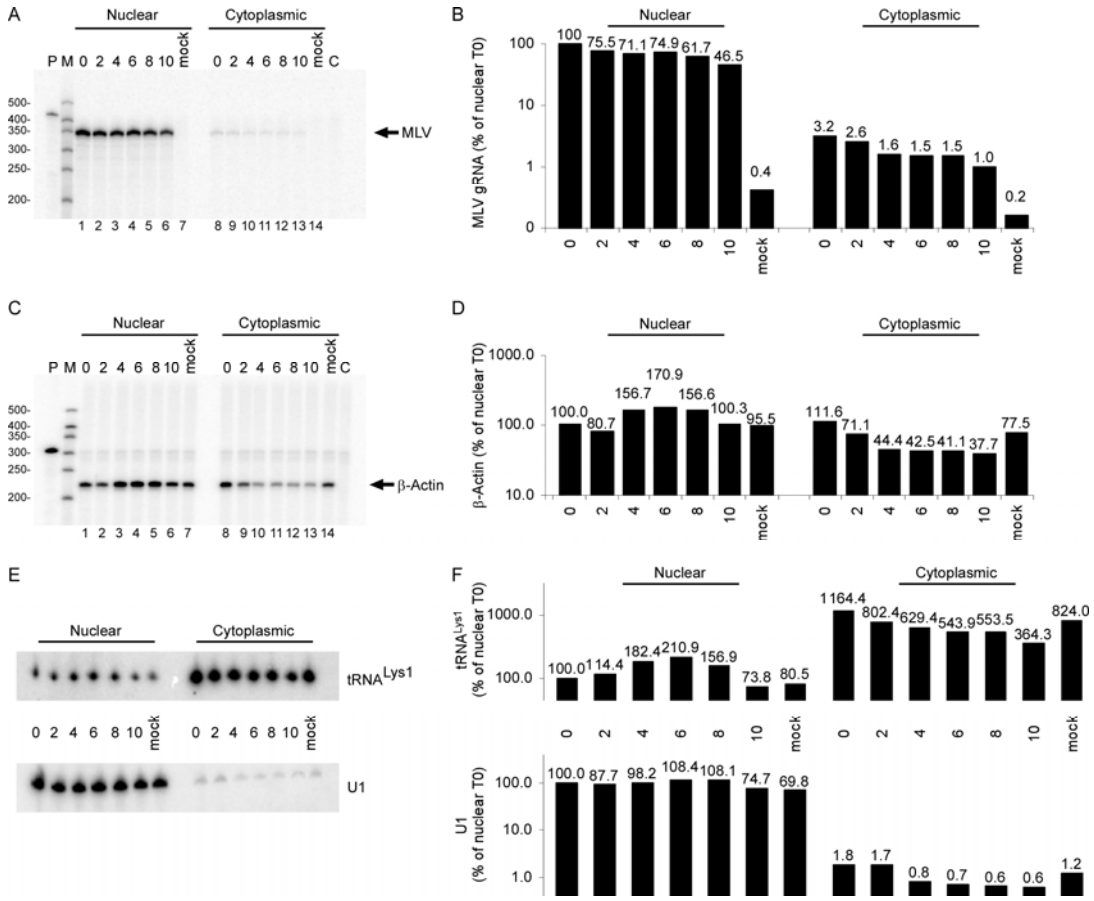

Figure 3-4. MLV unspliced RNA and total β-actin mRNA nuclear and cytoplasmic levels post ActD. (A) RPA of MLV unspliced RNA extracted from nuclear and cytoplasmic fractions of chronically infected NIH-3T3 cells before or after ActD treatment or from mock-infected NIH-3T3 cells. Cells were fractionated with 0.01% (wt/vol) digitonin. (B) Quantification of RPA from (A). (C) RPA of nuclear and cytoplasmic fractions from (A) for total mouse β-actin mRNA. (D) Quantification of RPA from (C). (E) northern blot of nuclear and cytoplasmic fractions from (A) probed separately for nuclear U1 snRNA and cytoplasmic $tRNA^{Lys1}$ for use as fractionation controls. (F) Quantification of northern blots in (E).

Discussion

Where and when retroviral gRNAs are initially recruited for virion inclusion affects the recombinogenic potential of the virus by influencing the make up of gRNA dimer populations. Work performed here tested hypotheses with regards to the initial point of recruitment of MLV gRNAs. Upon specific Tet-repression of MLV transcription, a more rapid decline in gRNA packaging relative to virion production was observed. These observations are consistent with previous findings with ActD which suggested the bisection of MLV unspliced RNA into separate pools of gRNA and mRNA. In order to test the hypothesis that this bisection in RNA fates occurs early in the biogenesis of the RNAs, the effect of transcription inhibition on gRNA dimer populations was analyzed for levels of randomness, using biochemical and genetic assays. Transcription inhibition led to increases in gRNA dimer partner selection and recombination, to levels that were consistent with later gRNA pairings but belied a residual bias for partitioning between gRNA and mRNA fates. Overall, these data are consistent with the initial recruitment of MLV gRNAs from host cell nuclei.

In combination, the more rapid decrease in gRNA packaging relative to virion production and the increases in the randomness of gRNA dimer partner associations and recombination led to our model in which the bisection of MLV unspliced RNAs takes place in the host cell nucleus (Fig. 3-5). In this model, high local concentrations of nascent transcripts favor preferential self associations at or near sites of transcription(Fig. 3-5). This model, however, also suggests that a subset of gRNAs may escape early dimer partner associations and either diffuse or be actively relocated within the nucleus to areas de-enriched for self (Fig. 3-5). Thus, this latter subset of gRNAs may form partner

associations more randomly (Fig. 3-5) and may contribute disproportionately to the small portion of heterozygous virions that are present in co-expression studies. It may be possible that some dimer partner associations do not arise until the unspliced RNAs reach the cytoplasm, but genetic differences between HIV-1 and MLV, differences in the rates of recombination and in the randomness of dimer partner associations in co-expression studies, suggest that very few MLV gRNAs take this route. Whether among the pool of nascent transcripts or the low level gRNA dimers that form later, nuclear dimer partner associations represent an initial point of recruitment and a likely branch point in the divergence of MLV unspliced RNA to separate fates of gRNA or mRNA.

In this model, nuclear dimer partner associations could function to switch the RNA into a fold that is subsequently recruited by MLV Gag to sites of assembly. In the upcoming Chapter IV, the RNA switch hypothesis linking gRNA dimerization to packaging is discussed in more detail. Briefly, *in vitro* evidence suggests that gRNA dimerization exposes high affinity NC binding sites within the MLV Ψ that function in gRNA packaging (36). Our results suggest that MLV gRNA may form dimers in the host cell nucleus which would lead to exposure of high affinity NC binding sites. Thus, binding of Gag to dimeric RNA in the host cell nucleus could function in the bisection of MLV unspliced RNA fates by routing this dimeric gRNA to plasma membrane sites of assembly.

Consistent with results from general transcription inhibition, specific Tet-repression of MLV transcription led to a decline in gRNA packaging that was more rapid than the decline in virion production; however, gRNA packaging levels did not decrease to the same extent after Tet-repression as was observed after global inhibition with ActD.

The more moderate decline in gRNA packaging from specific Tet-repression of MLV transcription could indicate that other factors, which are involved in the initial recruitment of MLV gRNAs, are disrupted by general transcription inhibition but not by specific inhibition of MLV transcription.

Disruptions to protein shuttling between the nucleus and cytoplasm caused by ActD treatment may sequester cellular or viral factors that function in MLV gRNA recruitment. Cellular factors demonstrated to be disrupted by ActD treatment include the protein components of heterogenous nuclear ribonucleoprotein complexes (hnRNPs) (159) which are highly abundant in the host cell nucleus and are among the first proteins to bind nascent Pol II transcripts (44, 45). Candidates among the transcription-dependent hnRNPs that may differentially effect MLV versus HIV-1 unspliced RNA pools are hnRNP A1 and hnRNP A2, which are retained in the cytoplasm after ActD treatment (159). HIV-1 over-expression has been shown to induce the cytoplasmic retention of hnRNP A1 (125), and over-expression of either hnRNP A1 or A2 decreases virion production and increases nuclear retention of HIV-1 unspliced RNAs (85). Disruption of hnRNP A2-response elements leads to increased nuclear retention of HIV-1 unspliced RNA and decreased packaging (12). These data suggest that hnRNP proteins may function in the localization and initial recruitment of HIV-1 gRNAs to sites of assembly. HIV-1 unspliced RNAs, which likely form dimers in the cytoplasm (128), are not, therefore, sequestered from these potential recruitment cofactors after ActD treatment, but MLV gRNAs, which likely form nuclear dimer partner associations, might be compartmentally isolated from these cellular RNA binding proteins after ActD treatment.

Alternatively, the disruption to nuclear-cytoplasmic shuttling could impact a viral factor involved in the initial recruitment of MLV gRNA. MLV Gag has not been demonstrated conclusively to shuttle between the nucleus and cytoplasm. However, Nash et al. (137) reported that 18% of MLV-infected cell-associated Gag immunoprecipitated from nuclear fractions. Gag trafficking through the nucleus at late phases in replication is not widely established among retroviruses, but studies of avian sarcoma virus have shown that a portion of Gag transits through the nucleus en route to sites of assembly (176-178). Gag, in particular the NC domain of Gag, has been demonstrated to function in activating gRNA dimerization *in vitro* (68). The NC domain of Gag also mediates gRNA recruitment (72, 168, 169). General transcription inhibition could sequester Gag in the cytoplasm and prevent interaction with nuclear MLV unspliced RNAs. Tet-repression of MLV transcription might not alter this trafficking pattern, and the more modest decline in gRNA recruitment relative to that seen with general transcription inhibition could be indicative of the singular effect of reducing nascent transcripts but not exposure to the *trans* acting protein component of the initial retroviral RNP.

Perhaps the simplest explanation for the discrepancy between the declines in gRNA packaging from Tet-removal versus ActD treatment is that the repression in the Tet-inducible system results in an incomplete shut off of MLV transcription. Media from Tet-regulated MLV expressing cells that were never exposed to tetracycline contain low levels of 7SL and MLV gRNAs (~30-fold less than On levels and ~10-fold above no RNA controls). When used to initiate a spreading infection in fresh target cells, supernatants from uninduced cells gave rise to RT positive supernatants at 5 days post

infection, which was 2 days later than cells infected from a comparable volume of supernatants from induced cells. Together, these data suggest that even uninduced Tet-regulated MLV expressing cells produce low levels of virus. Thus, low level expression of MLV transcripts may continue to be recruited into assembling virions. Low level MLV expression could then account for the more moderate effect on gRNA packaging seen here by specific Tet-repression. The observed more rapid decline in gRNA packaging relative to virion production might then represent a direct effect of inhibiting MLV expression rather than an indirect effect on an additional viral or cellular factor involved in gRNA recruitment.

Increases in the randomness of MLV dimer partner associations and in recombination at late time points suggest the existence of an alternate pathway of initial gRNA recruitment. However, the levels of increase in both randomness of dimerization and recombination do not reach the level of randomness exhibited by HIV-1. Therefore, this alternate pathway continues to exhibit dimer partner associations which are consistent with gRNA recruitment taking place prior to nuclear egress.

The mode of nuclear export may function further in the subcellular spatial-segregation of partitioned MLV gRNAs and viral mRNAs. Retroviruses use different pathways to export their unspliced RNAs from the nucleus, and the manner of export affects subsequent protein functions as well as the cytoplasmic compartmentalization of viral unspliced RNAs. How MLV unspliced RNA is exported from the nucleus is not known, but the mode of unspliced RNA nuclear export is known for other retroviruses. To translocate from the nucleus to the cytoplasm, a constitutive transport element (CTE) on Mason-Pfizer monkey virus (M-PMV) unspliced RNA interacts directly with the

cellular nuclear export factor Nxf1 (32, 78). In HIV-1, the viral protein Rev mediates translocation of HIV-1 unspliced RNA from the nucleus to the cytoplasm through interaction with a Rev response element in the unspliced viral RNA (31) and the cellular shuttling protein Crm1 (138). Changing the mode of nuclear export of HIV-1 gag-pol mRNAs from the native Rev/RRE/Crm1 pathway to the CTE/Nxf1pathway restored Gag trafficking to cellular membranes and HIV-1 budding in murine cells (200). Recently, Moore et al. (128) showed that HIV-1 co-expressed gRNAs randomly associate and exhibit normal high level recombination when they both exit the nucleus via the same (either Crm1 or Nxf1) pathway. However, when co-expressed HIV-1 gRNAs exit through different pathways, they exhibit non-random dimer associations or preferential self-associations, and lower levels of recombination (128). In the context of our results here, in which MLV unspliced RNAs appear to sort in the host cell nucleus, nuclear export of monomeric viral mRNAs versus dimeric gRNA likely further spatially segregates these RNA pools (Fig. 3-5).

Previous work in our lab on the packaging of mY RNAs provides additional support for the model of nuclear gRNA recruitment. Mouse mY RNAs are among the most highly packaged noncoding cellular RNAs by MLV (149). While mY RNA levels are severely reduced in cells that lack Ro60 (185), the cognate cellular mY RNA-associated RNP protein, virions produced from Ro60 knockout cells continue to package very high levels of mY RNAs (65). This suggests that mY RNAs may be recruited early in their biogenesis within the host cell nucleus. The recruitment of cellular mY RNAs, therefore, indicates a nuclear subassembly step in MLV replication which may represent

a nuclear intersection between cellular noncoding mY RNA recruitment and the initial recruitment of MLV gRNAs.

The findings here, which support an early bisection in MLV unspliced RNA fates, add to the growing evidence for a nuclear subassembly step in MLV replication. This nuclear step in MLV assembly contrasts with the recent findings of cytoplasmic gRNA dimerization in HIV-1 (128). The results here suggest a distinct RNA trafficking pathway that transits dimeric MLV gRNA rapidly and directly from the nucleus to plasma membrane sites of MLV assembly.

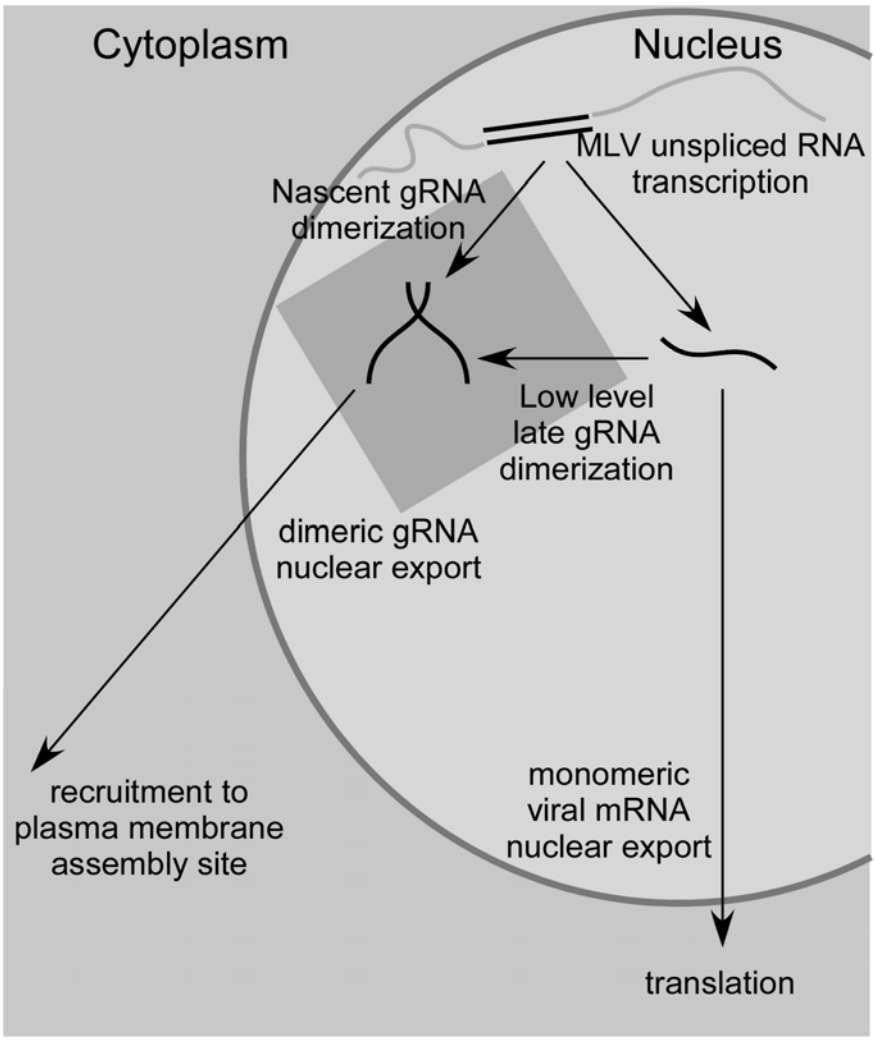

Figure 3-5. Model of nuclear MLV unspliced RNA sorting. A model for the bisection of MLV unspliced RNA into gRNA and viral mRNA fates, based on observations reported here. The majority of MLV gRNAs are subject to an early dimerization event. However, a subset of MLV gRNAs may escape early dimerization and form dimer partner associations more randomly later. The oval represents the nucleus, and the gray box within the nucleus indicates the likely stages of MLV unspliced RNA biogenesis where dimeric gRNAs are first recruited towards sites of assembly.

CHAPTER IV

An RNA structural switch in the 5' leader of Moloney murine leukemia virus genomic RNA regulates diploid genome packaging.

Abstract

Retroviral genomic RNAs (gRNA) are recruited in pairs. This fundamental property of retroviruses suggests that the mechanism of gRNA pair associations is coupled to how gRNAs are recruited into assembling virions. Recent *in vitro* studies of Moloney murine leukemia virus (MLV) gRNA interactions with the nucleocapsid (NC) protein, a domain of Gag, support an RNA switch model whereby dimerization exposes *cis*-acting gRNA residues that participate in high affinity interactions with NC, as part of Gag. These high affinity interactions then are hypothesized to recruit the gRNA dimer into assembling virions. Further testing this model in collaboration with work performed here, Miyazaki et al (124) quantified the number of high affinity NC interactions of *in vitro* transcribed RNAs corresponding to wild type Ψ (Ψ^{WT}) and a dimerization-defective mutant Ψ (Ψ^{M}) that contained GNRA residues which stabilized Ψ-hairpins. The Ψ^{WT} RNA bound ~12 NC molecules with high affinity (Kd ~17 nM), and the Ψ^{M} RNA, in contrast, only bound 1 NC molecule with high affinity. Here, the *in vivo* packaging of Ψ^{M}-containing full length MLV gRNAs was compared to the packaging of Ψ^{WT}-containing gRNAs, and results indicated that Ψ^{M} mutations which disrupt dimerization *in vitro* also led to a near 100-fold decrease in gRNA packaging *in vivo*. The low level of

gRNA packaged into virions produced from Ψ^{M} constructs also exhibited lower thermostability than Ψ^{WT} gRNAs, which indicates an *in vivo* dimer stability defect that parallels the *in vitro* phenotype. Using a mutant NC that disrupts the hydrophobic cleft of the zinc finger and impairs high affinity RNA binding, NC function in specific (Ψ^{WT}) and nonspecific (Ψ^{M}) gRNA packaging was quantified, and results indicated that the relatively efficient packaging of Ψ^{M} gRNAs produced by transient transfection was likely due to low affinity NC-RNA interactions. Our results here provide *in vivo* support for an RNA conformational switch model of gRNA packaging, and they also demonstate the potential use of *cis* and *trans*-acting mutants with defects in gRNA dimerization and/or packaging in the further study of our model of MLV nuclear gRNA dimerization.

Introduction

Retroviruses selectively package two unspliced genomic RNAs (gRNAs) from a large excess of cellular mRNAs. The nucleocapsid domain (NC) of Gag has been demonstrated to function in the specific recruitment of retroviral unspliced RNAs which contain *cis*-acting packaging signals (called Psi or Ψ) (36, 168). The exact mechanism by which NC mediates gRNA recruitment and the specific incorporation of Ψ-containing RNAs into assembling virions is an area of active research (36).

In vitro structure and function analysis of NC-Ψ interactions suggests that Moloney murine leukemia virus (MLV) uses an RNA switch mechanism for gRNA packaging whereby gRNA dimerization functions to switch the RNA into a conformation that exposes high affinity NC binding sites (34, 36). The previous findings in support of this model include observations of high NC binding affinities for synthetic oligoribonucleotides that contain portions of Ψ (Kd of ~55 nM) (35). Also, NMR analysis of a 101 nucleotide (nt) mutant Ψ-construct, designed to remain monomeric but retain intramolecular base pairing of the dimer, revealed a single NC-Ψ interaction between the CCHC zinc finger of NC and UCUG nucleotides on the RNA (34). Synthetic oligoribonucleotides with similar Py-Py-Py-G sequences (Py = pyrimidines) bound NC with high affinities between 94 to 315 nM (42). This motif and similar UCUG sequences are more abundant in the 5' UTR and Ψ region than in the rest of the gRNA. Because most of these sequences are sequestered by base pairing in the monomeric form of the RNA, the observations of high affinity NC binding to this motif supports a model in which dimerization functions to expose single stranded UCUG motifs that then bind NC with high affinity.

The MLV Ψ within the 5' UTR functions in both gRNA dimerization and packaging. Pair associations near the 5' ends of MLV gRNAs, termed the dimer linkage structure (DLS), were first visualized by electron microscopy (134). The importance of this region on gRNA packaging was demonstrated by a 353 nt deletion within the 5' UTR of MLV gRNA that reduced gRNA packaging to undetectable levels by northern blot (115). A ~70 nt portion of this region was shown to be sufficient to confer packaging of heterologous RNAs into MLV particles, and it was termed the core encapsidation signal (CES) (2, 129). *In vitro* synthesized RNAs of this region, including downstream sequences that extend into *gag*, spontaneously form dimers in a process that can be catalyzed by NC (162). Using oligo-accessibility mapping and competition experiments, Prats et al. (162) demonstrated that nts 280 to 308 and 310 to 329 (nt positions relative to the 5' end of the gRNA) function in the DLS of MLV. Additional sequences that function in the DLS were subsequently mapped to nts 204 to 228 (152). Ly and Parslow (111) used point mutations and antisense inhibition to show that nts 204 to 228 and 283 to 298 function as a bipartite signal in MLV gRNA dimer initiation and DLS stabilization *in vitro*. These regions were termed dimer initiation site 1 and 2 (DIS-1 and DIS-2). The region of MLV Ψ from DIS-1 through the end of the CES forms four putative stem loops (termed DIS-1, DIS-2, SL-C and SL-D) which have been extensively studied and further demonstrated to function in gRNA dimerization and NC-dependent gRNA packaging (Fig. 4-1) (36).

The NC domain of Gag specifically recruits MLV gRNA into assembling virions (13, 38, 168). The importance of NC in MLV gRNA packaging was first demonstrated by point mutations in the zinc finger of the NC domain that disrupted gRNA packaging and

infectivity (72, 121). The specificity of the MLV NC domain for recruitment of MLV Ψ-containing RNAs was demonstrated using chimeric Gag polyproteins (14). Packaging of MLV Ψ-containing RNAs was achieved by swapping the human immunodeficiency virus type 1 (HIV-1) NC domain for the MLV NC domain (14). Thus, the MLV NC domain is sufficient to confer packaging of heterologous RNAs that contain the MLV Ψ into HIV-1-derived virus like particles.

The MLV NC domain participates in low and high affinity interactions which may function in the RNA switch mechanism of gRNA packaging. In addition to its role in specific gRNA packaging, the NC domain has been shown to catalyze gRNA dimerization through low affinity gRNA-protein interactions (68, 162). In the context of the RNA switch model of MLV gRNA packaging mentioned above, this suggests that low affinity NC-gRNA interactions lower the activation energy of gRNA dimerization which then exposes high affinity NC binding sites on the gRNA. Using an *in vitro* NC binding assay and isothermal titration calorimetry, Miyazaki et al. (124) quantified the number of high affinity NC binding sites in 476 nt *in vitro* transcribed Ψ-containing RNAs with a wild type Ψ (Ψ^{WT}) or a dimerization mutant Ψ (Ψ^{M}) (Fig. 4-1A). The Ψ^{WT} RNA bound approximately 12 molecules of NC with high affinity (Kd ~17 nM) in contrast to the Ψ^{M} RNA which bound 1 molecule of NC with high affinity (Kd ~29 nM) (124). These data directly support the model that gRNA dimerization functions as an RNA switch that exposes additional high affinity NC binding sites.

Here, the packaging of gRNAs that contain Ψ^{M} dimer disrupting mutations or three Ψ sub-deletions were quantified relative to Ψ^{WT}-containing gRNAs in a tissue culture-based packaging system(Fig. 4-1A and 1B). MLV gRNA packaging was

measured using RNA isolated from MLV virions produced by transient transfection with a Ψ^{WT} competitor, and by single-copy integrated proviruses. Results indicated that mutations which disrupt dimerization and NC binding *in vitro* inhibit gRNA packaging *in vivo*. Furthermore, the NC dependence of gRNA packaging was addressed using an NC point mutant with a change that disrupts the hydrophobic cleft of the NC zinc finger pocket which NMR data suggest mediates specific NC-gRNA binding. Finally, Ψ^{M}-containing gRNAs were used to test predictions from the model presented in Chapter III that nuclear MLV unspliced RNA bifurcation and dimer partner associations lead to MLV gRNA preferential self-associations. Together, our results provide further evidence that gRNA dimerization acts as a switch to expose high affinity NC binding sites that can then function in gRNA recruitment, and our preliminary observations suggest that disrupting gRNA dimerization inhibits nuclear gRNA associations.

Materials and Methods

Plasmids for virology. MLV RNA packaging was assessed using derivatives of the MLV-based *gag-pol-puro* plasmid, pGPP (pSRK876-15) (indicated in the figures here as "WT"), which contains an intact provirus modified by the replacement of the *env* open reading frame with a puromycin N-acetyltransferase gene (puroR) driven by a simian virus 40 (SV40) promoter (158) (Fig. 4-1C). The "classic Ψ" deletion of Mann and Baltimore (Δ215-568) (pEG455-11) (115), sub-deletions Δ215-367 (pEG455-8) and Δ375-568 (pEG455-24), and the Ψ^{M} mutant (pSRK910-1) were generated by overlap extension PCR, sequenced, and used to replace the corresponding portions of pGPP (Fig. 4-1A and 1B). The W35G NC mutation was generated by overlap extension PCR and used to replace the corresponding portion of pGPP; the resulting plasmid used here was pEG479-1. The double mutant containing Ψ^{M} and W35G NC, pSRK1342-3 was generated by restriction fragment subcloning. The helper plasmid pNGVL-3'-gag-pol, which expresses MLV Gag and Gag-Pol from a 5' leader-deleted transcript driven by the CMV promoter, has been described previously (225). The competitor plasmid pBAG encodes a retroviral vector with a wild type MLV 5'-UTR and *lacZ* (163).

For RNA capture experiments, MΨPuro (pAM86-5 (98))-derived vectors were created that contained short sequences from *pol* (nts. 2741-3141 from MLV transcription start site, BclI-MfeI) which were complementary to the biotinylated oligo (the oligo binding domain, OBD) used for the captures. These MΨPuro-OBD plasmids were subcloned to contain either Ψ^{WT} (pEG402-1) or Ψ^{M} (pEG427-3). Ψ^{WT} pEG402-1 was co-transfected with pAM86-5 as a control for wild

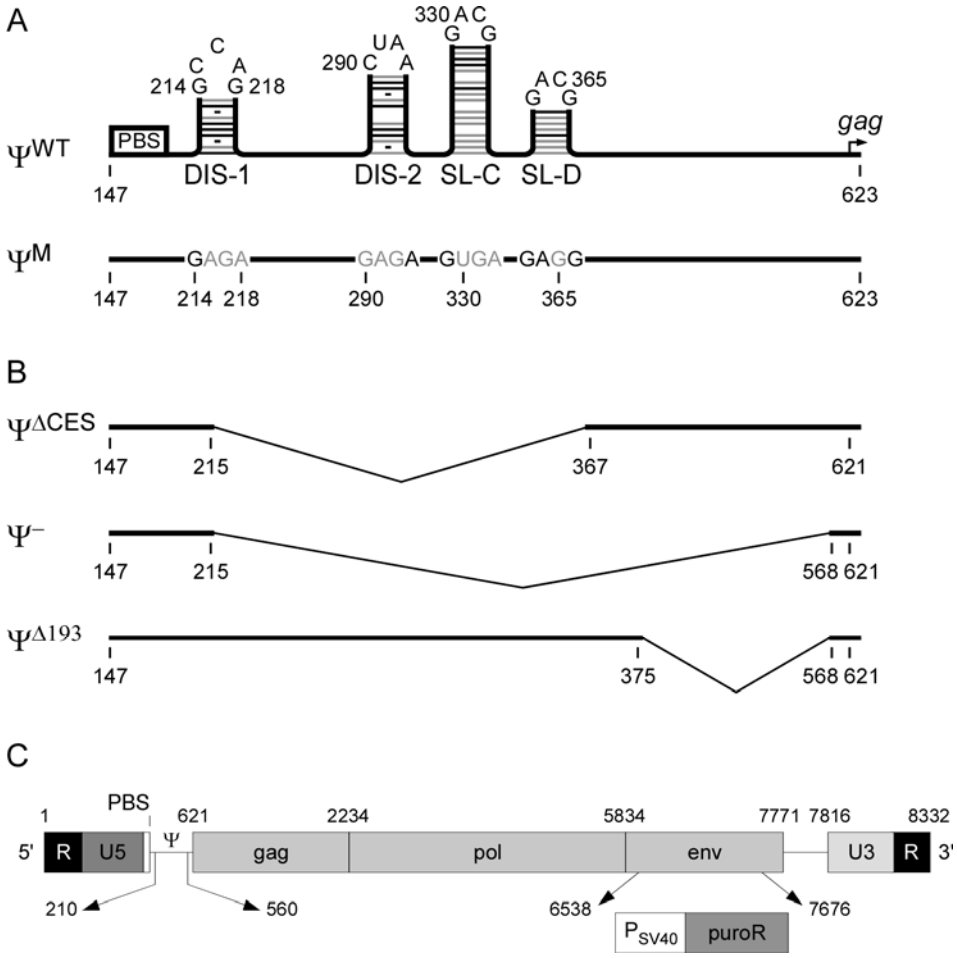

Figure 4-1. Ψ constructs and MLV-based *gag-pol-puro* (GPP) cassette. (A), location of Ψ^{WT} DIS-1 and core encaspsidation signal (CES) hairpins (DIS-2, SL-C, and SL-D) and the corresponding hairpin stabilizing mutations in the Ψ^{M} dimerization mutant, indicated as gray bases in Ψ^{M}. (B), location of the three Ψ deletions ($\Psi^{\Delta CES}$—a deletion of DIS-1 thru SL-D; Ψ^{-}—a "classic Ψ" deletion of Mann et al. (115); and $\Psi^{\Delta 193}$—a deletion sequences downstream of the CES but within the classic Ψ) in relation to the PBS, the four Ψ stem loops, and the first base of *gag*, nt. 621. (C), the location of Ψ and the puromycin resistance expression cassette (P_{SV40}; puroR) in the GPP-derivative plasmids used for all the work reported here. Portions of Fig. 4-1, A & B, were adapted from Miyazaki et al. (124). Figures are not to scale.

type in RNA capture assays, and a Ψ^M version of pAM86-5 (pEG427-6) was cotransfected with pEG427-3 to test the randomness of Ψ^M gRNAs.

All riboprobe templates were derivatives of pBSII SK(+) (Stratagene). The insert in pEG467-10, which was generated by PCR and subcloned into the pBSII SK(+) EcoRV site, included complementarity to portions of both the MLV 5' untranslated region (nts. 55-214) and 100nt of 7SL RNA (149). pSRK38-7 is an HIV-1 *pol*-7SL chimeric riboprobe template described previously and used here as a probe for 7SL RNA (150). pSRK1216-71 was generated by sequentially subcloning a Cla I-Ssp I fragment of *lacZ* and a Bgl II-Xba I MLV *pol* fragment from pNCA (28) into pBSII SK(+) digested from Cla I-EcoRV and BamHI-Xba I, respectively. The insert in pEG349-1 included 92 nts. of *pol* (nts. 3050-3141) and an adjacent 324 nts. of SV40 promoter sequences.

Cells and virus. 293T cells (human embryonic kidney cells expressing SV40 T antigen) were grown in Dulbecco's modified Eagle's medium supplemented with 10% fetal calf serum and 1% penicillin-streptomycin. Virus was produced by transient transfection of the pGPP or pNGVL-3'-gag-pol plasmids into 293T cells by calcium phosphate precipitation (225). Virus-containing media were harvested at 24, 36, and 48 hours post transfection, pooled, filtered through a 0.2-μm filter, and stored at -70ºC prior to use. Some of this transiently produced virus was used to infect ET cells, which are a 293T derivative that constitutively expresses ecotropic envelope (158). These infections were used for measuring titers and creating the pools of stably integrated proviruses used in later experiments. Virus-containing media harvested from the ET cell pools were harvested and analyzed for RT content and packaged RNA content using the assays described below.

Exogenous reverse transcriptase (RT) assay. Virus was harvested, filtered through 0.2-μm filters, and stored at -70 ºC. Quantitative RT assays of media supernatants as a means of quantifying virion production were performed using modifications of a standard protocol (70) as described previously (172). Products were quantified by PhosphorImager analysis.

Ribonuclease protection assays. Cellular RNA was extracted using TRIzol ® reagent (Invitrogen) according to the manufacturer's protocol. To generate riboprobes for measuring cellular gRNA/7SL levels, two riboprobes were used. To detect 7SL, pSRK38-7 was linearized with SalI and transcribed using T7 RNA polymerase (Promega) and [γ-^{32}P] rCTP to create a 344 nt transcript which protected 101 nt of 7SL RNA. To detect MLV gRNA, pSRK1216-71 was linearized with XhoI and transcribed using T3 RNA polymerase (Promega) to generate a 693 nt transcript which protected 206 nt of MLV *pol* RNA (nts. 5120-5325). In packaging competition experiments, pSRK1216-71 693 nt transcript was used to detect both Test RNAs (by protecting a 206 nt *pol* fragment) and the Control pBag vector (by protecting a 408 nt *lacZ* fragment).

For measuring viral gRNA/7SL ratios and for RNA capture assays, RNA was isolated from pelleted virions using a previously described proteinase K-based extraction protocol (53) and quantified by RPA using a 365 nt chimeric MLV-7SL riboprobe templated by linearized pEG467-10, which protected 160 nt of Ψ^{M} or 163 nt of wild type and Ψ deletion mutant gRNAs, plus 100 nt of 7SL RNA.

For measuring gRNA ratios in RNA capture assays, pEG349-1 was linearized with HindIII and transcribed with T3 RNA polymerase (Promega) to generate a 491 nt

transcript which protected 440 nts. of MΨPuro-OBD-type gRNAs (designated as "MLV" in Fig. 4-6) and 324 nts. of MΨPuro-type gRNAs (designated as "MΨPuro" in Fig. 4-6).

Previously described RPA approaches (149) were modified by extending hybridization times to 16h and digesting using only RNase T1. Bands were quantified by PhosphorImager and adjusted for the number of radiolabelled Cs protected. RNA packaging was quantified by normalizing the amount of MLV RNA in each lane to the amount of co-packaged 7SL.

Non-denaturing northern blot. MLV viral RNA was isolated from pelleted virus by the proteinase K-based extraction protocol above and resuspended in 1× TENS buffer (10 mM Tris pH [8.0], 1 mM EDTA, 1% (w/v) SDS, and 100 mM NaCL). Samples were incubated for 10 min at the indicated temperatures then placed on ice until loaded on a non-denaturing 0.7% (w/v) agarose gel. RNA was electrophoretically transferred to a Zeta-Probe® GT nylon membrane (Bio-Rad). Prehybridization was performed at 45ºC for 2h in 6× SSC (1× SSC is 0.15 M NaCL plus 0.015 M sodium citrate) – 5× Denhardt's solution–0.5% sodium dodecyl sulfate (SDS) – 0.025 M sodium phosphate – 625 μg/ml of denatured salmon sperm DNA. The oligonucleotide probe was an anti-MLV R probe: 5'-actgcaagagggtttattggatacacgggtacc-3' that was 5'-end labeled using [γ-^{32}P] ATP (Perkin-Elmer) and T4 polynucleotide kinase (NEB). Hybridization was performed at 45ºC for 16 h. The blot was washed twice with 2× SSC – 0.1% (w/v) SDS at 50ºC for 15 min followed by 2 washes with 0.33× SSC – 0.1% (w/v) SDS at 50ºC for 15 min. Washed blots were exposed to PhosphorImager screens for subsequent ImageQuant analysis/band quantification.

RNA capture assay. The RNA capture assay protocol--an oligo-mediated dimer pull down assay--was adapted from that previously described and used to measure the randomness of dimer partner associations (53). The modifications included increasing the number of washes to 7 and increasing the stringency of the washes by lowering the salt concentration of the wash buffer to 0.33× SSC (50 mM NaCl).

Results

Mutations that inhibit dimerization and NC binding *in vitro* inhibit RNA packaging *in vivo*.

The effects of Ψ region mutations on MLV RNA packaging were assessed initially by quantifying RNA packaging levels in virions produced by transient transfection. An MLV-based vector construct, pGPP, containing the 5' terminal two-thirds of the MLV genome, including the 5'-UTR, *gag* and *pol* genes, and a puromycin N-acetyltransferase expression cassette in place of *env* (158) was used to generate both viral proteins and genomic RNAs (gRNAs) (Fig. 4-1C). Derivatives of pGPP containing wild type or mutant 5'-UTRs (Fig. 4-1A and 1B) were expressed in 293T cells, and gRNA levels in the cells and the resulting virions were determined by RNase protection assay. Virions were normalized with 7SL RNA, a host RNA that is packaged in HIV-1 and MLV at levels proportionate to virion proteins (149, 150). Results are shown in Figure 4-2.

Intracellular levels of wild type and mutant gRNAs differed by less than three-fold (Fig. 4-2A), and virus production (as determined by reverse transcriptase (RT) activity) was roughly proportionate to intracellular viral RNA levels. This indicated that the 5' UTR mutations did not significantly affect transcription, translation, or virion assembly. However, deletion of either the core encapsidation region (Δ215-367, $\Psi^{\Delta CES}$) or the extended packaging region (Δ215-568, Ψ^{-}) (115) reduced RNA packaging to roughly 1% of wild type levels. In contrast, deletion of a large fragment located immediately downstream of the core encapsidation region (Δ375-568, $\Psi^{\Delta 193}$) decreased

packaging by less than two-fold (Fig. 4-2B and 4-2C). Packaging levels measured by quantifying gRNA per virion, normalized to either RT or to 7SL RNA packaging, yielded very similar results (Fig. 4-2B and 4-2C), and both measures indicated that the Ψ^{M} is packaged at ~8% of wild type levels. Thus, the UTR variants that were dimerization defective *in vitro* were also packaging defective in virus. When normalized by RT levels, the puromycin-resistant colony forming unit (cfu) titer of Ψ^{M} mutant virion-containing media was about 10-fold less than either wild type or $\Psi^{\Delta 193}$, and both Ψ^{-} and $\Psi^{\Delta CES}$ titers were reduced an additional 10- to 20-fold (data not shown). Thus, reverse transcription was not altered by these 5' UTR mutations.

Although packaging levels of the Ψ^{M} mutants were reduced in the above experiments, the over-production of the mutant RNAs in transfected cells might have caused packaging levels to be artificially high, since retroviruses can efficiently package RNAs that lack Ψ sequences under conditions in which the native genomes are not present (48). Therefore, we next measured packaging efficiencies using a competition assay, in which "test" genomic RNAs (gRNAs) containing either wild type or mutant 5' UTRs were co-expressed with a control gRNA containing a wild type 5' UTR, and ratios of test to control gRNAs were determined in both virus and cells (Fig. 4-2D). As shown in Fig. 4-2D, the presence of a wild type competitor gRNA depressed packaging of both the Ψ^{M} and $\Psi^{\Delta CES}$ mutants to ~ 1% of wild type levels, suggesting that at least some Ψ mutant RNA packaging observed under the transient transfection conditions above was nonspecific.

Finally, gRNA packaging was assessed in virions produced by cells that contained single-integrated proviruses. Pools of puromycin-resistant cells generated by infection

with GPP derivatives at low (<0.01) multiplicity of infection were used to generate virions, and the virion and intracellular levels of the respective gRNAs were compared. As shown in Fig. 4-2E-2G, Ψ^{M} gRNA packaging levels were reduced 100-fold relative to wild-type levels under these conditions, which resemble those that occur during natural infection. These results are consistent with those obtained using the competition assay, and provide further evidence that much of the Ψ^{M} packaging observed under transient transfection conditions was due to non-specific packaging of the overproduced RNA.

Inefficiently packaged Ψ^{M} gRNAs exhibit reduced thermal stability

The relatively efficient encapsidation of Ψ^{M} gRNAs under transient transfection conditions provided a way to generate Ψ^{M} gRNAs in sufficient quantities for examination on non-denaturing northern blots, to test whether or not the encapsidated RNAs existed in the metastable dimer linkage characteristic of wild type MLV gRNAs (82). To address this, vectors with Ψ^{WT}, Ψ^{M}, and $\Psi^{\Delta CES}$ – containing 5' UTRs were overexpressed by transient transfection, and virion RNAs were purified under non-denaturing conditions. Virion RNA samples normalized for gRNA content were subjected to heat treatments based on previously determined genome melting profiles (82), and examined on non-denaturing northern blots (Fig. 4-3). The results showed that wild type gRNAs displayed properties as described previously (58, 81): running as a fairly discrete dimer when unheated, displaying a small amount of monomer but principally residual dimer at 58 °C, and denaturing fairly completely to the monomer form—albeit with a significant amount of the RNA degradation characteristic of retroviral gRNAs—when incubated at 65 °C (Fig. 4-3). In contrast, unheated Ψ^{M} and $\Psi^{\Delta CES}$ virion gRNAs appeared as diffuse, slowly-migrating bands that resolved mainly to monomers or a smear with reduced mobility at

Figure 4-2. RPA quantification of gRNA packaging for gRNAs containing wild type and mutant Ψs. (A-C) Packaging of Ψ mutant gRNAs in virus produced by transient transfection. (A) Intracellular expression of Ψ mutant RNAs. MLV wild type and Ψ mutant gRNA levels were normalized to 7SL RNA by RNase protection assay (RPA) of total RNA extracted from transiently transfected cells. Lane 1: mock-transfected cell sample; lane 2: cells transfected with pGPP Ψ^{WT}; lane 3: cells transfected with pGPP derivative with Ψ^{M}; lane 4: with $\Psi^{\Delta CES}$; lane 5: with Ψ^{-}; lane 6: with $\Psi^{\Delta 193}$; lane 7: cells transfected with pNGVL-3', which is a helper construct that expresses MLV Gag and Pol but contains a large 5' UTR deletion; and lane C: no RNA control. Migrations of probe fragments protected by MLV wild type and mutant gRNAs, and by 7SL RNA, are indicated on the right. (B) Packaging of Ψ mutant RNAs. RPA of virion RNA extracted from media samples normalized by RT activity. The helper plasmid, pNGVL-3'-gag-pol, lacks native 5' UTR sequences, and thus no MLV-derived fragment was detected in lane 6. (C) Quantification of gRNA RNA packaging in virions produced by transient transfection. Reported as percent of wild type levels, using 7SL to normalize number of virions. Data are from three separate RPAs of viral RNA as shown in (B). (D) Packaging of Ψ mutant gRNAs under competition with co-expressed wild type gRNAs. RPA of cell and viral RNA from 293T cells transiently co-transfected with plasmids expressing test gRNAs (Ψ variant GPPs) and a wild type 5' UTR control gRNA (pBAG (163)). Calculation of %WT packaging was as described in text. (E-G) Packaging of Ψ mutant gRNAs under single copy expression conditions (E) RPA of cellular RNA extracted from cells expressing MLV Ψ variants as single stably integrated proviruses. (F) RPA of gRNA in virions produced by single integrants. Migration of probe fragments protected by MLV gRNA and 7SL are indicated on the right. (G) Quantification of gRNA/7SL ratios from three separate RPAs of viral RNA. For all RPAs, lanes include undigested probe (P); RNA size markers (M); and digested probe alone control (C). MLV gRNA protected fragments occasionally run as two bands due to a single-base mismatch between the 5' end of the gRNA and the 3' end of the riboprobe which cleaves under conditions of excess RNAse T1 to RNA. The MLV gRNA riboprobe protects the 5' UTR region of MLV gRNA which contains the different mutations tested, and this accounts for discrete differences in the size of protected fragments exhibited by the mutant MLV gRNAs versus the wild type MLV gRNAs. 7SL protected fragments appear as multiple bands possibly due to the existence of different 7SL isoforms and experimental differences in the degree of RNase cleavage. The altered mobility 7SL bands in lane 6 (B) and in lane 4 (F) were likely due to minor variations in salt concentrations in those individual samples as these differences were not reproducibly observed.

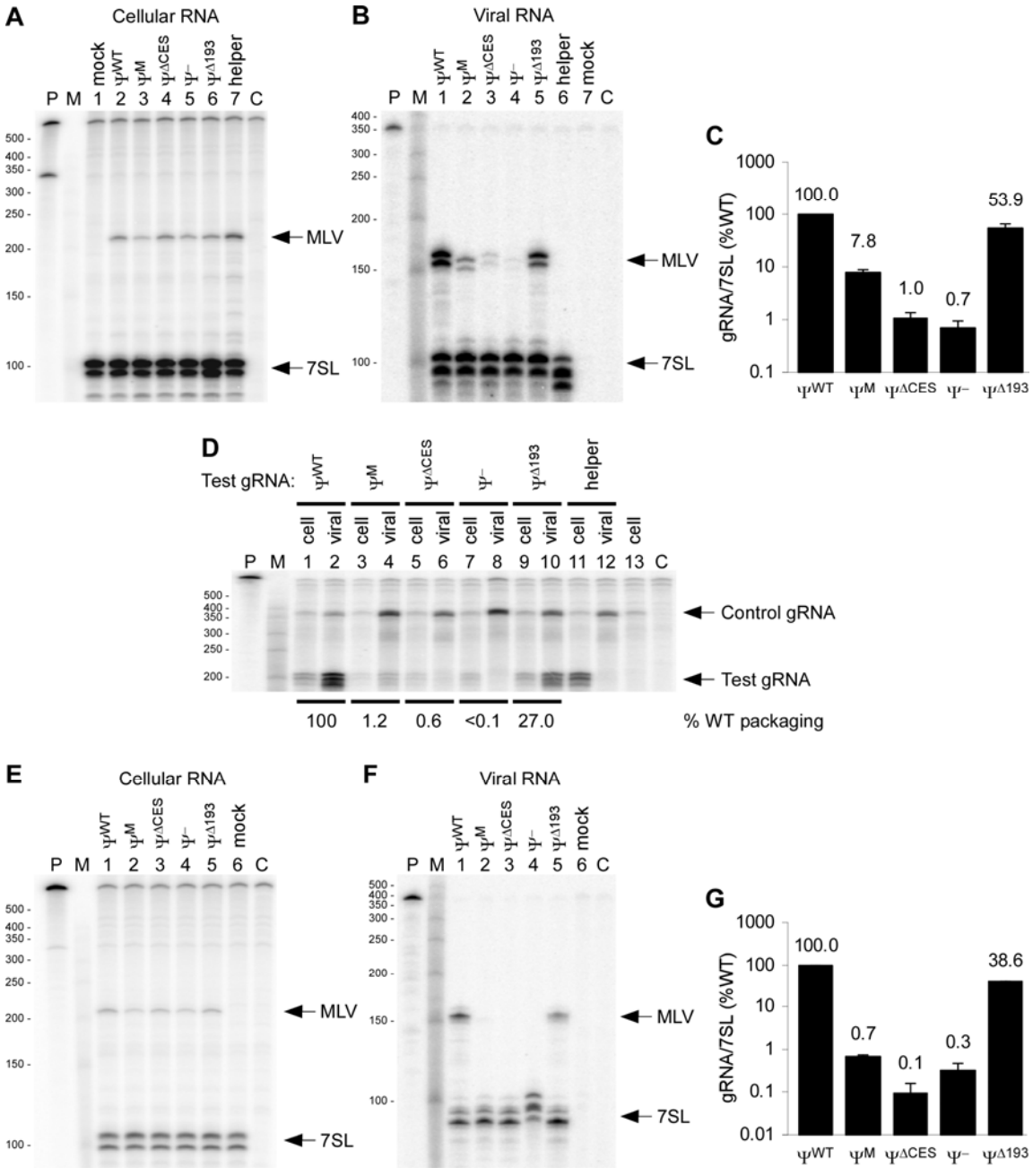
A
Cellular RNA
P M 1 2 3 4 5 6 7 C
mock
ΨWT
ΨM
ΨΔCES
Ψ–
ΨΔ193
helper
500 -
400 -
350 -
300 -
250 -
200 -
150 -
100 -
MLV
7SL
B
Viral RNA
P M 1 2 3 4 5 6 7 C
ΨWT
ΨM
ΨΔCES
Ψ–
ΨΔ193
helper
mock
400 -
350 -
300 -
250 -
200 -
150 -
100 -
MLV
7SL
C
gRNA/7SL (%WT)
1000
100
10
1
0.1
100.0
7.8
1.0
0.7
53.9
ΨWT
ΨM
ΨΔCES
Ψ–
ΨΔ193
D
Test gRNA:
ΨWT
ΨM
ΨΔCES
Ψ–
ΨΔ193
helper
cell
viral
P M 1 2 3 4 5 6 7 8 9 10 11 12 13 C
500 -
400 -
350 -
300 -
250 -
200 -
Control gRNA
Test gRNA
100
1.2
0.6
<0.1
27.0
% WT packaging
E
Cellular RNA
P M 1 2 3 4 5 6 C
ΨWT
ΨM
ΨΔCES
Ψ–
ΨΔ193
mock
500 -
400 -
350 -
300 -
250 -
200 -
150 -
100 -
MLV
7SL
F
Viral RNA
P M 1 2 3 4 5 6 C
ΨWT
ΨM
ΨΔCES
Ψ–
ΨΔ193
mock
500 -
400 -
350 -
300 -
250 -
200 -
150 -
100 -
MLV
7SL
G
gRNA/7SL (%WT)
1000
100
10
1
0.1
0.01
100.0
0.7
0.1
0.3
38.6
ΨWT
ΨM
ΨΔCES
Ψ–
ΨΔ193

58 °C, followed by nearly complete denaturation to the monomer form at 65 °C (Fig. 4-3). This later thermal denaturation profile is highly reminiscent of the so-called "tethering" interactions that have been described within and between co-packaged MLV gRNAs in RNA regions outside the dimer linkage region (82). This suggests that the slow migrating forms of both Ψ^{M} and $\Psi^{\Delta CES}$ RNAs were retarded largely by non-specific interactions that occur during condensation of the RNAs in assembling virions rather than by specific, more stable interactions involving their 5' UTRs. Together, these findings demonstrate that when Ψ^{M} RNAs are packaged, they do not exist in the dimer linkage with a fairly discrete melting point that is characteristic of wild type MLV gRNAs, but instead exist in heterogeneous form that is condensed by various tethering interactions, at least most of which are significantly less thermostable than wild type gRNAs' dimer linkages.

Packaging of MLV Ψ^{WT} and Ψ^{M} gRNAs is NC dependent.

The elevated level of packaging of Ψ^{M} gRNAs observed in transient transfection experiments above suggested that overexpression of mutant Ψ^{M} gRNAs led to the observed relatively efficient packaging. The subsequent analysis of packaging in competition and single-integrated copy experiments showed a further 10-fold drop in Ψ^{M} gRNA packaging, which further supports the notion that overexpression led to increased nonspecific packaging.

Because the NC domain of the Gag polyprotein mediates specific recruitment of MLV gRNA (14), the specificity of gRNA recruitment in transient transfection experiments could be assessed with an NC mutant that is defective in gRNA packaging. Ψ^{WT} and Ψ^{M} gRNA packaging were, therefore, quantified in the context of MLV Gag polyproteins which contained mutated NC domains. We used W35G, an NC mutant with

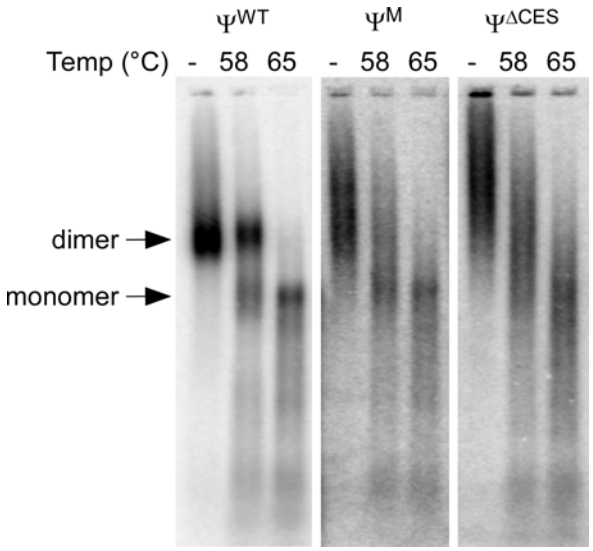

Figure 4-3. Non-denaturing northern analysis of wild type, Ψ^{M}, and $\Psi^{\Delta CES}$ containing gRNAs. Virion RNA samples were normalized to contain roughly the same number of gRNAs per lane and were subjected to the indicated treatments as described in the text. Arrowheads at right indicate the mobilities of wild type products. That the slightly reduced mobility of the wild type dimeric RNA observed at 58^{o}, relative to the unheated sample, is consistent with previous findings (58, 81).

a glycine in place of a tryptophan at amino acid number 35 of the NC protein. This mutation disrupts an aromatic amino acid in the hydrophobic cleft of the zinc finger domain that binds sequences in Ψ^{WT} gRNAs with high affinity (37). The W35G NC mutant is defective for gRNA packaging *in vivo* (71, 226) and NC-Ψ interactions *in vitro* (Michael Summers, personal communication). The NC W35G mutant in the context of Ψ^{WT} (Fig. 4-4, lanes 4 and 5) disrupted gRNA packaging 2 to 3 fold more than the Ψ^{M} mutations with wild type NC (Fig. 4-4, lane 3). The gRNA packaging levels in the W35G mutant were about $1/20^{th}$ wild type levels. The levels of gRNA in the double mutant, Ψ^{M} and W35G, were further decreased to less than 1% of wild type levels. These data indicate that, while the Ψ^{M} mutant exhibits reduced NC binding *in vitro* and gRNA packaging *in vivo*, residual Ψ^{M} gRNA packaging is still NC dependent.

Packaging quantification in transient transfection experiments can yield variable results. For example, we observed 2 to 3 fold differences in gRNA packaging in virions produced by transfection with different plasmids of identical genotype, Ψ^{WT} W35G NC mutant (Fig. 4-4, lanes 4 and 5). Also, the level of Ψ^{M} gRNA packaged in the RPA shown (Fig. 4-4, lane3) was about 3 fold greater than previous experiments reported above. To test whether or not varying expression would lead to parallel changes in gRNA packaging, we performed 3 fold serial dilutions of DNA used in the transfection of one of the double mutants (Fig. 4-4, lanes 7 through 9). Indeed, the gRNA packaging levels declined concomitantly with the amount of DNA used for transfection (Fig. 4-3, lanes 7 through 9). These data suggest that MLV proteins are not a limiting component in gRNA packaging, and further demonstrate that transient transfection experiments used to analyze gRNA packaging may underestimate packaging defects.

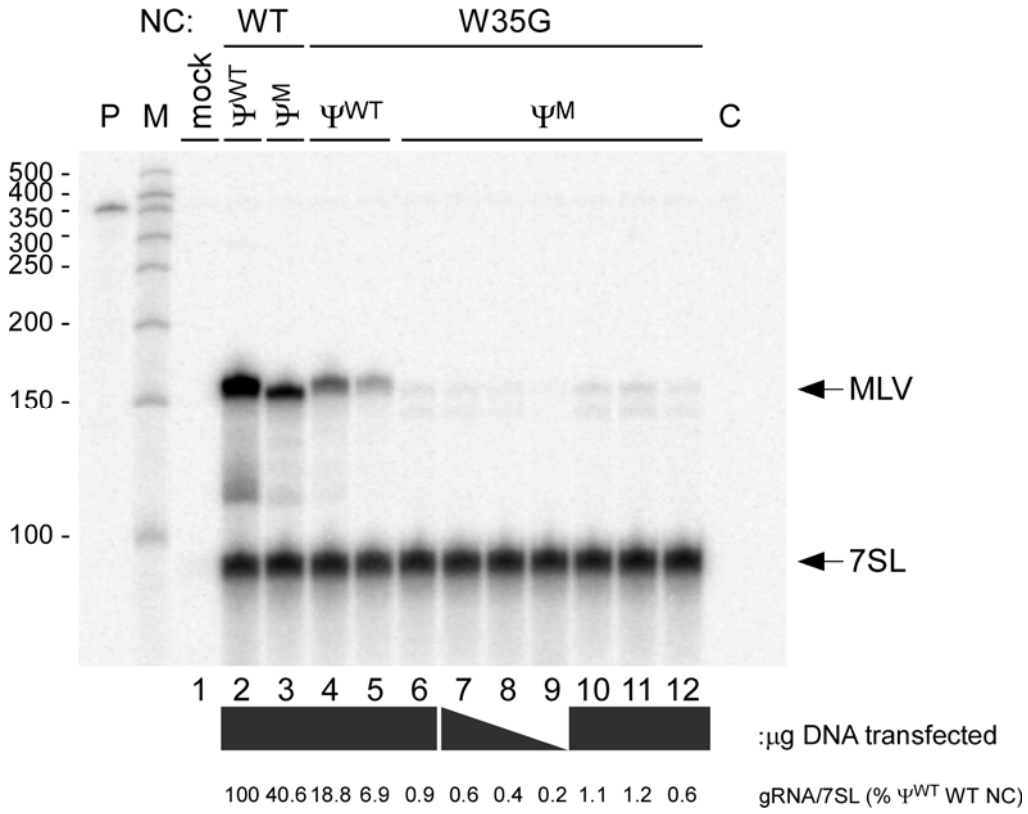

Figure 4-4. RPA quantification of Ψ^{WT} and Ψ^{M} gRNAs with wild type or W35G mutant NCs. Packaging of Ψ^{WT} and Ψ^{M} gRNAs in WT NC and W35G NC mutant virions produced by transient transfection and analyzed here by RPA. Viral RNA samples were normalized to RT activity. Migrations of probe fragments protected by MLV wild type and mutant gRNAs, and by 7SL RNA, are indicated on the right. Lanes 4 and 5 are RNAs from virus produced by transfection with different plasmid preparations of Ψ^{WT} W35G NC mutant pGPPs. Lanes 6, 7-9, 10, 11 and 12 are RNAs from virus produced by transfection with different plasmid preparations of Ψ^{M} W35G NC mutant pGPPs. Lane 8 and 9 were 3-fold serial dilutions of the same preparation of the Ψ^{M} W35G NC mutant pGPP plasmid used for lane 7, represented by the gray triangle below the lane numbers. Lanes include undigested probe (P); RNA size markers (M); and digested probe alone control (C). Ψ^{M} W35G MLV gRNAs appear as two bands due to a single-base mismatch near the 5' end of the gRNA with the 3' end of the riboprobe which produces two bands under conditions of excess RNase T1 to RNA. The gRNA levels normalized to 7SL are quantified below the RPA as the % of Ψ^{WT} with a WT NC domain.

W35G NC mutant is defective in gRNA packaging but does not disrupt gRNA dimerization.

The MLV NC domain takes part in high (124) and low affinity (39, 161) RNA interactions which function in both gRNA recruitment (72, 168) and activation of gRNA dimerization (68, 162), respectively (reviewed in (38) and (170)). Because NC functions in both packaging and dimerization, we sought to determine the effect of the W35G mutation on gRNA dimer stability *in vivo.* To determine whether or not the W35G mutation disrupts Ψ^{WT} gRNA dimer stability, we performed a nondenaturing northern blot on viral RNA from W35G mutant virions produced by transient transfection (Fig. 4-5). The northern blot was normalized for virion abundance by RT activity. As quantified in the RPA above, the W35G NC mutant exhibited decreased gRNA packaging relative to wild type NC (Fig. 4-5). However, in contrast to the diffuse dimers exhibited by Ψ^{M}, $\Psi^{\Delta CES}$, and Ψ^{-} gRNAs, the Ψ^{WT} gRNA from the W35G NC mutant displayed a tight dimer profile similar to the Ψ^{WT} gRNA with wild type NC domains (Fig. 4-5). This provides *in vivo* support that the W35G NC mutation specifically disrupts high affinity NC-RNA interactions required for dimer recruitment, but this mutation does not inhibit the low affinity NC-RNA interactions which likely function in dimer formation and stabilization.

Dimer partner selection of packaged Ψ^{M} gRNAs is more random that Ψ^{WT} gRNAs.

If dimer partner selection acts as a mechanism for routing gRNAs towards sites of assembly and encapsidation, then the low level of gRNAs packaged by the dimer mutant Ψ^{M} would be expected to exhibit increased randomness in dimer partner associations. The nonrandom dimerization of MLV gRNAs expressed from separate loci (53) and the

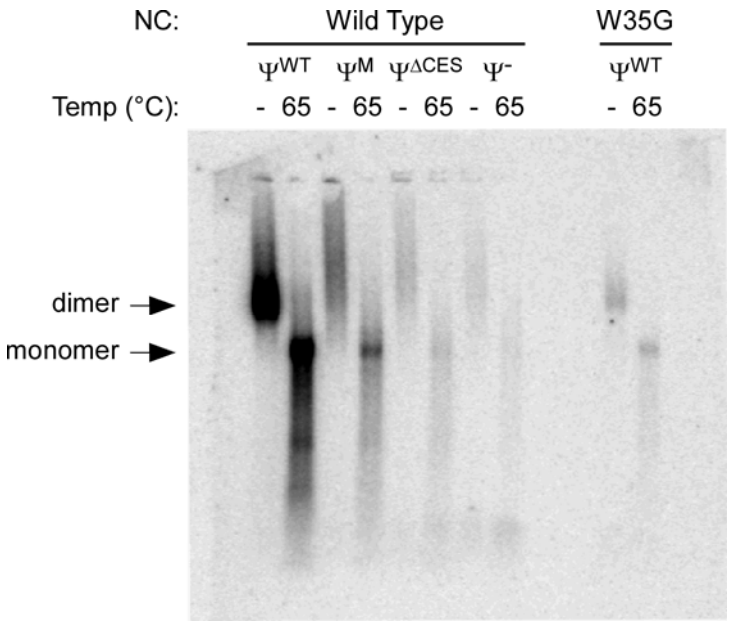

Figure 4-5. Non-denaturing northern blot analysis of the NC W35G mutant compared to wild type NCs containing Ψ^{WT}, Ψ^{M}, $\Psi^{\Delta CES}$, or Ψ^{-}. Nondenaturing northern blot of MLV gRNAs extracted from virions produced by transient transfection. Viral RNAs were either kept on ice prior to agarose gel electrophoresis or subjected to 65ºC for 10 min. Virus-containing media were normalized by RT activity to ensure the loading of RNA from an equivalent number of virions. Migrations of either the tight WT gRNA dimer or the denatured gRNA monomer are indicated on the left.

random dimerization of MLV gRNAs expressed from a single locus (54) observed in previous studies suggest that dimer partner selection occurs early in the biogenesis of MLV gRNAs. This implies that gRNA dimerization acts as an early mechanism for routing gRNAs towards sites of assembly. Additionally, the increase in the randomness of gRNA dimerization that we observed upon transcription inhibition in studies described in Chapter III of this dissertation further argues that the majority of MLV gRNA dimer partner associations occur early. In those studies, transcription inhibition disrupted the entire nascent pool of transcripts which comprise the earliest potential gRNAs capable of dimer partner associations, but it did not alter the ability of the gRNAs to form dimer partner associations later.

To test the prediction that disrupting gRNA dimerization would lead to an increase in the randomness of dimer partner associations, we performed RNA captures on gRNA dimers from virions produced by transient transfection with the Ψ^{M} dimer mutant (Fig. 4-6). Data from two separate RNA captures showed a small but reproducible increase in the randomness of gRNA dimerization of the Ψ^{M} dimer mutant relative to Ψ^{WT}, from 1.84 to 1.58 with 1 being random (Fig. 4-6). In these experiments, the level of nonrandomness exhibited by Ψ^{WT} gRNAs was lower than that reported in Chapter III here or in Flynn et al. (53). However these results are preliminary. The wash conditions used in the captures represented here were less stringent than those used in acquiring the data presented in Chapter III, and the variation in the stringency of wash conditions could account for the observed discrepancies. While only a small increase in randomness was observed here, these trends are, nevertheless, consistent with the hypothesis that

disrupting the ability of MLV gRNAs to initially form dimers impairs their ability to be routed towards sites of assembly and leads to more random gRNA partner associations.

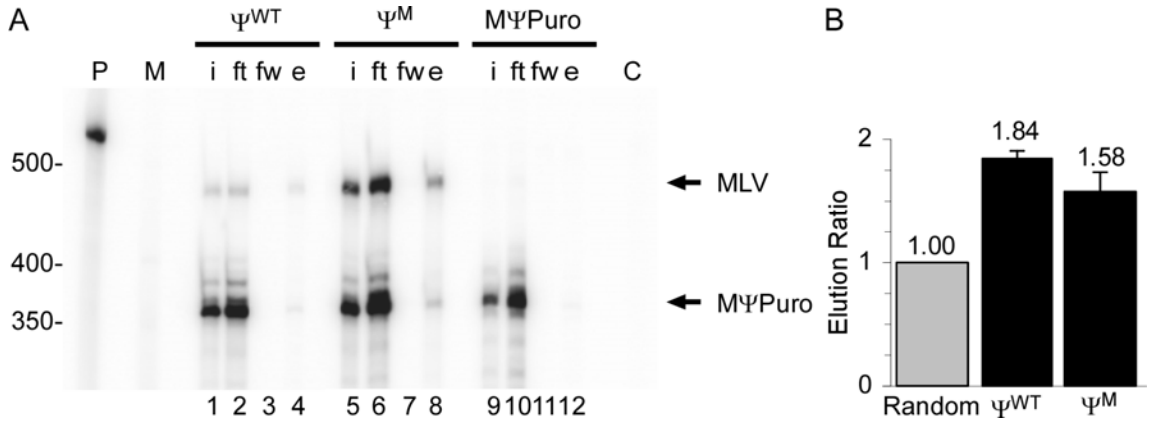

Figure 4-6. RNA capture measurement of the randomness of dimer partner associations in Ψ^{M} gRNAs versus Ψ^{WT} gRNAs. (A) RPA of RNA capture of packaged Ψ^{WT} and Ψ^{M} gRNA dimers. Mobilities of MLV and MΨPuro RNAs indicated on the right. For each capture, input (i), flow through (ft), final wash (fw), and elution (e) are indicated on the top. Lanes also include undigested probe (P); RNA size markers (M); and digested probe alone control (C). (B) elution ratios of Ψ^{WT} and Ψ^{M} quantified from 2 separate RPAs of RNA captures normalized to 1 being the expected elution ratio from random dimerization.

Discussion

The *in vivo* quantification of Ψ^{M} versus Ψ^{WT}-containing gRNA packaging supports an RNA switch model of gRNA recruitment. The mutations in Ψ^{M} stabilize the stem loops of DIS-1 and the core encapsidation signal which disrupts dimerization and NC binding *in vitro* (124) and, as demonstrated here, inhibits gRNA packaging *in vivo*. Also, the inhibitory effect of Ψ^{M} mutations on gRNA dimerization led to a decreased thermal stability of Ψ^{M}-containing gRNA dimers *in vivo*. This suggests that the defect in gRNA dimerization is causing the decrease in gRNA packaging, and it provides *in vivo* support for the model that gRNA dimerization switches the conformation of the gRNA to expose high affinity NC binding sites that recruit the gRNA into assembling virions.

The contribution of the zinc finger domain of NC to specific gRNA recruitment was also quantified here with an NC mutant that contained a disruption to the hydrophobic cleft in the zinc finger. Virions with a W35G mutant NC domain packaged 20-fold less Ψ^{WT}-containing gRNA than virions with a wild type NC domain. Also, the hydrophobic cleft disruption of the NC domain had a two-fold greater defect in gRNA packaging than the *cis*-acting Ψ^{M} mutations. In combination, virions produced from a double mutant of Ψ^{M}-containing gRNA and a W35G mutant NC packaged 10-fold less gRNA than single mutants with only Ψ^{M} mutations. This suggests that the relatively efficient packaging of Ψ^{M}-containing gRNAs observed in virions produced by transient transfection is NC dependent. It also provides *in vivo* support for the notion that the W35G NC mutation disrupts high affinity NC-RNA interactions which mediate specific gRNA recruitment but not low affinity NC-RNA interactions that might contribute to low level nonspecific RNA packaging by MLV.

Observations from non-denaturing northern blot analysis of the W35G NC mutant further suggest that this residue of NC functions in specific gRNA recruitment and not other functions associated with low affinity interactions. Functions of the NC domain of Gag include specific recruitment of MLV gRNAs and low affinity RNA interactions which function in catalyzing MLV gRNA dimerization (68, 162). The tight dimer profile exhibited by gRNA isolated from virions produced with the W35G mutant suggests that this mutation is not disrupting the ability of the gRNAs to form strong dimer partner associations. The effect of this mutation on high affinity gRNA recruitment and not low affinity dimer stabilization suggests that it could prove useful in disrupting other high affinity interactions that are necessary in retroviral replication. For example, NC residues have been shown to play a role in viral DNA synthesis *in vivo* (71), and previous reports indicate that mutations to the same tryptophan residue abrogate virus spread (71, 72, 121). However, the results here suggest that transient overexpression could produce gRNA-containing virions in sufficient quantity to study the impact of the W35G mutation on DNA synthesis in a single round of infection.

The ten-fold difference in Ψ^M gRNA packaging in virus produced by transient transfection versus single copy expression and competition experiments suggests that overexpression leads to non-specific incorporation of Ψ^M gRNAs. Since virus particles produced without Ψ-containing RNAs package an excess of cellular mRNAs (132, 133), the elevated packaging of the Ψ^M mutant likely represents non-specific incorporation. As mentioned above, the further decrease in packaging observed with the Ψ^M W35G double mutant suggests that this packaging of RNA is mediated by the NC zinc finger.

The decreased packaging of the gRNA exhibited by the Ψ^M dimerization mutant is consistent with our model (Fig. 3-5) that gRNA dimer partner associations function in the initial recruitment of MLV gRNAs. The mutations of Ψ^M disrupt dimerization and therefore likely disrupt the early bisection of the unspliced RNA into separate fates of gRNA and mRNA. To test for this impairment in nuclear gRNA dimerization and the predicted outcome that nonspecific incorporation of Ψ^M gRNAs should exhibit more random dimer partner associations, we performed an RNA capture experiment on packaged viral gRNAs produced from coexpressed Ψ^M mutants. Our preliminary results indicate that Ψ^M gRNAs associated more randomly which is consistent with predictions based on our model. However, the difference was small relative to Ψ^{WT} internal controls. Subsequent to these experiments, modifications to the RNA capture procedure have reproducibly produced levels of nonrandom Ψ^{WT} gRNA dimerization that are two-fold greater than those obtained here (Fig. 3-2A and C, pre-ActD and –DRB treatments). Incorporating these procedural modifications to an analysis of Ψ^M dimerization could bolster the small change in randomness seen here, with the expectation that Ψ^{WT} gRNAs would exhibit about two-fold greater levels of nonrandomness and the more random associations of Ψ^M-containing gRNAs wouldn't display a parallel increase in nonrandomness.

MLV Ψ^{WT} has been previously demonstrated to function in the nuclear egress and intracellular localization of MLV unspliced RNAs, and the participation of Ψ in gRNA dimerzation may, therefore, also regulate these aspects of MLV RNA trafficking (7, 192). Levels of virion production for Ψ^M-containing provirus constructs were comparable to Ψ^{WT} which suggests that MLV unspliced RNAs with either Ψ were efficiently exported

from the nucleus and trafficked to sites of viral mRNA translation. However, the inefficient packaging of Ψ^M gRNA could also indicate aberrant gRNA intracellular localization. In the context of our model of MLV unspliced RNA nuclear dimerization and corresponding bisection in RNA fates (Fig. 3-5), the impaired ability of Ψ^M to form dimers might alter the manner of its nuclear egress. Recent results in HIV-1 demonstrate that nuclear egress of coexpressed unspliced RNAs via separate host cell pathways disrupts normal random dimer partner associations (128). If Ψ^M gRNAs are exiting the nucleus via an alternate pathway than dimeric Ψ^{WT} gRNAs, then co-expression of Ψ^{WT} with Ψ^M gRNAs might be expected to exhibit even greater levels of nonrandomness in dimer partner associations. The opposite result of increase randomness between Ψ^{WT} and Ψ^M might be consistent with the nonspecific incorporation of Ψ^M gRNAs and inconsistent with the hypothesis that dimeric gRNAs and monomeric viral unspliced RNAs traffic to separate intracellular locations.

CHAPTER V

CONCLUSIONS AND FUTURE DIRECTIONS

OVERVIEW

Results presented in this dissertation suggest that MLV recruits cellular and viral RNAs from the host cell nucleus. Chapter II observations of MLV high level mY RNA packaging and mY RNA intracellular redistribution suggest that mY RNAs are recruited early in their biogenesis in the nucleus, which is consistent with prior findings of high level mY RNA recruitment from Ro60 knockout cells by Onafuwa-Nuga (148). Data presented in Chapter II were obtained in collaboration with the Sandra Wolin lab at Yale University and published in Garcia et al. (65). Chapter III results support the nuclear bisection in MLV unspliced RNAs into mRNA or gRNA functions. Observations in Chapter III are consistent with the hypothesis that MLV gRNAs form nuclear dimer partner associations and suggest a subset of MLV unspliced RNAs, which escape dimer partner associations at or near sites of transcription, may disproportionately contribute to heterozygous virions. Results in Chapter IV that demonstrate the ~100-fold reductions in MLV packaging of Ψ^{M}-containing gRNAs, which contain Ψ stem loop stabilizing mutations which disrupt dimerization and NC binding *in vitro*, are consistent with an RNA switch model of MLV gRNA recruitment, and preliminary observations suggest that this gRNA dimerization-dependent switch functions in nuclear gRNA recruitment by MLV. Chapter IV results were obtained in collaboration with the Mike Summers lab at the University of Maryland Baltimore County and published in Miyazaki et al. (124).

Together, the findings of nuclear recruitment of viral gRNAs and cellular mY RNAs suggest a potential intersection in MLV replication with a cellular RNA quality control pathway.

The main findings presented in this dissertation are:

Chapter II

- MLV expressed in wild type MEFs packages 3 to 5 copies of mY1 and mY3 RNAs each, and MLV expressed in Ro60 knockout cells packages ~2 copies each of mY1 and mY3 RNAs.

- Levels of mY RNAs in Ro60 knockout cells are redistributed more evenly between the nucleus and the cytoplasm than in wild type cells where the majority of mY RNAs are cytoplasmic.

- MLV recruitment of mY RNAs occurs independent of mY RNA 3' end maturation.

- Ro60 is necessary for the accumulation of 3' end-processed mature mY RNAs in cells.

Chapter III

- Specific repression of MLV transcription leads to a more rapid decline in gRNA packaging than virion production.

- The randomness of co-expressed MLV gRNA dimer partner associations increases over time after general transcription inhibition.

- An increase in the frequency of recombination between co-expressed MLV gRNAs parallels the increase in the randomness of gRNA dimerization after general transcription inhibition.

- gRNA co-packaging and the frequency of recombination between co-expressed MLV gRNAs also increases after expression declines at late time points post transfection.

Chapter IV

- Mutations that stabilize MLV Ψ stem loops and inhibit dimerization and nucleocapsid (NC) binding *in vitro* decrease gRNA packaging into MLV by 100-fold in a tissue culture system of single-copy integrated proviruses.

- Quantification of MLV gRNA packaging in virus produced by transient transfection underestimates defects in gRNA packaging.

- Packaged MLV gRNAs which contain Ψ deletions or Ψ stem loop stabilizing mutations exhibit reduced thermal stability compared to gRNAs with wild type Ψs.

- Disruption of a hydrophobic cleft in MLV NC decreases MLV gRNA packaging by 20-fold compared to MLV with a wild type NC in a transient transfection tissue culture system.

- MLV gRNAs packaged by a hydrophobic cleft NC mutant exhibit wild type dimer mobility on non-denaturing gels.

- Packaged MLV gRNAs with Ψ stem loop stabilizing mutations exhibit slightly increased randomness in MLV gRNA dimer partner associations relative to wild type gRNAs.

CONCLUSIONS

Chapter II

In Ro60 knockout cells, the cellular mY1 and mY3 RNAs are more highly recruited by MLV than the retroviral gRNA. Ro60 knockout cells contain ~30-fold less mY1 RNAs than wild type cells, and the mY1 RNA levels in knockout cells are redistributed more evenly between the nucleus and the cytoplasm. This redistribution shifts the levels of mY RNAs away from cytoplasmic sites of MLV assembly on the plasma membrane. The continued packaging of high levels of mY RNAs from Ro60 knockout cells suggests that mY RNAs are actively recruited by MLV from the host cell nucleus at an early stage in their biogenesis.

Chapter III

Specific repression of MLV transcription reveals a similar bisection in MLV unspliced RNA fates as that previously seen when transcription is inhibited with actinomycin D (ActD). Tetracycline-regulated repression of MLV transcription leads to a more rapid decline in MLV gRNA packaging than virion production. This result is consistent with previous findings using ActD (107) which suggest that MLV gRNAs sort

into separate non-equilibrating pools of viral mRNAs and gRNAs. However, the decrease in MLV gRNA packaging upon specific repression of MLV transcription is less than that seen with ActD. This suggests either that the tetracycline-regulated repression of MLV transcription is incomplete or that ActD treatment disrupts an additional component of MLV gRNA recruitment, possibly by sequestering or re-localizing viral and/or cellular factors required for gRNA recruitment.

Transcription inhibition leads to increases in the randomness of MLV gRNA dimer partner selection and recombination over time in co-expression assays. Results presented in this dissertation are consistent with previous results that demonstrated that the majority of MLV gRNAs expressed from separate nuclear loci preferentially self-associate (53). However, the increases in the randomness of gRNA dimerization and frequency of recombination that occur concurrent with decreases in gRNA packaging after transcription inhibition suggest that some MLV gRNAs are forming dimer partner associations more randomly. This subset of MLV gRNAs may contribute disproportionately to the number of heterodimers packaged by MLV in coexpression studies.

Chapter IV

MLV gRNA dimerization functions in the subsequent recruitment of the dimeric gRNA into MLV particles. Disrupting MLV gRNA dimer formation abrogates gRNA recruitment into MLV particles. Mutations to Ψ that stabilize Ψ-associated stem loops and inhibit RNA dimerization and NC binding *in vitro* disrupt gRNA packaging *in vivo*. These results support an RNA switch model of MLV gRNA recruitment. In this model,

dimerization switches MLV gRNA to a fold that exposes high affinity NC binding sites which then recruit the dimeric gRNA into MLV particles.

The hydrophobic cleft in MLV NC functions in gRNA recruitment but not gRNA dimerization. Substitution of a tryptophan with an alanine residue at amino acid 35 in MLV NC (W35G) disrupts gRNA packaging but not gRNA dimerization. This W35G mutant NC decreases packaging by 20-fold compared to wild type NC, but the gRNA packaged into W35G NC mutant particles exhibits wild type dimer mobility on non-denaturing gels. This suggests that this mutant NC is defective in high affinity RNA binding but not low affinity RNA chaperone activity.

PRELIMINARY DATA AND FUTURE DIRECTIONS

The nuclear recruitment of MLV gRNAs and cellular noncoding mY RNAs suggests an intersection in MLV ribonucleoprotein (RNP) assembly with a cellular RNA quality control pathway. Emerging evidence suggests that Y RNAs function together with the Ro60 protein in the recognition of misfolded noncoding RNAs within the host cell nucleus (171). Data presented in this dissertation suggest that mY RNAs and MLV gRNA are recruited by MLV from the same subcellular compartment: the host cell nucleus. This Chapter will present additional preliminary data which further support this intersection and future directions to explore this.

Decreased gRNA packaging leads to increased mY1 RNA packaging by MLV

Increased packaging of human hY RNAs has been reported in human immunodeficiency virus type 1 (HIV-1) particles produced by a 5' UTR-deleted helper construct that packages undetectable levels of HIV-1 gRNA (91). HIV-1 virions with wild type 5'-UTRs package very low levels of Y RNAs (148). This suggests potential

differences in the RNP formation and Y RNA recruitment in HIV-1 versus MLV, since the latter packages high levels of Y RNAs. The increased packaging of hY RNAs by HIV-1 virions with reduced levels of gRNA suggests competition between gRNA and Y RNA recruitment. Despite the demonstrated differences in Y RNA recruitment by HIV-1 and MLV, we sought to test for similar competition in Y RNA and gRNA recruitment in MLV.

To determine if decreased levels of gRNA packaging correlated with more mY1 RNA packaging, MLV mY1 RNA packaging was analyzed in virus produced with Ψ^{M}-containing proviruses in a transient transfection system. MLV packages approximately 12-fold less Ψ^{M}-containing gRNAs, which contain Ψ stem loop stabilizing GNRA mutations (G, guanosine; N, any nucleotide; R, purine; and A, adenosine) that disrupt dimerization and NC binding *in vitro*, than Ψ^{WT}-containing gRNAs in transient transfection experiments (as quantified in Chapter IV). However, MLV virions produced from Ψ^{M}-containing proviruses packaged nearly two-fold more mY1 RNAs than virions produced from Ψ^{WT}-containing proviruses (Fig. 5-1). This result is demonstrated by a non-denaturing northern blot that was first probed for mY1 and subsequently stripped and re-probed for 7SL to normalize for the number of virions (Fig. 5-1). Quantification of total mY1 RNA per total 7SL RNA for each lane revealed an approximately two-fold increase in mY1 RNA packaging in the Ψ^{M} mutant (Fig. 5-1). These data are consistent with the earlier results with HIV-1 (212) and suggest MLV gRNA recruitment may intersect with MLV mY RNA recruitment.

The increased packaging of hY RNAs by particles produced from HIV-1 5'-UTR deleted helper constructs was reported to be NC dependent (91). Khan et al. (91) used an

HIV-1 NC double mutant, in which the zinc-chelating cysteine residues of both zinc fingers had been replaced by serine residues, to test for the NC dependence of hY RNA packaging. RT-PCR levels of hY RNAs were below the limit of detection in particles produced from their NC double mutant (91). This suggested to the authors that the increased hY RNA recruitment into HIV-1 particles produced from the 5'-UTR deleted helper was NC dependent.

To determine if mY1 RNA packaging was increased in MLV virions with Ψ deletions, mY1 RNA packaging was analyzed in MLV virions produced by proviral constructs containing Ψ deletions. Using the core encapsidation signal ($\Psi^{\Delta CES}$) and the "classic" Ψ deletion (Ψ^{-}) described in Chapter IV, which packaged ~100-fold less MLV gRNA by transient transfection, mY1 RNA packaging was assessed by nondenaturing northern blot. Results show that mY1 RNA packaging in virions generated from Ψ deletion expression constructs was increased to a similar extent (~two-fold) as that observed with the Ψ^{M} mutant (Fig. 5-2, lanes 1 through 8). These data are consistent with those of Khan et al. (91) for the HIV-1 5'-UTR deleted helper virus, and they also demonstrate that large reductions in MLV gRNA packaging lead to increases in mY RNA packaging (Fig. 5-2, lanes 1 through 8 and Chapter IV Fig. 4-1B and 1C). The two-fold increase in mY1 RNA packaging in virions with large reductions in gRNA packaging suggests that mY RNA recruitment may intersect with gRNA recruitment and MLV assembly. Also, this inverse relationship in mY RNA and gRNA packaging may suggest that mY RNAs can compete with MLV gRNAs for NC binding and recruitment into particles.

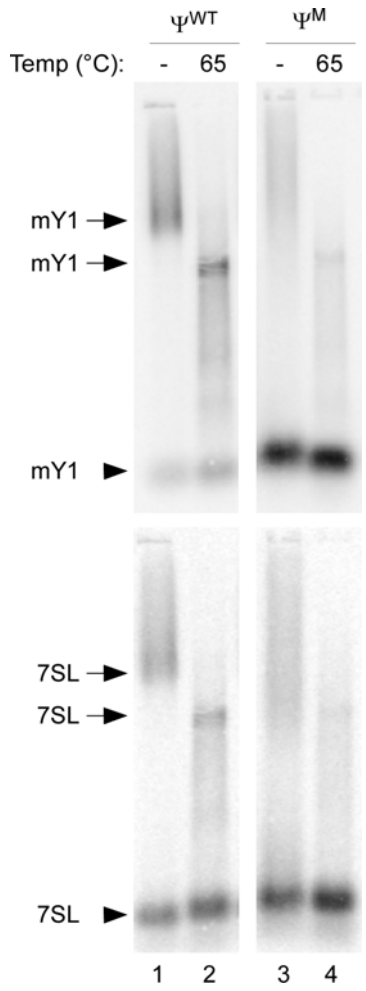

Figure 5-1. Nondenaturing northern analysis of mY1 (top) and 7SL (bottom) of viral RNA from MLV with Ψ^{WT}- or Ψ^{M}-containing proviruses. RNA extracted from virions was probed for mY1 RNAs (top) stripped and reprobed for 7SL RNAs (bottom). Arrows indicate the co-migration of mY1 and 7SL RNAs with viral gRNAs. Arrowheads indicate the mobility of mY1 and 7SL RNAs that are not annealed to longer RNAs.

Next, to determine if the recruitment of mY RNAs into MLV particles is NC dependent, mY1 RNA packaging was analyzed with the W35G hydrophobic cleft NC mutant that disrupts high affinity NC-RNA interactions. Results demonstrate that mY RNA packaging in the MLV W35G NC mutant was comparable to that in MLV virions with wild type NC (Fig. 5-2, lanes 1 and 2 and lanes 9 and 10). This suggests that mY RNAs do not compete with gRNAs for high affinity NC binding. However, it remains possible that mY RNAs are recruited by low affinity NC-RNA interactions.

Future directions to address the potential intersection in mY RNA recruitment with MLV gRNA recruitment could build upon these preliminary data. The results presented in Figures 5-1 and 5-2 were obtained by nondenaturing northern blots which, because of differences in the specific activities of separate probes for mY1 and 7SL, are not as quantitative as RNase protection assays. RNAse protection assays also have the potential to be more sensitive which could reveal subtle differences in mY1 RNA packaging that are not evident by northern blot analysis. Such approaches could assess differences in mY RNA recruitment into virions from Ψ^{M} versus Ψ deletion-containing constructs which differ in gRNA packaging by as much as 10-fold in transient transfection experiments. Also, measuring differences in mY RNA packaging into virions produced by single-copy integrated proviruses could provide a more biologically relevant measurement of differences between MLV mY RNA recruitment into virions from Ψ^{WT} versus Ψ^{M}-containing gRNAs.

Speculatively, the results indicating wild type levels of mY RNA packaging by the W35G NC mutant may suggest that low affinity NC-RNA interactions are involved in the recruitment of mY RNAs. To address this question, mY RNA packaging could be

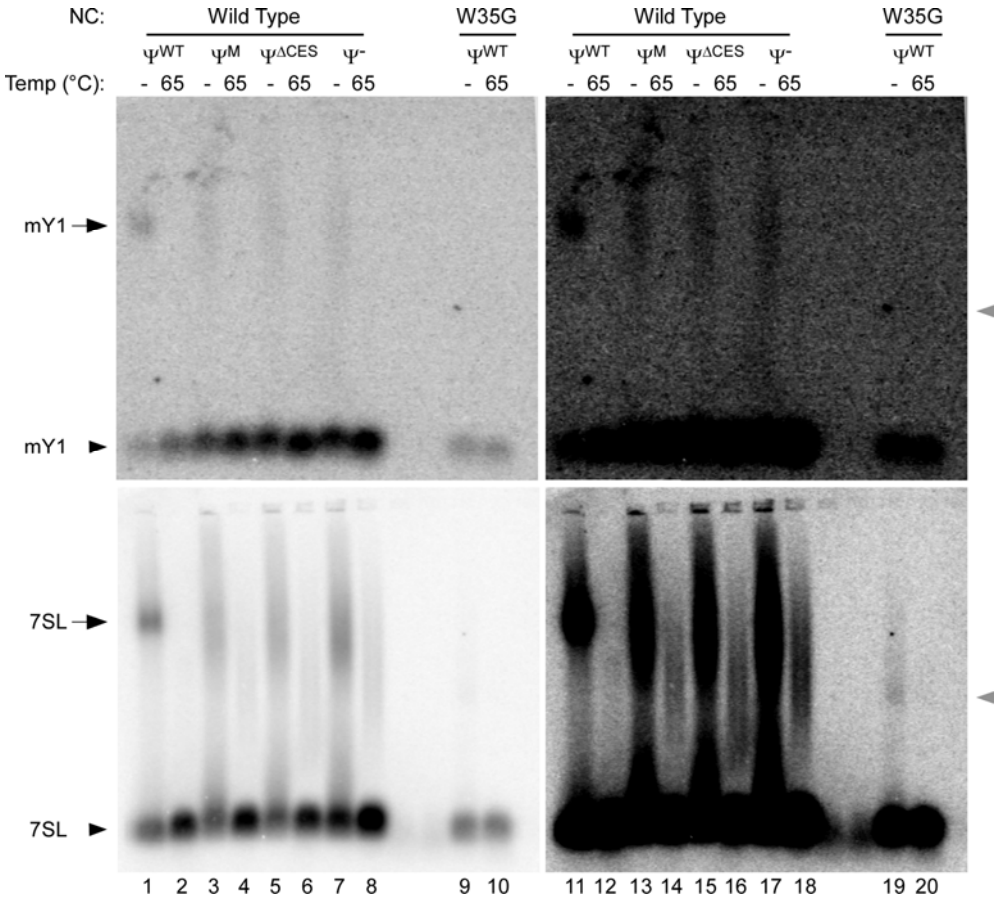

Figure 5-2. . Nondenaturing northern analysis of mY1 (top) and 7SL (bottom) of viral RNA from MLV particles containing: wild type NC with Ψ^{WT}, Ψ^{M}, ΨΔCES, or Ψ^{-} gRNAs or the W35G mutant NC with Ψ^{WT} gRNAs. RNA extracted from virions was probed for mY1 RNAs (top) stripped and reprobed for 7SL RNAs (bottom). Blots on the right are overexposure of the same blots on the left. Arrows indicate the co-migration of mY1 and 7SL RNAs with viral gRNAs (Fig. 4-5). Black arrowheads indicate the mobility of mY1 and 7SL RNAs that are not annealed to longer RNAs. The gray arrowheads indicate a band of intermediate mobility between free noncoding RNAs and noncoding RNAs annealed to the retroviral gRNA. In addition to the results mentioned in the text, the lack of visible mY1 and 7SL RNAs co-migrating with packaged MLV gRNAs in the W35G mutant serves as a negative control for cross-hybridization of the probes used here with the retroviral gRNA.

quantified using additional NC mutants that disrupt low affinity NC-RNA interactions, both by NC zing finger disruptions and by disruptions to the two basic regions surrounding the NC zinc finger. Onafuwa-Nuga (148) observed a reproducible two-fold decrease in 7SL packaging in NC basic region mutants. This suggests that NC low affinity RNA chaperone activity may function to a limited extent in 7SL RNA recruitment. To address the mechanism of 7SL recruitment, our lab is currently studying 7SL and 7SL-derivative RNA packaging in HIV-1-derived minimal VLPs (Keene and Telesnitsky, *in preparation*). These minimal VLPs contain a leucine zipper motif in place of HIV-1 NC, to mediate protein-protein interactions required in particle assembly (1). The design and testing of RNA packaging with a similar mutant in MLV could aid in determining whether or not MLV NC functions in mY RNA recruitment.

Nondenaturing northern blot analysis of mY1 and 7SL RNAs packaged by the MLV W35G NC mutant revealed a couple of intriguing observations that could be further tested (Fig. 5-2). First, the W35G mutant disrupted MLV gRNA packaging but not MLV gRNA dimerization, as demonstrated when the blot shown in Fig. 5-2 was probed with an oligo complementary to the R-region (Fig. 4-5). In contrast to wild type, no mY1 RNA or 7SL RNA co-migrated with the dimeric or denatured-monomeric gRNA for this mutant. This may suggest that when NC binds to gRNA with high affinity it concurrently traps some molecules of mY1 and 7SL. These RNAs then continue to anneal to the gRNA during RNA extraction from virions and subsequently migrate with the gRNA on nondenaturing gels (Fig. 5-2 and Fig. 4-5). Basic residue substitutions in MLV NC that preserve high affinity interactions but reduce RNA chaperone activity could be used to test this hypothesis. The MLV NC domain is highly basic, and this

basic nature may function in an RNA chaperone capacity (170). Substitution of basic residues in and around the NC zinc finger (e.g. K30A) has been demonstrated to disrupt replication (71) and 7SL packaging (148), and these mutations could provide a starting point for testing outcomes of NC RNA chaperone disruption on noncoding RNA packaging. Expectations consistent with this hypothesis would entail mY and 7SL RNAs migrating with the gRNA in nondenaturing northern blots and potentially lower total mY and 7SL RNA packaging in low affinity-disrupted MLV NC mutants. Alternatively, low affinity-disrupted mutants might display a similar phenotype to the W35G mutant and contain no or less mY and 7SL co-migrating with MLV gRNA. Such an outcome would suggest that both low and high affinity NC-RNA interactions function in the annealing of noncoding cellular RNAs to the viral gRNA.

Second, overexposure of the nondenaturing northern blot of 7SL RNA revealed a band that had an intermediate mobility (Fig. 5-2, bottom right, lane 19, gray arrowhead) between the faster migrating majority of 7SL RNAs (Fig. 5-2, bottom left, lane 9, black arrow head) and the slower migrating dimeric gRNA bands (Fig. 5-2, black arrow and Fig. 4-5). This band was not evident upon probing for the viral gRNA with the anti-R region probe that was used in Chapter IV (Fig. 4-5). Speculatively, this could indicate elevated packaging of a cellular RNA by the W35G mutant. The annealing of 7SL to this RNA might occur in a manner distinct from how 7SL anneals to the viral gRNA.

Alternatively, the W35G NC mutant might alter the intracellular localization of Gag which would disrupt nuclear recruitment of MLV gRNAs and concurrent nuclear recruitment of noncoding cellular RNAs. This hypothesis asserts that a portion of Gag traffics through the nucleus, where it recruits RNA en route to sites of assembly. If this

alternative speculation is correct, the co-migration of 7SL and mY RNAs with MLV gRNAs might provide further support for the model of nuclear RNA recruitment proposed in this hypothesis. Analysis of the intracellular localization of the W35G NC mutant Gag compared to wild type Gag by either immunofluorescence or GFP-tagged molecules could provide a means of testing this hypothesis. Because this hypothesis speculates that MLV Gag is recruiting RNA in the nucleus, slowing RNA nuclear export machinery might aid in attempts to observe wild type of W35G mutant Gag nuclear localization. In combination with fluorescent microscopy of the Gag molecules, host cell RNA nuclear export machinery could be slowed or perturbed with drugs, dominant negatives, RNAi, or RNA competitors, and host cell nuclei could be monitored for wild type and W35G Gag co-localization.

Analyzing the randomness of gRNA dimer partner associations with the W35G mutant NC could also address this question of potential mis-localization of W35G mutant Gag molecules. If the W35G mutant Gag does not translocate to the nucleus, it could not function in nuclear gRNA recruitment. Thus, gRNAs packaged into W35G mutant virions would likely be recruited from the cytoplasm and be expected to display increased randomness in gRNA dimer partner associations. As detailed by the methodology in Chapter III, this hypothesis could be tested by both biochemical RNA capture assays and genetic recombination assays.

A nuclear intersection of MLV gRNA recruitment with a host cell noncoding RNA quality control pathway might be expected to perturb the intracellular localization of components of the cellular RNA quality control pathway. To determine if MLV infection altered the subcellular localization of mY RNAs, mock and chronically-infected

NIH-3T3 cells were fractionated and analyzed by northern blot. MLV infection did not alter the nuclear to cytoplasmic distribution of mY1 RNAs (Fig. 5-3A, time 0 and mock). However, high level recruitment of mY RNAs by MLV in cells with or without the Ro60 protein suggests that these RNAs are recruited early in their biogenesis by MLV. Because prior studies have indicated that mY RNAs normally translocate and localize to the cytoplasm with the Ro60 protein in uninfected cells (164), the nuclear recruitment of mY RNAs by MLV might be expected to disrupt the normal subcellular localization of Ro60. The localization of Ro60 could be monitored by immunofluorescence in mock and chronically-infected cells, or its subceullar distribution in these cells could be determined by fractionation and subsequent western blots.

Lastly, in Chapter III, attempts to determine the relative half-life of nuclear unspliced MLV RNA were complicated by the global effects of general transcription inhibition with actinomycin D. A wide range of cellular noncoding RNAs were monitored for use as controls for Chapter III Figure 3-4 (Fig. 5-3A and 3B). General transcription inhibition with actinomycin D led to decreased cytoplasmic levels of all the non-coding RNAs tested (Fig. 5-3). Future experiments to determine the nuclear half-life of MLV unspliced RNA could use the tetracycline-inducible MLV cells also described in Chapter III. Specific repression of MLV transcription would not be expected to alter the intracellular distribution of cellular noncoding RNA which could then be used as controls for sample loading. Also, alterations in noncoding cellular RNA packaging after tetracycline-regulated repression of MLV might imply either co-recruitment with MLV gRNA or competition with MLV gRNA for recruitment. If non-competitive co-recruitment is occurring, then tetracycline-regulated repression of MLV would be

expected to result in a decrease in packaging of this RNA. Alternatively, repression of MLV transcription would be expected to increase packaging of RNAs which compete with MLV gRNA for recruitment into particles.

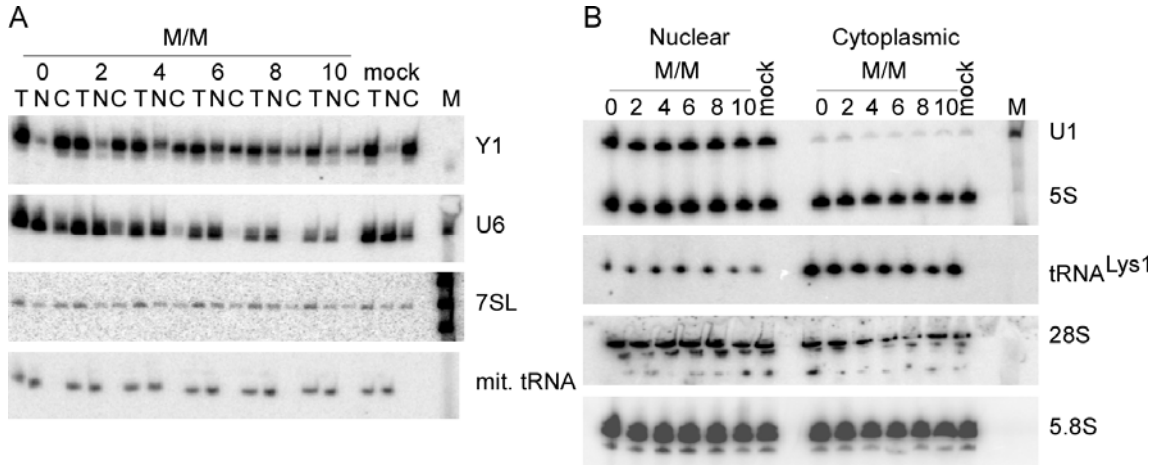

Figure 5-3. Northern blot of total, nuclear, and cytoplasmic fractions from NIH 3T3 fibroblasts that are mock or chronically-infected with MLV (M/M). (A) Total (T), nuclear (N), and cytoplasmic (C) fractions were probed for mY1 (Y1) RNAs, U6 snRNAs, 7SL RNAs, and mitochondrial tRNAs. (B) Nuclear and cytoplasmic fractions probed for U1 snRNA, 5S rRNA, $tRNA^{Lys1}$, 28S rRNA, and 5.8S rRNA. M/M cells are NIH 3T3 cells that are chronically infected with MLV. Mock cells were uninfected NIH 3T3 cells. The time in hours pre- and post-actinomycin D treatment is indicated on the top. Fractions were obtained by methods described in Chapter II and III which used digitonin to permeabilize the plasma membrane. Figures A and B represent two different blots that were repetitively stripped and re-probed for the indicated noncoding RNAs. On the right of each blot is an RNA size marker (M). The co-fractionation of mitochondrial tRNA with the nuclear fraction suggests that mitochondria were retained in the nuclear fraction, and this also suggests that the permeabilization of the plasma membrane with digitonin created holes in the plasma membrane that were smaller than the mitochondria.

REFERENCES

1. **Accola, M. A., B. Strack, and H. G. Gottlinger.** 2000. Efficient particle production by minimal Gag constructs which retain the carboxy-terminal domain of human immunodeficiency virus type 1 capsid-p2 and a late assembly domain. J Virol **74:**5395-402.

2. **Adam, M. A., and A. D. Miller.** 1988. Identification of a signal in a murine retrovirus that is sufficient for packaging of nonretroviral RNA into virions. J Virol **62:**3802-6.

3. **Alford, R. L., S. Honda, C. B. Lawrence, and J. W. Belmont.** 1991. RNA secondary structure analysis of the packaging signal for Moloney murine leukemia virus. Virology **183:**611-9.

4. **Andersen, J., and G. W. Zieve.** 1991. Assembly and intracellular transport of snRNP particles. Bioessays **13:**57-64.

5. **Andrei, M. A., D. Ingelfinger, R. Heintzmann, T. Achsel, R. Rivera-Pomar, and R. Luhrmann.** 2005. A role for eIF4E and eIF4E-transporter in targeting mRNPs to mammalian processing bodies. RNA **11:**717-27.

6. **Bach, D., S. Peddi, B. Mangeat, A. Lakkaraju, K. Strub, and D. Trono.** 2008. Characterization of APOBEC3G binding to 7SL RNA. Retrovirology **5:**54.

7. **Basyuk, E., S. Boulon, F. Skou Pedersen, E. Bertrand, and S. Vestergaard Rasmussen.** 2005. The packaging signal of MLV is an integrated module that mediates intracellular transport of genomic RNAs. J Mol Biol **354:**330-9.

8. **Basyuk, E., T. Galli, M. Mougel, J. M. Blanchard, M. Sitbon, and E. Bertrand.** 2003. Retroviral genomic RNAs are transported to the plasma membrane by endosomal vesicles. Dev Cell **5:**161-74.

9. **Beliakova-Bethell, N., C. Beckham, T. H. Giddings, Jr., M. Winey, R. Parker, and S. Sandmeyer.** 2006. Virus-like particles of the Ty3 retrotransposon assemble in association with P-body components. RNA **12:**94-101.

10. **Bender, M. A., T. D. Palmer, R. E. Gelinas, and A. D. Miller.** 1987. Evidence that the packaging signal of Moloney murine leukemia virus extends into the gag region. J Virol **61:**1639-46.

11. **Bender, W., Y. H. Chien, S. Chattopadhyay, P. K. Vogt, M. B. Gardner, and N. Davidson.** 1978. High-molecular-weight RNAs of AKR, NZB, and wild mouse viruses and avian reticuloendotheliosis virus all have similar dimer structures. J Virol **25:**888-96.

12. **Beriault, V., J. F. Clement, K. Levesque, C. Lebel, X. Yong, B. Chabot, E. A. Cohen, A. W. Cochrane, W. F. Rigby, and A. J. Mouland.** 2004. A late role for the association of hnRNP A2 with the HIV-1 hnRNP A2 response elements in genomic RNA, Gag, and Vpr localization. J Biol Chem **279:**44141-53.

13. **Berkowitz, R., J. Fisher, and S. P. Goff.** 1996. RNA packaging. Curr Top Microbiol Immunol **214:**177-218.

14. **Berkowitz, R. D., A. Ohagen, S. Hoglund, and S. P. Goff.** 1995. Retroviral nucleocapsid domains mediate the specific recognition of genomic viral RNAs by chimeric Gag polyproteins during RNA packaging in vivo. J Virol **69:**6445-56.

15. **Bishop, J. M., W. E. Levinson, N. Quintrell, D. Sullivan, L. Fanshier, and J. Jackson.** 1970. The low molecular weight RNAs of Rous sarcoma virus. I. The 4 S RNA. Virology **42:**182-95.

16. **Bishop, J. M., W. E. Levinson, D. Sullivan, L. Fanshier, N. Quintrell, and J. Jackson.** 1970. The low molecular weight RNAs of Rous sarcoma virus. II. The 7 S RNA. Virology **42:**927-37.

17. **Butsch, M., and K. Boris-Lawrie.** 2000. Translation is not required To generate virion precursor RNA in human immunodeficiency virus type 1-infected T cells. J Virol **74:**11531-7.

18. **Carmody, S. R., and S. R. Wente.** 2009. mRNA nuclear export at a glance. J Cell Sci **122:**1933-7.

19. **Cen, S., H. Javanbakht, S. Kim, K. Shiba, R. Craven, A. Rein, K. Ewalt, P. Schimmel, K. Musier-Forsyth, and L. Kleiman.** 2002. Retrovirus-specific packaging of aminoacyl-tRNA synthetases with cognate primer tRNAs. J Virol **76:**13111-5.

20. **Chatel-Chaix, L., K. Boulay, A. J. Mouland, and L. Desgroseillers.** 2008. The host protein Staufen1 interacts with the Pr55Gag zinc fingers and regulates HIV-1 assembly via its N-terminus. Retrovirology **5:**41.

21. **Chatel-Chaix, L., J. F. Clement, C. Martel, V. Beriault, A. Gatignol, L. DesGroseillers, and A. J. Mouland.** 2004. Identification of Staufen in the human immunodeficiency virus type 1 Gag ribonucleoprotein complex and a role in generating infectious viral particles. Mol Cell Biol **24:**2637-48.

22. **Chen, J., O. Nikolaitchik, J. Singh, A. Wright, C. E. Bencsics, J. M. Coffin, N. Ni, S. Lockett, V. K. Pathak, and W. S. Hu.** 2009. High efficiency of HIV-1 genomic RNA packaging and heterozygote formation revealed by single virion analysis. Proc Natl Acad Sci U S A **106:**13535-40.

23. **Chen, X., A. M. Quinn, and S. L. Wolin.** 2000. Ro ribonucleoproteins contribute to the resistance of Deinococcus radiodurans to ultraviolet irradiation. Genes Dev **14:**777-82.

24. **Chen, X., J. D. Smith, H. Shi, D. D. Yang, R. A. Flavell, and S. L. Wolin.** 2003. The Ro autoantigen binds misfolded U2 small nuclear RNAs and assists mammalian cell survival after UV irradiation. Curr Biol **13:**2206-11.

25. **Chen, X., and S. L. Wolin.** 2004. The Ro 60 kDa autoantigen: insights into cellular function and role in autoimmunity. J Mol Med **82:**232-9.

26. **Chen, X., E. J. Wurtmann, J. Van Batavia, B. Zybailov, M. P. Washburn, and S. L. Wolin.** 2007. An ortholog of the Ro autoantigen functions in 23S rRNA maturation in D. radiodurans. Genes Dev **21:**1328-39.

27. **Coffin, J. M., S. H. Hughes, and H. E. Varmus.** 1997. Retroviruses. Cold Spring Harbor Laboratory Press, Plainview, NY.

28. **Colicelli, J., and S. P. Goff.** 1988. Sequence and spacing requirements of a retrovirus integration site. J Mol Biol **199:**47-59.

29. **Cougot, N., S. Babajko, and B. Seraphin.** 2004. Cytoplasmic foci are sites of mRNA decay in human cells. J Cell Biol **165:**31-40.

30. **Crist, R. M., S. A. Datta, A. G. Stephen, F. Soheilian, J. Mirro, R. J. Fisher, K. Nagashima, and A. Rein.** 2009. Assembly properties of human immunodeficiency virus type 1 Gag-leucine zipper chimeras: implications for retrovirus assembly. J Virol **83:**2216-25.

31. **Cullen, B. R.** 1992. Mechanism of action of regulatory proteins encoded by complex retroviruses. Microbiol Rev **56:**375-94.

32. **Cullen, B. R.** 2003. Nuclear mRNA export: insights from virology. Trends Biochem Sci **28:**419-24.

33. **Curry, S., and M. R. Conte.** 2006. A terminal affair: 3'-end recognition by the human La protein. Trends Biochem Sci **31:**303-5.

34. **D'Souza, V., A. Dey, D. Habib, and M. F. Summers.** 2004. NMR structure of the 101-nucleotide core encapsidation signal of the Moloney murine leukemia virus. J Mol Biol **337:**427-42.

35. **D'Souza, V., J. Melamed, D. Habib, K. Pullen, K. Wallace, and M. F. Summers.** 2001. Identification of a high affinity nucleocapsid protein binding element within the Moloney murine leukemia virus Psi-RNA packaging signal: implications for genome recognition. J Mol Biol **314:**217-32.

36. **D'Souza, V., and M. F. Summers.** 2005. How retroviruses select their genomes. Nat Rev Microbiol **3:**643-55.

37. **D'Souza, V., and M. F. Summers.** 2004. Structural basis for packaging the dimeric genome of Moloney murine leukaemia virus. Nature **431:**586-90.

38. **Darlix, J. L., M. Lapadat-Tapolsky, H. de Rocquigny, and B. P. Roques.** 1995. First glimpses at structure-function relationships of the nucleocapsid protein of retroviruses. J Mol Biol **254:**523-37.

39. **De Rocquigny, H., D. Ficheux, C. Gabus, B. Allain, M. C. Fournie-Zaluski, J. L. Darlix, and B. P. Roques.** 1993. Two short basic sequences surrounding the zinc finger of nucleocapsid protein NCp10 of Moloney murine leukemia virus are critical for RNA annealing activity. Nucleic Acids Res **21:**823-9.

40. **Dejardin, J., G. Bompard-Marechal, M. Audit, T. J. Hope, M. Sitbon, and M. Mougel.** 2000. A novel subgenomic murine leukemia virus RNA transcript results from alternative splicing. J Virol **74:**3709-14.

41. **Demirov, D. G., and E. O. Freed.** 2004. Retrovirus budding. Virus Res **106:**87-102.

42. **Dey, A., D. York, A. Smalls-Mantey, and M. F. Summers.** 2005. Composition and sequence-dependent binding of RNA to the nucleocapsid protein of Moloney murine leukemia virus. Biochemistry **44:**3735-44.

43. **Dorman, N., and A. Lever.** 2000. Comparison of viral genomic RNA sorting mechanisms in human immunodeficiency virus type 1 (HIV-1), HIV-2, and Moloney murine leukemia virus. J Virol **74:**11413-7.

44. **Dreyfuss, G.** 1986. Structure and function of nuclear and cytoplasmic ribonucleoprotein particles. Annu Rev Cell Biol **2:**459-98.

45. **Dreyfuss, G., V. N. Kim, and N. Kataoka.** 2002. Messenger-RNA-binding proteins and the messages they carry. Nat Rev Mol Cell Biol **3:**195-205.

46. **Duesberg, P. H., and W. S. Robinson.** 1966. Nucleic acid and proteins isolated from the Rauscher mouse leukemia virus (MLV). Proc Natl Acad Sci U S A **55:**219-27.

47. **Edwards, S. A., and H. Fan.** 1980. Sequence relationship of glycosylated and unglycosylated gag polyproteins of Moloney murine leukemia virus. J Virol **35:**41-51.

48. **Embretson, J. E., and H. M. Temin.** 1987. Lack of competition results in efficient packaging of heterologous murine retroviral RNAs and reticuloendotheliosis virus encapsidation-minus RNAs by the reticuloendotheliosis virus helper cell line. J Virol **61:**2675-83.

49. **Eulalio, A., I. Behm-Ansmant, and E. Izaurralde.** 2007. P bodies: at the crossroads of post-transcriptional pathways. Nat Rev Mol Cell Biol **8:**9-22.

50. **Evans, M. J., E. Bacharach, and S. P. Goff.** 2004. RNA sequences in the Moloney murine leukemia virus genome bound by the Gag precursor protein in the yeast three-hybrid system. J Virol **78:**7677-84.

51. **Fabini, G., R. Raijmakers, S. Hayer, M. A. Fouraux, G. J. Pruijn, and G. Steiner.** 2001. The heterogeneous nuclear ribonucleoproteins I and K interact with a subset of the ro ribonucleoprotein-associated Y RNAs in vitro and in vivo. J Biol Chem **276:**20711-8.

52. **Flynn, J. A.** 2005. Retroviral genomic RNA dimer partner selection. Ph.D. Dissertation. University of Michigan, Ann Arbor.

53. **Flynn, J. A., W. An, S. R. King, and A. Telesnitsky.** 2004. Nonrandom dimerization of murine leukemia virus genomic RNAs. J Virol **78:**12129-39.

54. **Flynn, J. A., and A. Telesnitsky.** 2006. Two distinct Moloney murine leukemia virus RNAs produced from a single locus dimerize at random. Virology **344:**391-400.

55. **Fok, V., K. Friend, and J. A. Steitz.** 2006. Epstein-Barr virus noncoding RNAs are confined to the nucleus, whereas their partner, the human La protein, undergoes nucleocytoplasmic shuttling. J Cell Biol **173:**319-25.

56. **Fouraux, M. A., P. Bouvet, S. Verkaart, W. J. van Venrooij, and G. J. Pruijn.** 2002. Nucleolin associates with a subset of the human Ro ribonucleoprotein complexes. J Mol Biol **320:**475-88.

57. **Freed, E. O.** 1998. HIV-1 gag proteins: diverse functions in the virus life cycle. Virology **251:**1-15.

58. **Fu, W., and A. Rein.** 1993. Maturation of dimeric viral RNA of Moloney murine leukemia virus. J Virol **67:**5443-9.

59. **Fuchs, G., A. J. Stein, C. Fu, K. M. Reinisch, and S. L. Wolin.** 2006. Structural and biochemical basis for misfolded RNA recognition by the Ro autoantigen. Nat Struct Mol Biol **13:**1002-9.

60. **Fukata, M., S. Kuroda, K. Fujii, T. Nakamura, I. Shoji, Y. Matsuura, K. Okawa, A. Iwamatsu, A. Kikuchi, and K. Kaibuchi.** 1997. Regulation of cross-linking of actin filament by IQGAP1, a target for Cdc42. J Biol Chem **272:**29579-83.

61. **Fukata, M., T. Watanabe, J. Noritake, M. Nakagawa, M. Yamaga, S. Kuroda, Y. Matsuura, A. Iwamatsu, F. Perez, and K. Kaibuchi.** 2002. Rac1 and Cdc42 capture microtubules through IQGAP1 and CLIP-170. Cell **109:**873-85.

62. **Gallois-Montbrun, S., R. K. Holmes, C. M. Swanson, M. Fernandez-Ocana, H. L. Byers, M. A. Ward, and M. H. Malim.** 2008. Comparison of cellular ribonucleoprotein complexes associated with the APOBEC3F and APOBEC3G antiviral proteins. J Virol **82:**5636-42.

63. **Ganser-Pornillos, B. K., M. Yeager, and W. I. Sundquist.** 2008. The structural biology of HIV assembly. Curr Opin Struct Biol **18:**203-17.

64. **Garbitt-Hirst, R., S. P. Kenney, and L. J. Parent.** 2009. Genetic evidence for a connection between Rous sarcoma virus gag nuclear trafficking and genomic RNA packaging. J Virol **83:**6790-7.

65. **Garcia, E. L., A. Onafuwa-Nuga, S. Sim, S. R. King, S. L. Wolin, and A. Telesnitsky.** 2009. Packaging of host mY RNAs by murine leukemia virus may occur early in Y RNA biogenesis. J Virol **83:**12526-34.

66. **Gerace, L.** 1995. Nuclear export signals and the fast track to the cytoplasm. Cell **82:**341-4.

67. **Giles, K. E., M. Caputi, and K. L. Beemon.** 2004. Packaging and reverse transcription of snRNAs by retroviruses may generate pseudogenes. RNA **10:**299-307.

68. **Girard, P. M., H. de Rocquigny, B. P. Roques, and J. Paoletti.** 1996. A model of PSI dimerization: destabilization of the C278-G303 stem-loop by the nucleocapsid protein (NCp10) of MoMuLV. Biochemistry **35:**8705-14.

69. **Glynn, J. M., T. G. Cotter, and D. R. Green.** 1992. Apoptosis induced by Actinomycin D, Camptothecin or Aphidicolin can occur in all phases of the cell cycle. Biochem Soc Trans **20:**84S.

70. **Goff, S., P. Traktman, and D. Baltimore.** 1981. Isolation and properties of Moloney murine leukemia virus mutants: use of a rapid assay for release of virion reverse transcriptase. J Virol **38:**239-48.

71. **Gonsky, J., E. Bacharach, and S. P. Goff.** 2001. Identification of residues of the Moloney murine leukemia virus nucleocapsid critical for viral DNA synthesis in vivo. J Virol **75:**2616-26.

72. **Gorelick, R. J., L. E. Henderson, J. P. Hanser, and A. Rein.** 1988. Point mutants of Moloney murine leukemia virus that fail to package viral RNA: evidence for specific RNA recognition by a "zinc finger-like" protein sequence. Proc Natl Acad Sci U S A **85:**8420-4.

73. **Graham, F. L., J. Smiley, W. C. Russell, and R. Nairn.** 1977. Characteristics of a human cell line transformed by DNA from human adenovirus type 5. J Gen Virol **36:**59-74.

74. **Greatorex, J., and A. Lever.** 1998. Retroviral RNA dimer linkage. J Gen Virol **79 (Pt 12):**2877-82.

75. **Green, C. D., K. S. Long, H. Shi, and S. L. Wolin.** 1998. Binding of the 60-kDa Ro autoantigen to Y RNAs: evidence for recognition in the major groove of a conserved helix. RNA **4:**750-65.

76. **Griffin, S. D., J. F. Allen, and A. M. Lever.** 2001. The major human immunodeficiency virus type 2 (HIV-2) packaging signal is present on all HIV-2 RNA species: cotranslational RNA encapsidation and limitation of Gag protein confer specificity. J Virol **75:**12058-69.

77. **Grimm, C., E. Lund, and J. E. Dahlberg.** 1997. In vivo selection of RNAs that localize in the nucleus. EMBO J **16:**793-806.

78. **Gruter, P., C. Tabernero, C. von Kobbe, C. Schmitt, C. Saavedra, A. Bachi, M. Wilm, B. K. Felber, and E. Izaurralde.** 1998. TAP, the human homolog of Mex67p, mediates CTE-dependent RNA export from the nucleus. Mol Cell **1:**649-59.

79. **Gwizdek, C., E. Bertrand, C. Dargemont, J. C. Lefebvre, J. M. Blanchard, R. H. Singer, and A. Doglio.** 2001. Terminal minihelix, a novel RNA motif that directs polymerase III transcripts to the cell cytoplasm. Terminal minihelix and RNA export. J Biol Chem **276:**25910-8.

80. **Gwizdek, C., B. Ossareh-Nazari, A. M. Brownawell, A. Doglio, E. Bertrand, I. G. Macara, and C. Dargemont.** 2003. Exportin-5 mediates nuclear export of minihelix-containing RNAs. J Biol Chem **278:**5505-8.

81. **Hibbert, C. S., J. Mirro, and A. Rein.** 2004. mRNA molecules containing murine leukemia virus packaging signals are encapsidated as dimers. J Virol **78:**10927-38.

82. **Hibbert, C. S., and A. Rein.** 2005. Preliminary physical mapping of RNA-RNA linkages in the genomic RNA of Moloney murine leukemia virus. J Virol **79:**8142-8.

83. **Houzet, L., J. L. Battini, E. Bernard, V. Thibert, and M. Mougel.** 2003. A new retroelement constituted by a natural alternatively spliced RNA of murine replication-competent retroviruses. Embo J **22:**4866-75.

84. **Houzet, L., J. C. Paillart, F. Smagulova, S. Maurel, Z. Morichaud, R. Marquet, and M. Mougel.** 2007. HIV controls the selective packaging of genomic, spliced viral and cellular RNAs into virions through different mechanisms. Nucleic Acids Res **35:**2695-704.

85. **Jablonski, J. A., and M. Caputi.** 2009. Role of cellular RNA processing factors in human immunodeficiency virus type 1 mRNA metabolism, replication, and infectivity. J Virol **83:**981-92.

86. **Kamath, R. V., D. J. Leary, and S. Huang.** 2001. Nucleocytoplasmic shuttling of polypyrimidine tract-binding protein is uncoupled from RNA export. Mol Biol Cell **12:**3808-20.

87. **Kawamura, H., Y. Tomozoe, T. Akagi, D. Kamei, M. Ochiai, and M. Yamada.** 2002. Identification of the nucleocytoplasmic shuttling sequence of heterogeneous nuclear ribonucleoprotein D-like protein JKTBP and its interaction with mRNA. J Biol Chem **277:**2732-9.

88. **Kaye, J. F., and A. M. Lever.** 1999. Human immunodeficiency virus types 1 and 2 differ in the predominant mechanism used for selection of genomic RNA for encapsidation. J Virol **73:**3023-31.

89. **Keenan, R. J., D. M. Freymann, R. M. Stroud, and P. Walter.** 2001. The signal recognition particle. Annu Rev Biochem **70:**755-75.

90. **Kelly, S. M., and A. H. Corbett.** 2009. Messenger RNA export from the nucleus: a series of molecular wardrobe changes. Traffic **10:**1199-208.

91. **Khan, M. A., R. Goila-Gaur, S. Opi, E. Miyagi, H. Takeuchi, S. Kao, and K. Strebel.** 2007. Analysis of the contribution of cellular and viral RNA to the packaging of APOBEC3G into HIV-1 virions. Retrovirology **4:**48.

92. **Kharytonchyk, S. A., A. I. Kireyeva, A. B. Osipovich, and I. K. Fomin.** 2005. Evidence for preferential copackaging of Moloney murine leukemia virus genomic RNAs transcribed in the same chromosomal site. Retrovirology **2:**3.

93. **Kim, W., Y. Tang, Y. Okada, T. A. Torrey, S. K. Chattopadhyay, M. Pfleiderer, F. G. Falkner, F. Dorner, W. Choi, N. Hirokawa, and H. C. Morse, 3rd.** 1998. Binding of murine leukemia virus Gag polyproteins to KIF4, a microtubule-based motor protein. J Virol **72:**6898-901.

94. **King, J. A., J. M. Bridger, F. Gounari, P. Lichter, T. F. Schulz, V. Schirrmacher, and K. Khazaie.** 1998. The extended packaging sequence of MoMLV contains a constitutive mRNA nuclear export function. FEBS Lett **434:**367-71.

95. **Kleeff, J., M. Kornmann, H. Sawhney, and M. Korc.** 2000. Actinomycin D induces apoptosis and inhibits growth of pancreatic cancer cells. Int J Cancer **86:**399-407.

96. **Klein, K. C., J. C. Reed, and J. R. Lingappa.** 2007. Intracellular destinies: degradation, targeting, assembly, and endocytosis of HIV Gag. AIDS Rev **9:**150-61.

97. **Konings, D. A., M. A. Nash, J. V. Maizel, and R. B. Arlinghaus.** 1992. Novel GACG-hairpin pair motif in the 5' untranslated region of type C retroviruses related to murine leukemia virus. J Virol **66:**632-40.

98. **Kulpa, D., R. Topping, and A. Telesnitsky.** 1997. Determination of the site of first strand transfer during Moloney murine leukemia virus reverse transcription and identification of strand transfer-associated reverse transcriptase errors. Embo J **16:**856-65.

99. **Kulpa, D. A., and J. V. Moran.** 2006. Cis-preferential LINE-1 reverse transcriptase activity in ribonucleoprotein particles. Nat Struct Mol Biol **13:**655-60.

100. **Kung, H. J., S. Hu, W. Bender, J. M. Bailey, N. Davidson, M. O. Nicolson, and R. M. McAllister.** 1976. RD-114, baboon, and woolly monkey viral RNA's compared in size and structure. Cell **7:**609-20.

101. **Labbe, J. C., S. Hekimi, and L. A. Rokeach.** 1999. The levels of the RoRNP-associated Y RNA are dependent upon the presence of ROP-1, the Caenorhabditis elegans Ro60 protein. Genetics **151:**143-50.

102. **LeBlanc, J. J., and K. L. Beemon.** 2004. Unspliced Rous sarcoma virus genomic RNAs are translated and subjected to nonsense-mediated mRNA decay before packaging. J Virol **78:**5139-46.

103. **LeBlanc, J. J., S. Uddowla, B. Abraham, S. Clatterbuck, and K. L. Beemon.** 2007. Tap and Dbp5, but not Gag, are involved in DR-mediated nuclear export of unspliced Rous sarcoma virus RNA. Virology **363:**376-86.

104. **Lee, S., M. Neumann, R. Stearman, R. Stauber, A. Pause, G. N. Pavlakis, and R. D. Klausner.** 1999. Transcription-dependent nuclear-cytoplasmic trafficking is required for the function of the von Hippel-Lindau tumor suppressor protein. Mol Cell Biol **19:**1486-97.

105. **Leung, J., A. Yueh, F. S. Appah, Jr., B. Yuan, K. de los Santos, and S. P. Goff.** 2006. Interaction of Moloney murine leukemia virus matrix protein with IQGAP. Embo J **25:**2155-66.

106. **Levesque, K., M. Halvorsen, L. Abrahamyan, L. Chatel-Chaix, V. Poupon, H. Gordon, L. DesGroseillers, A. Gatignol, and A. J. Mouland.** 2006. Trafficking of HIV-1 RNA is mediated by heterogeneous nuclear ribonucleoprotein A2 expression and impacts on viral assembly. Traffic **7:**1177-93.

107. **Levin, J. G., P. M. Grimley, J. M. Ramseur, and I. K. Berezesky.** 1974. Deficiency of 60 to 70S RNA in murine leukemia virus particles assembled in cells treated with actinomycin D. J Virol **14:**152-61.

108. **Levin, J. G., and M. J. Rosenak.** 1976. Synthesis of murine leukemia virus proteins associated with virions assembled in actinomycin D-treated cells: evidence for persistence of viral messenger RNA. Proc Natl Acad Sci U S A **73:**1154-8.

109. **Levin, J. G., and J. G. Seidman.** 1981. Effect of polymerase mutations on packaging of primer tRNAPro during murine leukemia virus assembly. J Virol **38:**403-8.

110. **Levin, J. G., and J. G. Seidman.** 1979. Selective packaging of host tRNA's by murine leukemia virus particles does not require genomic RNA. J Virol **29:**328-35.

111. **Ly, H., and T. G. Parslow.** 2002. Bipartite signal for genomic RNA dimerization in Moloney murine leukemia virus. J Virol **76:**3135-44.

112. **Maisel, J., W. Bender, S. Hu, P. H. Duesberg, and N. Davidson.** 1978. Structure of 50 to 70S RNA from Moloney sarcoma viruses. J Virol **25:**384-94.

113. **Mak, J., and L. Kleiman.** 1997. Primer tRNAs for reverse transcription. J Virol **71:**8087-95.

114. **Mann, R., and D. Baltimore.** 1985. Varying the position of a retrovirus packaging sequence results in the encapsidation of both unspliced and spliced RNAs. J Virol **54:**401-7.

115. **Mann, R., R. C. Mulligan, and D. Baltimore.** 1983. Construction of a retrovirus packaging mutant and its use to produce helper-free defective retrovirus. Cell **33:**153-9.

116. **Maraia, R. J., and R. V. Intine.** 2001. Recognition of nascent RNA by the human La antigen: conserved and divergent features of structure and function. Mol Cell Biol **21:**367-79.

117. **Martinez, N. W., X. Xue, R. G. Berro, G. Kreitzer, and M. D. Resh.** 2008. Kinesin KIF4 regulates intracellular trafficking and stability of the human immunodeficiency virus type 1 Gag polyprotein. J Virol **82:**9937-50.

118. **Marx, J.** 2005. Molecular biology. P-bodies mark the spot for controlling protein production. Science **310:**764-5.

119. **Matera, A. G., M. R. Frey, K. Margelot, and S. L. Wolin.** 1995. A perinucleolar compartment contains several RNA polymerase III transcripts as well as the polypyrimidine tract-binding protein, hnRNP I. J Cell Biol **129:**1181-93.

120. **Maurel, S., L. Houzet, E. L. Garcia, A. Telesnitsky, and M. Mougel.** 2007. Characterization of a natural heterodimer between MLV genomic RNA and the SD' retroelement generated by alternative splicing. RNA **13:**2266-76.

121. **Meric, C., and S. P. Goff.** 1989. Characterization of Moloney murine leukemia virus mutants with single-amino-acid substitutions in the Cys-His box of the nucleocapsid protein. J Virol **63:**1558-68.

122. **Messer, L. I., J. G. Levin, and S. K. Chattopadhyay.** 1981. Metabolism of viral RNA in murine leukemia virus-infected cells; evidence for differential stability of viral message and virion precursor RNA. J Virol **40:**683-90.

123. **Mikkelsen, J. G., S. V. Rasmussen, and F. S. Pedersen.** 2004. Complementarity-directed RNA dimer-linkage promotes retroviral recombination in vivo. Nucleic Acids Res **32:**102-14.

124. **Miyazaki, Y., E. L. Garcia, S. R. King, K. Iyalla, K. Loeliger, P. Starck, S. Syed, A. Telesnitsky, and M. F. Summers.** 2010. An RNA structural switch regulates diploid genome packaging by Moloney murine leukemia virus. J Mol Biol **396:**141-52.

125. **Monette, A., L. Ajamian, M. Lopez-Lastra, and A. J. Mouland.** 2009. Human immunodeficiency virus type 1 (HIV-1) induces the cytoplasmic retention of heterogeneous nuclear ribonucleoprotein A1 by disrupting nuclear import: implications for HIV-1 gene expression. J Biol Chem **284:**31350-62.

126. **Moore, M. D., M. P. Chin, and W. S. Hu.** 2009. HIV-1 recombination: an experimental assay and a phylogenetic approach. Methods Mol Biol **485:**87-105.

127. **Moore, M. D., W. Fu, O. Nikolaitchik, J. Chen, R. G. Ptak, and W. S. Hu.** 2007. Dimer initiation signal of human immunodeficiency virus type 1: its role in partner selection during RNA copackaging and its effects on recombination. J Virol **81:**4002-11.

128. **Moore, M. D., O. A. Nikolaitchik, J. Chen, M. L. Hammarskjold, D. Rekosh, and W. S. Hu.** 2009. Probing the HIV-1 genomic RNA trafficking pathway and dimerization by genetic recombination and single virion analyses. PLoS Pathog **5:**e1000627.

129. **Mougel, M., and E. Barklis.** 1997. A role for two hairpin structures as a core RNA encapsidation signal in murine leukemia virus virions. J Virol **71:**8061-5.

130. **Mouland, A. J., J. Mercier, M. Luo, L. Bernier, L. DesGroseillers, and E. A. Cohen.** 2000. The double-stranded RNA-binding protein Staufen is incorporated in human immunodeficiency virus type 1: evidence for a role in genomic RNA encapsidation. J Virol **74:**5441-51.

131. **Mouland, A. J., H. Xu, H. Cui, W. Krueger, T. P. Munro, M. Prasol, J. Mercier, D. Rekosh, R. Smith, E. Barbarese, E. A. Cohen, and J. H. Carson.** 2001. RNA trafficking signals in human immunodeficiency virus type 1. Mol Cell Biol **21:**2133-43.

132. **Muriaux, D., J. Mirro, D. Harvin, and A. Rein.** 2001. RNA is a structural element in retrovirus particles. Proc Natl Acad Sci U S A **98:**5246-51.

133. **Muriaux, D., J. Mirro, K. Nagashima, D. Harvin, and A. Rein.** 2002. Murine leukemia virus nucleocapsid mutant particles lacking viral RNA encapsidate ribosomes. J Virol **76:**11405-13.

134. **Murti, K. G., M. Bondurant, and A. Tereba.** 1981. Secondary structural features in the 70S RNAs of Moloney murine leukemia and Rous sarcoma viruses as observed by electron microscopy. J Virol **37:**411-19.

135. **Naghavi, M. H., and S. P. Goff.** 2007. Retroviral proteins that interact with the host cell cytoskeleton. Curr Opin Immunol **19:**402-7.

136. **Narita, T., Y. Yamaguchi, K. Yano, S. Sugimoto, S. Chanarat, T. Wada, D. K. Kim, J. Hasegawa, M. Omori, N. Inukai, M. Endoh, T. Yamada, and H. Handa.** 2003. Human transcription elongation factor NELF: identification of novel subunits and reconstitution of the functionally active complex. Mol Cell Biol **23:**1863-73.

137. **Nash, M. A., M. K. Meyer, G. L. Decker, and R. B. Arlinghaus.** 1993. A subset of Pr65gag is nucleus associated in murine leukemia virus-infected cells. J Virol **67:**1350-6.

138. **Neville, M., F. Stutz, L. Lee, L. I. Davis, and M. Rosbash.** 1997. The importin-beta family member Crm1p bridges the interaction between Rev and the nuclear pore complex during nuclear export. Curr Biol **7:**767-75.

139. **Nikolaitchik, O., T. D. Rhodes, D. Ott, and W. S. Hu.** 2006. Effects of mutations in the human immunodeficiency virus type 1 Gag gene on RNA packaging and recombination. J Virol **80:**4691-7.

140. **Nitta, T., Y. Kuznetsov, A. McPherson, and H. Fan.** 2010. Murine leukemia virus glycosylated Gag (gPr80gag) facilitates interferon-sensitive virus release through lipid rafts. Proc Natl Acad Sci U S A **107:**1190-5.

141. **O'Brien, C. A., K. Margelot, and S. L. Wolin.** 1993. Xenopus Ro ribonucleoproteins: members of an evolutionarily conserved class of cytoplasmic ribonucleoproteins. Proc Natl Acad Sci U S A **90:**7250-4.

142. **O'Brien, C. A., and S. L. Wolin.** 1994. A possible role for the 60-kD Ro autoantigen in a discard pathway for defective 5S rRNA precursors. Genes Dev **8:**2891-903.

143. **O'Hagan, H. M., and M. Ljungman.** 2004. Efficient NES-dependent protein nuclear export requires ongoing synthesis and export of mRNAs. Exp Cell Res **297:**548-59.

144. **O'Reilly, L., and M. J. Roth.** 2000. Second-site changes affect viability of amphotropic/ecotropic chimeric enveloped murine leukemia viruses. J Virol **74:**899-913.

145. **Ogert, R. A., and K. L. Beemon.** 1998. Mutational analysis of the rous sarcoma virus DR posttranscriptional control element. J Virol **72:**3407-11.

146. **Ogert, R. A., L. H. Lee, and K. L. Beemon.** 1996. Avian retroviral RNA element promotes unspliced RNA accumulation in the cytoplasm. J Virol **70:**3834-43.

147. **Onafuwa-Nuga, A., and A. Telesnitsky.** 2009. The remarkable frequency of human immunodeficiency virus type 1 genetic recombination. Microbiol Mol Biol Rev **73:**451-80, Table of Contents.

148. **Onafuwa-Nuga, A. A.** 2007. Host cell RNA packaging in retroviruses. Ph.D. Dissertation. University of Michigan, Ann Arbor.

149. **Onafuwa-Nuga, A. A., S. R. King, and A. Telesnitsky.** 2005. Nonrandom packaging of host RNAs in moloney murine leukemia virus. J Virol **79:**13528-37.

150. **Onafuwa-Nuga, A. A., A. Telesnitsky, and S. R. King.** 2006. 7SL RNA, but not the 54-kd signal recognition particle protein, is an abundant component of both infectious HIV-1 and minimal virus-like particles. RNA **12:**542-6.

151. **Onafuwa, A., W. An, N. D. Robson, and A. Telesnitsky.** 2003. Human immunodeficiency virus type 1 genetic recombination is more frequent than that of Moloney murine leukemia virus despite similar template switching rates. J Virol **77:**4577-87.

152. **Oroudjev, E. M., P. C. Kang, and L. A. Kohlstaedt.** 1999. An additional dimer linkage structure in Moloney murine leukemia virus RNA. J Mol Biol **291:**603-13.

153. **Pamballk, K., C. Hohenadl, B. Salmons, W. H. Gunzburg, and M. Renner.** 2002. Specific packaging of spliced retroviral vector transcripts lacking the Psi-region. Biochem Biophys Res Commun **293:**239-46.

154. **Paoletti, J., M. Mougel, N. Tounekti, P. M. Girard, C. Ehresmann, and B. Ehresmann.** 1993. Spontaneous dimerization of retroviral MoMuLV RNA. Biochimie **75:**681-6.

155. **Pasquinelli, A. E., R. K. Ernst, E. Lund, C. Grimm, M. L. Zapp, D. Rekosh, M. L. Hammarskjold, and J. E. Dahlberg.** 1997. The constitutive transport element (CTE) of Mason-Pfizer monkey virus (MPMV) accesses a cellular mRNA export pathway. Embo J **16:**7500-10.

156. **Peek, R., G. J. Pruijn, A. J. van der Kemp, and W. J. van Venrooij.** 1993. Subcellular distribution of Ro ribonucleoprotein complexes and their constituents. J Cell Sci **106 (Pt 3):**929-35.

157. **Peters, G., F. Harada, J. E. Dahlberg, A. Panet, W. A. Haseltine, and D. Baltimore.** 1977. Low-molecular-weight RNAs of Moloney murine leukemia virus: identification of the primer for RNA-directed DNA synthesis. J Virol **21:**1031-41.

158. **Pfeiffer, J. K., R. S. Topping, N. H. Shin, and A. Telesnitsky.** 1999. Altering the intracellular environment increases the frequency of tandem repeat deletion during Moloney murine leukemia virus reverse transcription. J Virol **73:**8441-7.

159. **Pinol-Roma, S., and G. Dreyfuss.** 1991. Transcription-dependent and transcription-independent nuclear transport of hnRNP proteins. Science **253:**312-4.

160. **Poole, E., P. Strappe, H. P. Mok, R. Hicks, and A. M. Lever.** 2005. HIV-1 Gag-RNA interaction occurs at a perinuclear/centrosomal site; analysis by confocal microscopy and FRET. Traffic **6:**741-55.

161. **Prats, A. C., V. Housset, G. de Billy, F. Cornille, H. Prats, B. Roques, and J. L. Darlix.** 1991. Viral RNA annealing activities of the nucleocapsid protein of Moloney murine leukemia virus are zinc independent. Nucleic Acids Res **19:**3533-41.

162. **Prats, A. C., C. Roy, P. A. Wang, M. Erard, V. Housset, C. Gabus, C. Paoletti, and J. L. Darlix.** 1990. Cis elements and trans-acting factors involved in dimer formation of murine leukemia virus RNA. J Virol **64:**774-83.

163. **Price, J., D. Turner, and C. Cepko.** 1987. Lineage analysis in the vertebrate nervous system by retrovirus-mediated gene transfer. Proc Natl Acad Sci U S A **84:**156-60.

164. **Pruijn, G. J., F. H. Simons, and W. J. van Venrooij.** 1997. Intracellular localization and nucleocytoplasmic transport of Ro RNP components. Eur J Cell Biol **74:**123-32.

165. **Rasmussen, S., and F. S. Pedersen.** 2004. Complementarity between RNA dimerization elements favors formation of functional heterozygous murine leukemia viruses. Virology **329:**440-53.

166. **Rasmussen, S. V., and F. S. Pedersen.** 2006. Co-localization of gammaretroviral RNAs at their transcription site favours co-packaging. J Gen Virol **87:**2279-89.

167. **Rehberger, S., F. Gounari, M. DucDodon, K. Chlichlia, L. Gazzolo, V. Schirrmacher, and K. Khazaie.** 1997. The activation domain of a hormone inducible HTLV-1 Rex protein determines colocalization with the nuclear pore. Exp Cell Res **233:**363-71.

168. **Rein, A.** 1994. Retroviral RNA packaging: a review. Arch Virol Suppl **9:**513-22.

169. **Rein, A., D. P. Harvin, J. Mirro, S. M. Ernst, and R. J. Gorelick.** 1994. Evidence that a central domain of nucleocapsid protein is required for RNA packaging in murine leukemia virus. J Virol **68:**6124-9.

170. **Rein, A., L. E. Henderson, and J. G. Levin.** 1998. Nucleic-acid-chaperone activity of retroviral nucleocapsid proteins: significance for viral replication. Trends Biochem Sci **23:**297-301.

171. **Reinisch, K. M., and S. L. Wolin.** 2007. Emerging themes in non-coding RNA quality control. Curr Opin Struct Biol **17:**209-14.

172. **Robson, N. D., and A. Telesnitsky.** 1999. Effects of 3' untranslated region mutations on plus-strand priming during moloney murine leukemia virus replication. J Virol **73:**948-57.

173. **Rodrigues, J. P., M. Rode, D. Gatfield, B. J. Blencowe, M. Carmo-Fonseca, and E. Izaurralde.** 2001. REF proteins mediate the export of spliced and unspliced mRNAs from the nucleus. Proc Natl Acad Sci U S A **98:**1030-5.

174. **Rulli, S. J., Jr., C. S. Hibbert, J. Mirro, T. Pederson, S. Biswal, and A. Rein.** 2007. Selective and nonselective packaging of cellular RNAs in retrovirus particles. J Virol **81:**6623-31.

175. **Rutjes, S. A., E. Lund, A. van der Heijden, C. Grimm, W. J. van Venrooij, and G. J. Pruijn.** 2001. Identification of a novel cis-acting RNA element involved in nuclear export of hY RNAs. RNA **7:**741-52.

176. **Scheifele, L. Z., R. A. Garbitt, J. D. Rhoads, and L. J. Parent.** 2002. Nuclear entry and CRM1-dependent nuclear export of the Rous sarcoma virus Gag polyprotein. Proc Natl Acad Sci U S A **99:**3944-9.

177. **Scheifele, L. Z., S. P. Kenney, T. M. Cairns, R. C. Craven, and L. J. Parent.** 2007. Overlapping roles of the Rous sarcoma virus Gag p10 domain in nuclear export and virion core morphology. J Virol **81:**10718-28.

178. **Scheifele, L. Z., E. P. Ryan, and L. J. Parent.** 2005. Detailed mapping of the nuclear export signal in the Rous sarcoma virus Gag protein. J Virol **79:**8732-41.

179. **Schultz, A. M., and A. Rein.** 1989. Unmyristylated Moloney murine leukemia virus Pr65gag is excluded from virus assembly and maturation events. J Virol **63:**2370-3.

180. **Sfakianos, J. N., R. A. LaCasse, and E. Hunter.** 2003. The M-PMV cytoplasmic targeting-retention signal directs nascent Gag polypeptides to a pericentriolar region of the cell. Traffic **4:**660-70.

181. **Shatkin, A. J., and J. L. Manley.** 2000. The ends of the affair: capping and polyadenylation. Nat Struct Biol **7:**838-42.

182. **Sheth, U., and R. Parker.** 2003. Decapping and decay of messenger RNA occur in cytoplasmic processing bodies. Science **300:**805-8.

183. **Shin, N. H., D. Hartigan-O'Connor, J. K. Pfeiffer, and A. Telesnitsky.** 2000. Replication of lengthened Moloney murine leukemia virus genomes is impaired at multiple stages. J Virol **74:**2694-702.

184. **Shinnick, T. M., R. A. Lerner, and J. G. Sutcliffe.** 1981. Nucleotide sequence of Moloney murine leukaemia virus. Nature **293:**543-8.

185. **Sim, S., D. E. Weinberg, G. Fuchs, K. Choi, J. Chung, and S. L. Wolin.** 2008. The Subcellular Distribution of an RNA Quality Control Protein, the Ro Autoantigen, Is Regulated by Noncoding Y RNA Binding. Mol Biol Cell.

186. **Sim, S., D. E. Weinberg, G. Fuchs, K. Choi, J. Chung, and S. L. Wolin.** 2009. The subcellular distribution of an RNA quality control protein, the Ro autoantigen, is regulated by noncoding Y RNA binding. Mol Biol Cell **20:**1555-64.

187. **Simons, F. H., G. J. Pruijn, and W. J. van Venrooij.** 1994. Analysis of the intracellular localization and assembly of Ro ribonucleoprotein particles by microinjection into Xenopus laevis oocytes. J Cell Biol **125:**981-8.

188. **Simons, F. H., S. A. Rutjes, W. J. van Venrooij, and G. J. Pruijn.** 1996. The interactions with Ro60 and La differentially affect nuclear export of hY1 RNA. RNA **2:**264-73.

189. **Simpson, S. B., L. Zhang, R. C. Craven, and C. M. Stoltzfus.** 1997. Rous sarcoma virus direct repeat cis elements exert effects at several points in the virus life cycle. J Virol **71:**9150-6.

190. **Singer, R. H., and S. Penman.** 1972. Stability of HeLa cell mRNA in actinomycin. Nature **240:**100-2.

191. **Siomi, M. C., P. S. Eder, N. Kataoka, L. Wan, Q. Liu, and G. Dreyfuss.** 1997. Transportin-mediated nuclear import of heterogeneous nuclear RNP proteins. J Cell Biol **138:**1181-92.

192. **Smagulova, F., S. Maurel, Z. Morichaud, C. Devaux, M. Mougel, and L. Houzet.** 2005. The highly structured encapsidation signal of MuLV RNA is involved in the nuclear export of its unspliced RNA. J Mol Biol **354:**1118-28.

193. **Song, R., J. Kafaie, L. Yang, and M. Laughrea.** 2007. HIV-1 viral RNA is selected in the form of monomers that dimerize in a three-step protease-dependent process; the DIS of stem-loop 1 initiates viral RNA dimerization. J Mol Biol **371:**1084-98.

194. **Sonstegard, T. S., and P. B. Hackett.** 1996. Autogenous regulation of RNA translation and packaging by Rous sarcoma virus Pr76gag. J Virol **70:**6642-52.

195. **St Johnston, D., D. Beuchle, and C. Nusslein-Volhard.** 1991. Staufen, a gene required to localize maternal RNAs in the Drosophila egg. Cell **66:**51-63.

196. **Stauber, R., G. A. Gaitanaris, and G. N. Pavlakis.** 1995. Analysis of trafficking of Rev and transdominant Rev proteins in living cells using green fluorescent protein fusions: transdominant Rev blocks the export of Rev from the nucleus to the cytoplasm. Virology **213:**439-49.

197. **Stein, A. J., G. Fuchs, C. Fu, S. L. Wolin, and K. M. Reinisch.** 2005. Structural insights into RNA quality control: the Ro autoantigen binds misfolded RNAs via its central cavity. Cell **121:**529-39.

198. **Stoltzfus, C. M., K. Dimock, S. Horikami, and T. A. Ficht.** 1983. Stabilities of avian sarcoma virus RNAs: comparison of subgenomic and genomic species with cellular mRNAs. J Gen Virol **64 (Pt 10):**2191-202.

199. **Swanson, C. M., and M. H. Malim.** 2006. Retrovirus RNA trafficking: from chromatin to invasive genomes. Traffic **7:**1440-50.

200. **Swanson, C. M., B. A. Puffer, K. M. Ahmad, R. W. Doms, and M. H. Malim.** 2004. Retroviral mRNA nuclear export elements regulate protein function and virion assembly. Embo J **23:**2632-40.

201. **Tabernero, C., A. S. Zolotukhin, A. Valentin, G. N. Pavlakis, and B. K. Felber.** 1996. The posttranscriptional control element of the simian retrovirus type 1 forms an extensive RNA secondary structure necessary for its function. J Virol **70:**5998-6011.

202. **Teixeira, D., U. Sheth, M. A. Valencia-Sanchez, M. Brengues, and R. Parker.** 2005. Processing bodies require RNA for assembly and contain nontranslating mRNAs. RNA **11:**371-82.

203. **Telesnitsky, A., S. Blain, and S. P. Goff.** 1995. Assays for retroviral reverse transcriptase. Methods Enzymol **262:**347-62.

204. **Tian, C., T. Wang, W. Zhang, and X. F. Yu.** 2007. Virion packaging determinants and reverse transcription of SRP RNA in HIV-1 particles. Nucleic Acids Res **35:**7288-302.

205. **Todaro, G. J., and H. Green.** 1963. Quantitative studies of the growth of mouse embryo cells in culture and their development into established lines. J Cell Biol **17:**299-313.

206. **Tounekti, N., M. Mougel, C. Roy, R. Marquet, J. L. Darlix, J. Paoletti, B. Ehresmann, and C. Ehresmann.** 1992. Effect of dimerization on the conformation of the encapsidation Psi domain of Moloney murine leukemia virus RNA. J Mol Biol **223:**205-20.

207. **Trubetskoy, A. M., S. A. Okenquist, and J. Lenz.** 1999. R region sequences in the long terminal repeat of a murine retrovirus specifically increase expression of unspliced RNAs. J Virol **73:**3477-83.

208. **Valadkhan, S.** 2005. snRNAs as the catalysts of pre-mRNA splicing. Curr Opin Chem Biol **9:**603-8.

209. **Vogel, U., and C. Scholtissek.** 1995. Inhibition of the intracellular transport of influenza viral RNA by actinomycin D. Arch Virol **140:**1715-23.

210. **Wada, T., T. Takagi, Y. Yamaguchi, A. Ferdous, T. Imai, S. Hirose, S. Sugimoto, K. Yano, G. A. Hartzog, F. Winston, S. Buratowski, and H. Handa.** 1998. DSIF, a novel transcription elongation factor that regulates RNA polymerase II processivity, is composed of human Spt4 and Spt5 homologs. Genes Dev **12:**343-56.

211. **Wada, T., T. Takagi, Y. Yamaguchi, D. Watanabe, and H. Handa.** 1998. Evidence that P-TEFb alleviates the negative effect of DSIF on RNA polymerase II-dependent transcription in vitro. Embo J **17:**7395-403.

212. **Wang, T., C. Tian, W. Zhang, P. T. Sarkis, and X. F. Yu.** 2008. Interaction with 7SL RNA but not with HIV-1 genomic RNA or P bodies is required for APOBEC3F virion packaging. J Mol Biol **375:**1098-112.

213. **Watanabe, T., S. Wang, J. Noritake, K. Sato, M. Fukata, M. Takefuji, M. Nakagawa, N. Izumi, T. Akiyama, and K. Kaibuchi.** 2004. Interaction with IQGAP1 links APC to Rac1, Cdc42, and actin filaments during cell polarization and migration. Dev Cell **7:**871-83.

214. **Wei, W., N. Gilbert, S. L. Ooi, J. F. Lawler, E. M. Ostertag, H. H. Kazazian, J. D. Boeke, and J. V. Moran.** 2001. Human L1 retrotransposition: *cis* preference versus *trans* complementation. Mol Cell Biol **21:**1429-39.

215. **Weldon, R. A., Jr., P. Sarkar, S. M. Brown, and S. K. Weldon.** 2003. Mason-Pfizer monkey virus Gag proteins interact with the human sumo conjugating enzyme, hUbc9. Virology **314:**62-73.

216. **Wickham, L., T. Duchaine, M. Luo, I. R. Nabi, and L. DesGroseillers.** 1999. Mammalian staufen is a double-stranded-RNA- and tubulin-binding protein which localizes to the rough endoplasmic reticulum. Mol Cell Biol **19:**2220-30.

217. **Wileman, T.** 2007. Aggresomes and pericentriolar sites of virus assembly: cellular defense or viral design? Annu Rev Microbiol **61:**149-67.

218. **Wolin, S. L., and T. Cedervall.** 2002. The La protein. Annu Rev Biochem **71:**375-403.

219. **Wolin, S. L., and J. A. Steitz.** 1983. Genes for two small cytoplasmic Ro RNAs are adjacent and appear to be single-copy in the human genome. Cell **32:**735-44.

220. **Wolin, S. L., and J. A. Steitz.** 1984. The Ro small cytoplasmic ribonucleoproteins: identification of the antigenic protein and its binding site on the Ro RNAs. Proc Natl Acad Sci U S A **81:**1996-2000.

221. **Xue, D., H. Shi, J. D. Smith, X. Chen, D. A. Noe, T. Cedervall, D. D. Yang, E. Eynon, D. E. Brash, M. Kashgarian, R. A. Flavell, and S. L. Wolin.** 2003. A lupus-like syndrome develops in mice lacking the Ro 60-kDa protein, a major lupus autoantigen. Proc Natl Acad Sci U S A **100:**7503-8.

222. **Yamaguchi, Y., T. Takagi, T. Wada, K. Yano, A. Furuya, S. Sugimoto, J. Hasegawa, and H. Handa.** 1999. NELF, a multisubunit complex containing RD, cooperates with DSIF to repress RNA polymerase II elongation. Cell **97:**41-51.

223. **Yamaguchi, Y., T. Wada, and H. Handa.** 1998. Interplay between positive and negative elongation factors: drawing a new view of DRB. Genes Cells **3:**9-15.

224. **Yang, J., and B. R. Cullen.** 1999. Structural and functional analysis of the avian leukemia virus constitutive transport element. RNA **5:**1645-55.

225. **Yang, S., R. Delgado, S. R. King, C. Woffendin, C. S. Barker, Z. Y. Yang, L. Xu, G. P. Nolan, and G. J. Nabel.** 1999. Generation of retroviral vector for clinical studies using transient transfection. Hum Gene Ther **10:**123-32.

226. **Yu, Q., and J. L. Darlix.** 1996. The zinc finger of nucleocapsid protein of Friend murine leukemia virus is critical for proviral DNA synthesis in vivo. J Virol **70:**5791-8.

227. **Yu, S. S., J. M. Kim, and S. Kim.** 2000. The 17 nucleotides downstream from the env gene stop codon are important for murine leukemia virus packaging. J Virol **74:**8775-80.

228. **Zhuang, J., S. Mukherjee, Y. Ron, and J. P. Dougherty.** 2006. High rate of genetic recombination in murine leukemia virus: implications for influencing proviral ploidy. J Virol **80:**6706-11.

229. **Zolotukhin, A. S., A. Valentin, G. N. Pavlakis, and B. K. Felber.** 1994. Continuous propagation of RRE(-) and Rev(-)RRE(-) human immunodeficiency virus type 1 molecular clones containing a cis-acting element of simian retrovirus type 1 in human peripheral blood lymphocytes. J Virol **68:**7944-52.